

---

Structures and Materials Research Report No. BC-050  
FINAL PROJECT REPORT

January 2000

UF Project No. 4910 45 04 680 12  
Contract No. BC-050

---

**DESIGN, TESTING, AND SPECIFICATION OF  
A MECHANICAL DAMPING DEVICE FOR  
MAST ARM TRAFFIC SIGNAL STRUCTURES**

---

Principle Investigators:	Ronald A. Cook, Ph.D., P.E. David Bloomquist, Ph.D., P.E.
Graduate Research Assistants:	Dylan S. Richard Michael A. Kalajian Victoria A. Cannon
Undergraduate Research Assistant:	David P. Arnold
Project Manager:	Marcus H. Ansley, P.E.

---

Department of Civil Engineering  
College of Engineering  
University of Florida  
Gainesville, Florida 32611

Engineering and Industrial Experiment Station

---



## DISCLAIMER

“The opinions, findings, and conclusions expressed in this publication are those of the authors and not necessarily those of the Florida Department of Transportation or the U.S. Department of Transportation.

Prepared in cooperation with the State of Florida Department of Transportation and the U.S. Department of Transportation.”

DESIGN, TESTING, AND SPECIFICATION OF  
A MECHANICAL DAMPING DEVICE FOR  
MAST ARM TRAFFIC SIGNAL STRUCTURES

State Job No. BC-050  
Contract No. BC-050  
UF No. 4910 45 04 680 12

Principle Investigators:	R. A. Cook D. Bloomquist
Graduate Research Assistants:	D. S. Richard M. A. Kalajian V. A. Cannon
Undergraduate Research Assistant	D. P. Arnold
FDOT Technical Coordinator:	M. H. Ansley

Engineering and Industrial Experiment Station  
Department of Civil Engineering  
University of Florida  
Gainesville, Florida

1. Report No. <b>BC-050</b>	2. Government Accession No.	3. Recipient's Catalog No.	
4. Title and Subtitle <b>Design, Testing, and Specification of a Mechanical Damping Device for Mast Arm Traffic Signal Structures</b>		5. Report Date <b>January 2000</b>	
		6. Performing Organization Code	
		8. Performing Organization Report No. <b>4910 45 04 680 12</b>	
7. Author(s) <b>R.A. Cook, D. Bloomquist, D.S. Richard, M.A. Kalajian, V.A. Cannon and D.P. Arnold</b>		10. Work Unit No. (TRAIS)	
9. Performing Organization Name and Address <b>University of Florida Department of Civil Engineering 345 Weil Hall / P.O. Box 116580 Gainesville, FL 32611-6580</b>		11. Contract or Grant No. <b>BC-050</b>	
		13. Type of Report and Period Covered <b>Final Report 12/15/98 - 2/15/00</b>	
		14. Sponsoring Agency Code	
12. Sponsoring Agency Name and Address <b>Florida Department of Transportation Research Management Center 605 Suwannee Street, MS 30 Tallahassee, FL 32301-8064</b>		15. Supplementary Notes <b>Prepared in cooperation with the Federal Highway Administration</b>	
16. Abstract <p>Several mast arm failures have been observed in Florida and other states from fatigue caused by wind-induced vibrations. An economical method to mitigate the effects of wind-induced vibration on these types of structures is to install mechanical damping systems directly on the mast arm. These devices limit the amplitude and duration of vibrations resulting in an increase in the design life of the structure.</p> <p>This report describes the development and testing of several different damping devices for cantilevered mast arm structures. Prototype damping devices were tested on a 37ft mast arm constructed in the Structures Laboratory at the University of Florida. Successful devices were then field tested on three existing mast arms to determine their effectiveness on a range of mast arm lengths. The optimum device was then placed on a mast arm in Tampa, Florida that had been observed to undergo significant wind-induced movement on a regular basis. The structure was monitored with and without the device in place to compare the overall effectiveness of the device. The specifications for a tapered impact damper (final device) are included.</p>			
17. Key Words <b>mast arms, damping, traffic signal supports, vibrations</b>		18. Distribution Statement <b>No restrictions. This document is available to the public through the National Technical Information Service, Springfield, VA, 22161</b>	
19. Security Classif. (of this report) <b>Unclassified</b>	20. Security Classif. (of this page) <b>Unclassified</b>	21. No. of Pages <b>135</b>	22. Price

## TABLE OF CONTENTS

	<u>Page</u>
DISCLAIMER .....	ii
TECHNICAL SUMMARY .....	iii
LIST OF TABLES .....	viii
LIST OF FIGURES .....	ix
CHAPTERS	
1 INTRODUCTION.....	1
1.1 Introduction.....	1
1.2 Objective.....	2
1.3 Scope.....	2
2 LITERATURE REVIEW.....	3
2.1 Introduction.....	3
2.2 Vortex Shedding .....	3
2.3 Galloping.....	6
2.4 Natural Wind Gusts.....	9
2.5 Truck-Induced Wind Gusts.....	10
2.6 Summary of Literature Review.....	11
3 REVIEW OF FDOT REPORT BY MICHAEL A. KALAJIAN .....	13
3.1 Introduction.....	13
3.2 University of Florida Test Facility.....	13
3.3 Instrumentation and Testing Procedures.....	15
3.4 Free Vibration of the Lab Mast Arm .....	15
3.5 Review of Kalajian’s Dampers and Lab Test Results .....	16
3.5.1 Damping at the Arm-Pole Connection .....	17
3.5.2 Stockbridge Type Version Dampers .....	20
3.5.3 Liquid Tuned Dampers.....	22
3.5.4 Tuned Mass Damper .....	22
3.5.5 Spring/Mass Friction Dampers.....	27

3.5.6	Spring/Mass Impact Friction Dampers.....	33
3.5.7	Woodpecker Damper.....	39
3.5.8	Summary of Kalajian’s Dampers .....	40
3.6	Field Testing of Damping Devices .....	40
3.7	Conclusion .....	45
4	DATA ACQUISITION AND INSTRUMENTATION .....	46
4.1	Data Required .....	46
4.2	Data Acquisition .....	46
4.3	Displacement Instrumentation .....	47
4.4	Calibration of Accelerometers .....	50
4.5	Wind Instrumentation .....	55
4.6	Instrument Effects on Mast Arm Structures .....	56
5	PRELIMINARY MAST ARM TESTING.....	57
5.1	Introduction.....	57
5.2	Mast Arms.....	57
5.3	Testing Procedures.....	61
5.4	Computer Modeling .....	64
5.5	Results.....	66
6	DAMPING DEVICES AND RESULTS .....	67
6.1	Introduction.....	67
6.2	Kalajian’s Selected Damping Device .....	67
6.3	Round Impact Damper .....	69
6.4	Eight-Inch Tapered Impact Damper .....	70
6.5	Long Four-Inch Tapered Impact Damper .....	71
6.6	Horizontal Damping Test.....	78
6.7	Semi-Tuned Tapered Impact Damper – Final Design .....	81
6.8	Conclusion .....	93
7	FIELD TESTING IN TAMPA, FL .....	95
7.1	Introduction.....	95
7.2	Procedure .....	96
7.3	Results.....	97
7.4	Conclusion .....	100
8	SUMMARY, CONCLUSIONS, AND RECOMMENDATIONS .....	102
8.1	Summary .....	102
8.2	Conclusions.....	104
8.3	Recommendations.....	105

## APPENDICES

A	SAMPLE DATA MANIPULATION MATHCAD WORKSHEET.....	106
B	SAMPLE SSTAN INPUT FILE OF THE LAB MAST ARM .....	118
C	FABRICATION OF TAPERED IMPACT DAMPER .....	124
	LIST OF REFERENCES .....	135

## LIST OF TABLES

<u>Tables</u>	<u>Page</u>
3.1 Summary of Kalajian’s Dampers .....	41
3.2 Mast Arm Frequency Results for Lab and Field Testing .....	44
3.3 Percent Critical Damping Results for Lab and Field Testing .....	44
5.1 Comparison of Computer Model and Free Vibration Mast Arm Testing Results .....	65
6.1 Spring/Mass Natural Frequency Comparisons (Mass held constant at 15 lbs) .....	73
6.2 Spring/Mass Combinations for Long 4 in Tapered Impact Damper (Variable Mass Testing) .....	76
6.3 Spring Lengths Required to Match Damper and Mast Arm Horizontal Frequencies .....	79
6.4 Summary of Percent Critical Damping Values for Each Tested Mast Arm .....	92
6.5 Summary of Total Displacements Allowed by the Dampers Under the Influence of the Eccentric Mass and Motor Device .....	92



## LIST OF FIGURES

<u>Figure</u>	<u>Page</u>
2.1 Vortex shedding illustration .....	3
2.2 Critical Wind Velocities Required for Vortex Shedding "Lock-In" for Circular Supports ( $f_n = 1\text{Hz}$ & $S = 0.18$ ) .....	5
2.3 Free body diagram to illustrate the galloping phenomena .....	7
3.1 Lab Mast Arm Dimensions .....	14
3.2 Lab Mast Arm (Photo 1) .....	14
3.3 Lab Mast Arm (Photo 2) .....	14
3.4 Free Vibration Response of Lab Mast Arm .....	16
3.5 Belleville Disc Spring Dimensions .....	17
3.6 Belleville Disc Springs Vibration Response .....	18
3.7 Neoprene Pad Dimensions .....	19
3.8 Connection where Belleville Disc Springs and Neoprene Pads were installed .....	19
3.9 Batten Damper .....	20
3.10 Stockbridge Version Damper .....	20
3.11 Batten Damper Vibration Response .....	21
3.12 Stockbridge Version Damper Vibration Response .....	21
3.13 20 ft Long PVC Liquid Damper .....	23
3.14 20 ft Long PVC Liquid Damper Vibration Response .....	23

<u>Figure</u>	<u>Page</u>
3.15 Short U-Tube Liquid Damper .....	24
3.16 Short U-Tube Liquid Damper Vibration Response.....	24
3.17 Long U-Tube Liquid Damper.....	25
3.18 Long U-Tube Liquid Damper Vibration Response .....	25
3.19 Tuned Mass Damper .....	26
3.20 Tuned Mass Damper Vibration Response.....	27
3.21 2 in Galvanized Pipe, Bungee and Mass Damper .....	28
3.22 2 in Galvanized Pipe, Bungee and Mass Damper Vibration Response.....	29
3.23 2 in PVC Pipe, Bungee and Mass Damper with Oil .....	30
3.24 2 in PVC Pipe, Bungee and Mass Damper with Oil Vibration Response.....	30
3.25 4 in PVC Pipe, Spring and Mass Damper with Oil .....	31
3.26 4 in PVC Pipe, Spring and Mass Damper with Oil Vibration Response .....	31
3.27 Compression Spring Damper .....	32
3.28 Compression Spring Damper Vibration Response.....	33
3.29 Tension Spring/Mass Binding on Joint Damper .....	34
3.30 Tension Spring/Mass Binding on Joint Damper Vibration Response.....	34
3.31 3 in to 2 in Tapered Spring/Mass Impact Damper .....	35
3.32 3 in to 2 in tapered Spring/Mass Impact Damper Vibration Response .....	36
3.33 4 in to 3 in Tapered Spring/Mass Impact Damper .....	37
3.34 4 in to 2 in Tapered Spring/Mass Impact Damper .....	37
3.35 4 in to 3 in Tapered Spring/Mass Impact Damper .....	38
3.36 4 in to 2 in Tapered Spring/Mass Impact Damper Vibration Response.....	38

<u>Figure</u>	<u>Page</u>
3.37 Woodpecker Damper.....	39
3.38 Woodpecker Damper Vibration Response.....	40
4.1 Wire-LVDT.....	47
4.2 Inclinator attached to tip of lab mast arm.....	48
4.3 Accelerometers attached to tip of lab mast arm.....	49
4.4 Accelerometer Power Supplies and Filter.....	50
4.5 Filtered Acceleration Data.....	51
4.6 Non-Filtered Acceleration Data.....	51
4.7 Acceleration Data Before FFT Filtering.....	53
4.8 Acceleration Data After FFT Filtering.....	53
4.9 Displacement Data Comparison without utilizing the Centering Function.....	54
4.10 Displacement Data Comparison utilizing the Centering Function.....	54
4.11 Anemometer and Vane.....	55
5.1 Gainesville Long (70ft) Mast Arm Dimensions.....	58
5.2 Gainesville Long (70ft) Mast Arm.....	58
5.3 Gainesville Short (40ft) Mast Arm Dimensions.....	59
5.4 Gainesville Short (40ft) Mast Arm.....	59
5.5 Tampa Mast Arm Dimensions.....	60
5.6 Tampa Mast Arm.....	60
5.7 Eccentric Mass and Motor Device (Photo 1).....	63
5.8 Eccentric Mass and Motor Device (Photo 2).....	63
6.1 4 in Tapered Impact Damper.....	68

<u>Figure</u>	<u>Page</u>
6.2 4 in Tapered Impact Damper Vibration Response .....	68
6.3 Round Impact Damper with Cover Plate .....	69
6.4 Round Impact Damper without Cover Plate .....	69
6.5 Round Impact Damper without Cover Plate, and Connected to the Tip of a Mast Arm.....	70
6.6 Eight-Inch Tapered Impact Damper.....	71
6.7 Cross Section Drawing of Long 4 in Tapered Impact Damper.....	73
6.8 Long 4 in Tapered Impact Damper .....	73
6.9 Long 4 in Tapered Impact Damper on Gainesville Short Mast Arm (Variable Springs with Constant Mass (15 lb)).....	74
6.10 Long 4 in Tapered Impact Damper on Lab Mast Arm (Variable Springs with Constant Mass (15 lb)) .....	75
6.11 Long 4 in Tapered Impact Damper on Gainesville Long Mast Arm (Variable Springs with Constant Mass (15 lb)).....	75
6.12 Variable Mass Testing for Long 4 in Tapered Impact Damper (Case 1).....	77
6.13 Variable Mass Testing for Long 4 in Tapered Impact Damper (Case 2).....	77
6.14 Variable Mass Testing for Long 4 in Tapered Impact Damper (Case 3).....	77
6.15 Results of 6 in Pipe with Various Spring Lengths and Consistent Mass (15lb) .....	80
6.16 Results of 6 in Pipe with Various Frequencies (Using Consistent Mass (15 lbs) and Variable Spring Lengths).....	80
6.17 Cross Section Drawing of 3 ft Tapered Impact Damper .....	82
6.18 3 ft Tapered Impact Damper .....	82
6.19 Free Vibration of the Lab Mast Arm.....	83
6.20 Free Vibration of the Lab Mast Arm with 3 ft Tapered Impact Damper .....	83

<u>Figure</u>	<u>Page</u>
6.21 Eccentric Mass and Motor Vibration of the Lab Mast Arm.....	84
6.22 Eccentric Mass and Motor Vibration of the Lab Mast Arm with 3 ft Tapered Impact Damper .....	84
6.23 Free Vibration of the Gainesville Short Mast Arm .....	85
6.24 Free Vibration of the Gainesville Short Mast Arm with 3 ft Tapered Impact Damper .....	85
6.25 Eccentric Mass and Motor Vibration of the Gainesville Short Mast Arm.....	86
6.26 Eccentric Mass and Motor Vibration of the Gainesville Short Mast Arm with 3 ft Tapered Impact Damper .....	86
6.27 Free Vibration of the Gainesville Long Mast Arm .....	87
6.28 Free Vibration of the Gainesville Long Mast Arm with 3 ft Tapered Impact Damper .....	87
6.29 Eccentric Mass and Motor Vibration of the Gainesville Long Mast Arm .....	88
6.30 Eccentric Mass and Motor Vibration of the Gainesville Long Mast Arm with 3 ft Tapered Impact Damper .....	88
6.31 Free Vibration of the Tampa Mast Arm.....	89
6.32 Free Vibration of the Tampa Mast Arm with 3 ft Tapered Impact Damper .....	89
6.33 Cross Section Drawing of 4 ft Tapered Impact Damper .....	90
6.34 4 ft Tapered Impact Damper .....	90
6.35 Free Vibration of the Lab Mast Arm with 4 ft Tapered Impact Damper .....	91
6.36 Eccentric Mass and Motor Vibration of the Lab Mast Arm with 4 ft Tapered Impact Damper .....	91
7.1 Plan View of Tampa Mast Arm Intersection.....	95
7.2 Instrumentation Setup for Tampa Mast Arm .....	96
7.3 Range of Wind Directions for Test Results.....	97

<u>Figure</u>	<u>Page</u>
7.4 Natural Vibration Displacements of the Tampa Mast Arm (Winds on the Front) .....	98
7.5 Natural Vibration Displacements of the Tampa Mast Arm with the 3 ft Tapered Impact Damper (Winds on the Front) .....	98
7.6 Natural Vibration Displacements of the Tampa Mast Arm (Winds on the Back) .....	99
7.7 Natural Vibration Displacements of the Tampa Mast Arm with the 3 ft Tapered Impact Damper (Winds on the Back).....	99

## CHAPTER 1 INTRODUCTION

### 1.1 Introduction

The Florida Department of Transportation (FDOT) currently requires mast arm support structures for traffic signs and signals within ten miles of the coast. These mast arms are also used off the coast of Florida and throughout the United States. Mast arm structures have been increasingly observed to be susceptible to structural vibrations resulting from both normal and extreme wind conditions. These wind-induced vibrations are typically caused by the vortex shedding or galloping phenomena. Vibrations are also caused by truck-induced wind gusts along mid to high-speed roadways. Mast arm cantilevered signal supports are susceptible to fatigue cracking from the numerous oscillations caused by these winds. This has caused a widespread concern regarding their reliability [5]. Recently, mast arm failures caused by wind effects have been observed in St. Augustine and Ft. Walton Beach, Florida. Mast arms are also being monitored for fatigue failure in Wyoming and Texas.

Light-poles along the Howard Franklin Bridge in Tampa, Florida and the New River Bridge in Ft. Lauderdale, Florida have also experienced failures from wind-induced vibrations. An economical method to mitigate the effects of wind-induced vibrations on these types of structures is to install mechanical damping systems in the structures. In the case of the Howard Franklin Bridge, such devices were retrofit to the existing poles. Similar mitigation techniques are necessary for mast arm structures subjected to wind-

induced oscillations [2]. Reducing the amplitude and number of vibration cycles will decrease the likelihood of fatigue failures, thus extending the structures life.

### 1.2 Objective

At this time, there are no FDOT specifications or qualification procedures for mechanical damping devices although, in some instances, they are required by the FDOT. The objective of this research was to develop a consistent, rationally based specification for a mechanical damping device. FDOT personnel and/or contractors could then use this specification in both the original design/construction and retrofit of cantilevered mast arm structures. Implementation of a specification will greatly reduce or possibly eliminate failures of mast arm and light pole structures caused by vibrations from wind effects.

### 1.3 Scope

The scope of this project is to design, test, and prepare a specification for a mechanical damping device that will effectively mitigate wind-induced vibrations on all lengths of mast arm structures under the FDOT's control. It is important to note that the specification will not only be appropriate in Florida, but in all areas of the United States where wind-induced vibrations are a problem. This project was divided as follows:

1. Literature review.
2. Review of previous report by Michael A. Kalajian [6].
3. Develop new damping devices.
4. Perform lab and field tests with the newly developed damping devices.
5. Present specification for the selected damping device.



## CHAPTER 2 LITERATURE REVIEW

### 2.1 Introduction

Cantilevered mast arms are susceptible to four types of wind loading that may induce vibrations that can lead to fatigue failures. The four wind-loading phenomena include vortex shedding, galloping, natural wind gusts, and truck-induced wind gusts [5]. The purpose of this chapter is to define these phenomena and present information from related research projects.

### 2.2 Vortex Shedding

The vortex shedding phenomena is illustrated in Figure 2.1. As a steady and uniform airflow travels over the face of a body, it reaches points of separation on each side where thin sheets of tiny vortices are generated. As the vortex sheets detach, they interact with one another and roll up into discrete vortices that are shed alternately from the sides of the object [10].

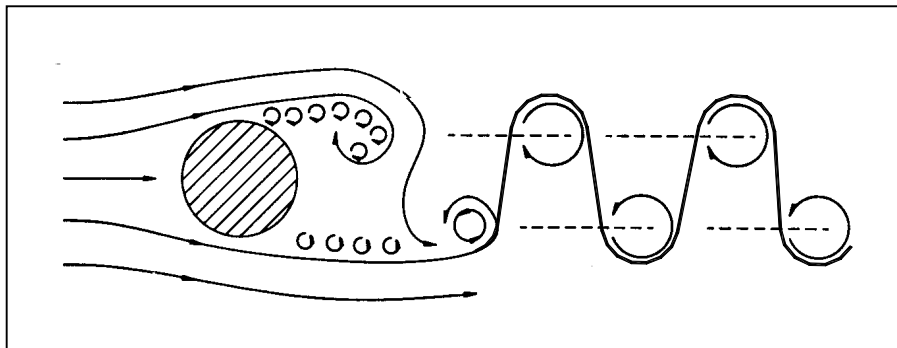


Figure 2.1 - Vortex shedding illustration

The sinusoidal pattern that forms in the wake of the object is known as a Von Karman street. The asymmetric pressure distribution created by the vortices around the cross section results in a sinusoidal forcing function transverse to the object. The Strouhal relation gives the frequency,  $f_s$ , of these shedding vortices in the equation:

$$f_s = \frac{S \cdot V}{D}$$

where  $S$  is the Strouhal number,  $D$  is the across-wind dimension of the element, and  $V$  is the free-stream wind velocity [5]. When the frequency of vortex shedding, as predicted by the Strouhal relation, does not match one of the natural frequencies of the structure, the shedding of vortices in the wake of a structure will attain only a nominal periodic response. However, when the frequency of vortex shedding approaches the frequency of a structure, the result is an increase in vortex strength, an increase in the spanwise correlation of the vortex shedding forces, and a tendency for the vortex shedding frequency to become coupled to the natural frequency of the structure. This phenomenon is called “lock in”. The critical wind velocity,  $V_{cr}$ , at which lock-in occurs is given by the Strouhal relation:

$$V_{cr} = \frac{f_n \cdot D}{S}$$

where  $f_n$  is the natural frequency of the structure [5]. The result of the vortex shedding lock-in phenomena is oscillations transverse to the wind that can lead to resonance of the structure.

Since uniform steady-state flow is required for vortex shedding, velocity boundaries can be determined for a mast arms susceptibility to vortex-induced oscillations. Previous research indicates that the level of turbulence associated with wind velocities above approximately 35 to 40 mph limits the symmetric formation of periodic vortices [7]. Also, vortex formation at wind velocities below approximately 10 mph generates forces with magnitudes insufficient to excite most structures. Therefore, structures may be susceptible to vortex-induced oscillations in the range of wind velocities between approximately 10 to 35 mph [5].

Figure 2.2 depicts the critical wind velocities necessary to initiate lock-in due to the shedding of vortices from circular supports of cantilevered structures subjected to a subcritical flow regime.

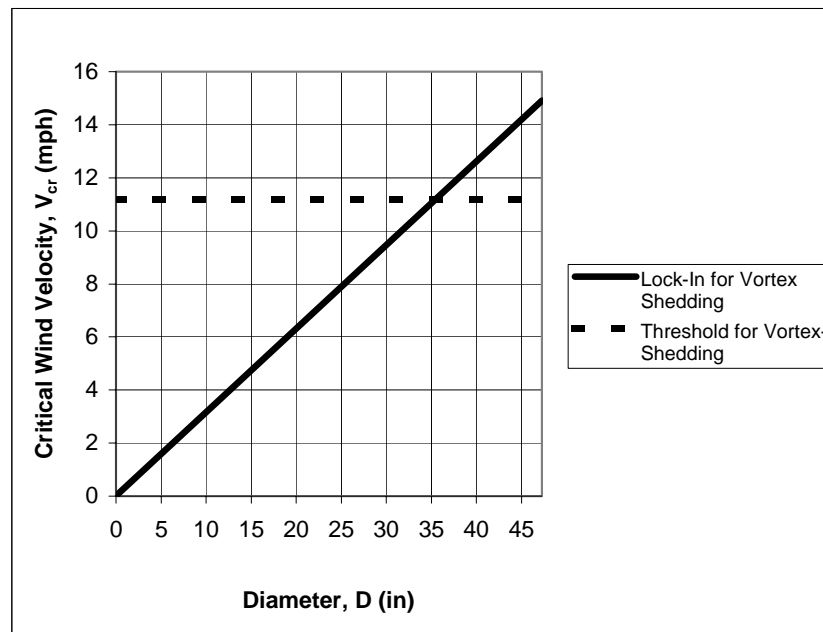


Figure 2.2 - Critical Wind Velocities Required for Vortex Shedding "Lock-In" for Circular Supports  
( $f_n = 1\text{Hz}$  &  $S = 0.18$ )

A typical diameter of a mast arm cantilever is anywhere from 3in to 15in. The lock-in graph indicates that the wind velocities for which vortices will be shed from the circular supports of the cantilevered support structures fall below the minimum wind velocity, of 10 mph, required to initiate vibrations in most structures. Thus, cantilevered mast arm structures are not expected to be susceptible to vortex-induced vibrations from the shedding of vortices [5].

It is also believed that tapered circular support members will be even less susceptible to vortex-induced oscillations than normal circular support members. Vortex shedding can only occur over some fraction of the member's length due to the variation in diameter of the member. Therefore, insufficient energy will be available to generate large amplitude vibrations of the structure [5].

The vortex-shedding phenomenon does not appear to have a significant effect on cantilevered mast arm structures with diameters less than 35 in. However, due to the height of most vertically mounted traffic signals (typically greater than 36in), it is possible that vortex shedding could play a role in the initiating of the galloping phenomena.

### 2.3 Galloping

Galloping is an unstable phenomenon caused by aerodynamic forces generated on certain cross-sectional shapes that result in displacements transverse to the wind [10].

This phenomenon can best be understood by observing Figure 2.3.

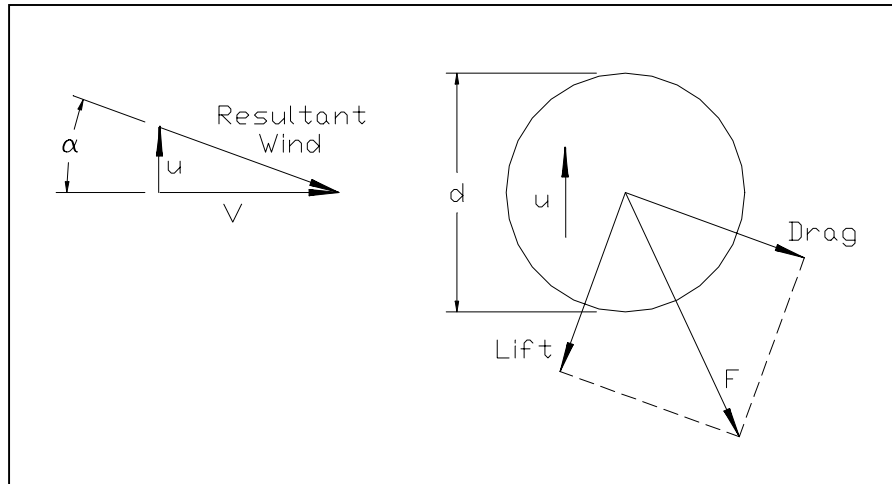


Figure 2.3 - Free body diagram to illustrate the galloping phenomena

Consider a circular section located in a steady air stream of velocity  $V$ . If the body moves upward at a velocity of  $u$ , a resultant wind force will act on it at a downward angle of attack,  $\alpha$ , given by:

$$\alpha = \arctan\left(\frac{u}{V}\right)$$

This resultant wind force will cause a drag force and a lift force on the section, which combine to produce a total damping force  $F$ . In the following equations,  $C_D$  and  $C_L$  are coefficients of drag and lift respectively,  $d$ =diameter of the body,  $\rho$ =air density, and  $L$ =length of the body [3].

$$\text{Drag} = C_D \cdot \rho \cdot d \cdot L \cdot \text{Resultant\_Wind}^2$$

$$\text{Lift} = C_L \cdot \rho \cdot d \cdot L \cdot \text{Resultant\_Wind}^2$$

$$F = \text{Lift} \cdot \cos\alpha + \text{Drag} \cdot \sin\alpha$$

The susceptibility of a structure to galloping can be determined from the Den Hartog's criterion given by [4]:

$$\frac{dF}{d\alpha} < 0 \quad (\text{unstable})$$

$$\frac{dF}{d\alpha} > 0 \quad (\text{stable})$$

Given that  $\alpha$  is a small angle, this criterion can be reduced to [4]:

$$\left( \frac{d\text{Lift}}{d\alpha} + \text{Drag} \right) < 0 \quad (\text{unstable})$$

$$\left( \frac{d\text{Lift}}{d\alpha} + \text{Drag} \right) > 0 \quad (\text{stable})$$

Positive damping of a system is apparent when an oscillating structure comes to rest with external forces present. A system found to be unstable by Den Hartog's criterion would contain negative damping, thus causing an increase in crosswind oscillations of the system. The minimum wind speeds for galloping are a function of this negative aerodynamic damping and the structural damping but are not affected by the critical or lock in velocity due to vortex shedding [8]. However, it is very important to note that galloping cannot start when the structure is at rest. Wind gusts usually start structural movement and then oscillations continue. Most galloping oscillations take place at low to medium wind speeds, but can occur in all wind velocities [9].

Most simple shapes have an unstable galloping characteristic at some attitude, except for a smooth circular cylinder [9]. Even though mast arms are circular, they

encounter galloping oscillations due to the sign and signal attachments on the horizontal cantilever. Kaczinski et al. [5] performed tests on mast arm models in both a wind tunnel and a water tank. They also observed cantilevered support structures in the field. It was determined that the galloping phenomenon is very sensitive to its surrounding conditions and does not occur frequently. Nevertheless, once a galloping instability was initiated, the resulting crosswind resonant vibrations persisted with both increases and reductions to the flow velocity. Kaczinski et al. [5] concluded that cantilevered signal support structures were more susceptible to galloping when the signal attachments with or without backplates were subject to wind flows from the rear. They also determined that signals are more likely to gallop when configured with the backplates. Finally, galloping of sign attachments was independent of aspect ratio and is more prevalent with wind flows from the front of the structure.

The effects of galloping oscillations on mast arm signal structures can be very significant. With the presence of damaging stress cycles, the structure's life could be greatly reduced due to fatigue in high stress-concentration areas.

#### 2.4 Natural Wind Gusts

Natural wind gusts arise from the variability in velocity and direction of airflow. These wind gusts are characterized by a spectrum of velocity components that oscillate over a broad range of frequencies as a result of turbulence inherently present in any natural airflow [5]. This broad range of frequencies causes the amplitude of a structure's response to natural wind gusts to be variable and randomly distributed.

The most common approach for estimating the maximum pressure imposed on a structure by a gust is through the use of a gust factor. A gust factor is the ratio of the expected peak displacement load during a specified period to the mean displacement load. Several parameters combine to produce the value of a gust factor including roughness of the surrounding terrain, height of the structure, and the structure's geometry. A design wind pressure can be determined from the gust factor. This design wind represents the maximum expected equivalent static wind pressure which produces the same response a structure would be subjected to under a maximum expected dynamic wind loading [5]. The gust factor currently used in the AASHTO specifications for the design of sign, signal, and luminaire support structures is 1.3. As reported by Kaczinski et al., all available evidence indicates that cantilevered support structures perform satisfactorily under extreme wind conditions and no reported failures have been directly attributed to extreme gust loading conditions. Therefore, the gust factor of 1.3 seems adequate for the ultimate strength design of cantilevered support structures [5]. However, natural wind gusts can still cause excessive displacements of mast arm structures. These excessive displacements could lead to fatigue cracking over the life of a cantilevered structure.

### 2.5 Truck-Induced Wind Gusts

Truck-induced wind gusts are the result of trucks repeatedly passing under sign and signal structures. These trucks cause wind gusts on both the front and underside areas of the cantilevered section of the structures. The magnitude of truck gusts on the front surface of the mast arms (horizontal direction) was reported by Kaczinski et al. to



be much less than the natural wind gust pressures. However, it is possible that the truck gusts on the underside surface of the mast arms (vertical direction) are causing vertical vibrations of cantilevered mast arm structures and perhaps fatigue damage. These vertical truck gusts are generated from deflectors on the truck cabs that are designed to divert the wind flow upward and minimize the drag created by the trailers. It's possible that these vertical wind gusts are equal to the speed of the truck or even higher if the truck is driving into a head wind.

One study performed by Cook et al., at the University of Florida, studied the wind pressures given off by semi-trucks along a major highway. Wind pressures were measured from 0° (horizontal) to 90° (vertical) in 15° increments. The pressures recorded in Cook's et al. study were lower than what would be produced by winds at the same speed as the truck, as suggested in Kaczinski's et al report. However, it was determined that the trucks produced wind gusts at frequencies around 2 Hz and 0.5 Hz [1]. Mast arm structures from 30 ft to 70 ft in length are known to have natural frequencies from 1.4 Hz to 0.6 Hz respectively. Therefore, it is very likely that truck induced-gusts are responsible for oscillations in long mast arms located along high-speed roads (ie. 55 mph plus).

## 2.6 Summary of Literature Review

The literature review revealed that vortex shedding, galloping, natural wind gusts, and truck-induced wind gusts are all phenomena that can induce vibrations in cantilevered mast arm structures. Vortex shedding was probably the least likely cause of oscillations due to the tapered geometry of most horizontal cantilevers. However, it is

possible that vertically mounted lights could experience vortex shedding enough to initiate galloping. Galloping is probably the main cause of excessive vibrations. The galloping phenomena can occur with winds from virtually any direction. Natural wind gusts are not thought to be the main cause of fatigue failure, but they are significant enough to be considered. Finally, truck-induced wind gusts cause relatively small and quick vibrations. However, some roads have high volumes of truck traffic and can inflict numerous oscillation cycles on a structure.

CHAPTER 3  
REVIEW OF FDOT REPORT BY MICHAEL A. KALAJIAN

3.1 Introduction

The purpose of this chapter is to review the procedures and results of the FDOT report written by Michael A. Kalajian [6]. The information in the remaining chapters of this report is an extension to the research performed by Kalajian in August of 1998.

3.2 University of Florida Test Facility

Kalajian's project began with the development of a mast arm test facility to be located in the structures laboratory at the University of Florida. The purpose of this facility was to evaluate the response of a mast arm structure and test the performance of his developed damping devices. A full-scale mast arm structure was proposed for the lab. It was determined that the lab could accommodate a cantilevered structure with a 37 ft arm length and 15 ft pole height. The mast arm was designed and built within these parameters.

The structure's foundation was an 8 ft x 8ft x 2 ft concrete block that was anchored to the structural floor of the laboratory with four 2.5 in bolts spaced at 6 ft on center. The foundation size was controlled by the spacing of the tie down bolt-holes in the lab's floor. The base of the pole was set in the center of the concrete block and anchored with four 1.75 in bolts embedded 24 in with 9 in free above the concrete. The clearance of the structure was limited to 20 ft from the floor surface due to the height of

the laboratory cranes. The final length of the mast arm's pole was 15 ft with a 37 ft cantilevered arm being attached at 14 ft. Three traffic signals were mounted on the arm. The outermost signal was a five light assembly (85 lbs), while the other two were three light assemblies (57 lbs each). All dimension details can be seen in Figure 3.1. Finally, a platform measuring 12 ft x 6 ft was built around the 4 ft tip of the cantilevered arm to act as the monitoring station for testing. Figures 3.2 and 3.3 are photographs of the University of Florida test facility.

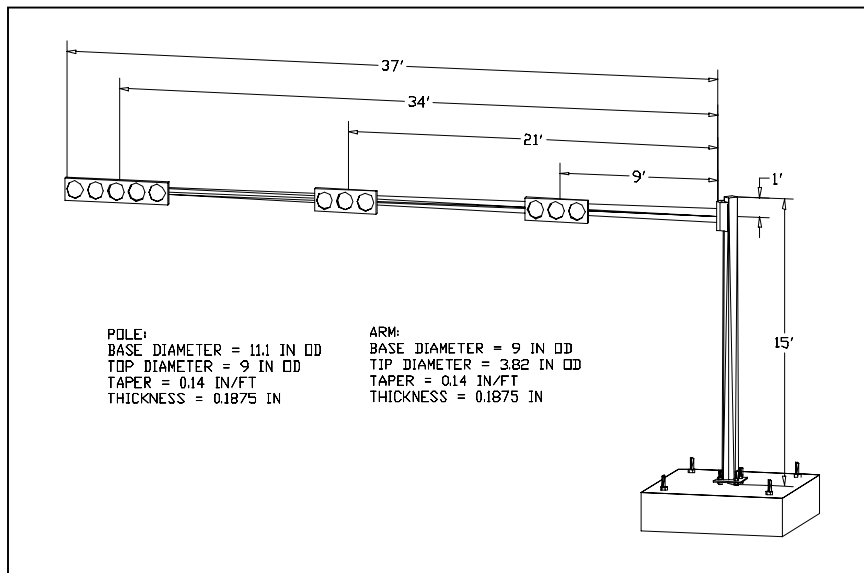


Figure 3.1 - Lab Mast Arm Dimensions



Figure 3.2 - Lab Mast Arm (Photo 1)



Figure 3.3 - Lab Mast Arm (Photo 2)

### 3.3 Instrumentation and Testing Procedures

Kalajian was interested in calculating the percent critical damping and natural frequency for each mast arm tested with and without his dampers attached. He selected PCB brand general-purpose accelerometers to record data for these calculations. Two accelerometers were mounted on a tri-axial mounting block that was then attached to a mast arm with wax. These sensors measured accelerations of the mast arm tip in the horizontal and vertical directions. Time was also recorded simultaneously with the acceleration data. The data acquisition used by Kalajian to record the acceleration and time data was identical to the one used in this report and will be covered in Chapter 4.

Each test consisted of giving the mast arm an initial vertical displacement and allowing it to oscillate freely. The recorded data was then used to plot a graph of normalized acceleration vs. time. As long as no external force was applied to the structure once it was placed into free vibration, the graph resulted in an exponentially damped function. This function was used to calculate the structure's percent critical damping and natural frequency.

### 3.4 Free Vibration of the Lab Mast Arm

The free vibration of the mast arm was the vibration of the arm due to a vertical displacement with no damping device on the arm. This test was done to determine the damping present in the mast arm itself. The free vibration response of the lab mast arm is represented in Figure 3.4.

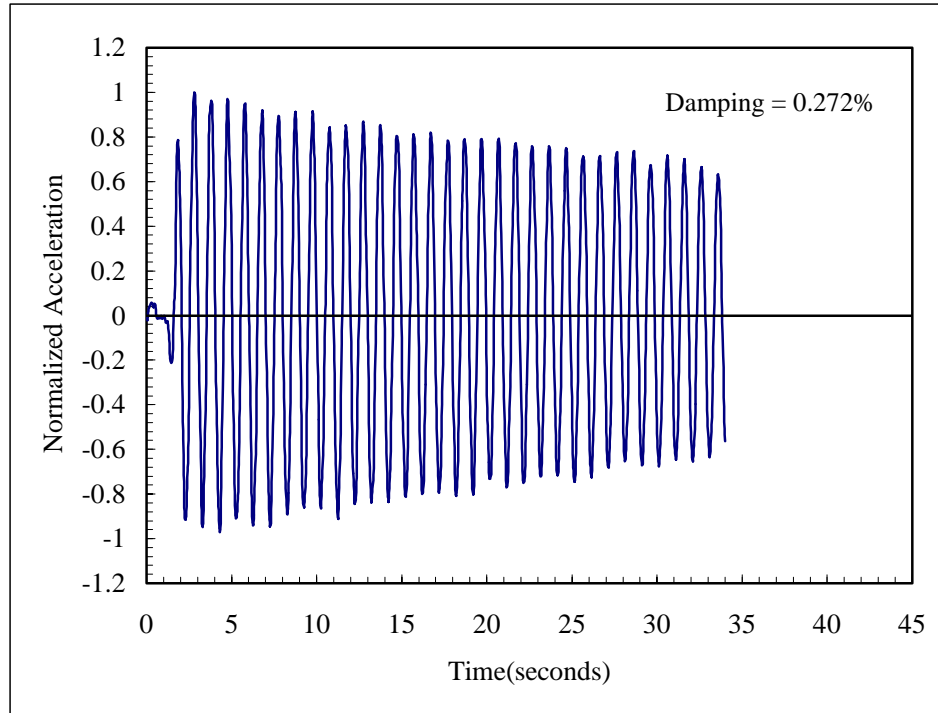


Figure 3.4 - Free Vibration Response of Lab Mast Arm

### 3.5 Review of Kalajian's Dampers and Lab Test Results

The purpose of a damping device is to decrease the number and amplitude of wind-induced oscillation cycles of a mast arm. This will in turn decrease fatigue on the structure, thus extending its life. The challenge in Kalajian's project was to develop a damping device that would work well on all types and lengths of mast arm structures. The target percent critical damping for a device was 5%. All the results given on Kalajian's devices in this section come from tests performed on the lab mast arm at the University of Florida.

### 3.5.1 Damping at the Arm-Pole Connection

Kalajian made two attempts towards damping the lab mast arm at its arm-pole connection. The first attempt was to add Belleville disc springs at the arm-pole connection. This connection consists of four 1.25 in diameter bolts. The springs were conically shaped and made to hold large loads in small space applications by maintaining tension and absorbing pressure in bolted assemblies and between plates. Dimensions of the Belleville disc springs are indicated in Figure 3.5. The springs were made of 1075 high carbon steel and were rated at 1584-1936 lbs. The purpose of the disc springs was to dissipate the energy due to the vibrations of the arm. However, the Belleville disc springs did not prove to be very effective for damping of the system. The vibration response of the lab mast arm with the Belleville disc springs in place is shown in Figure 3.6.

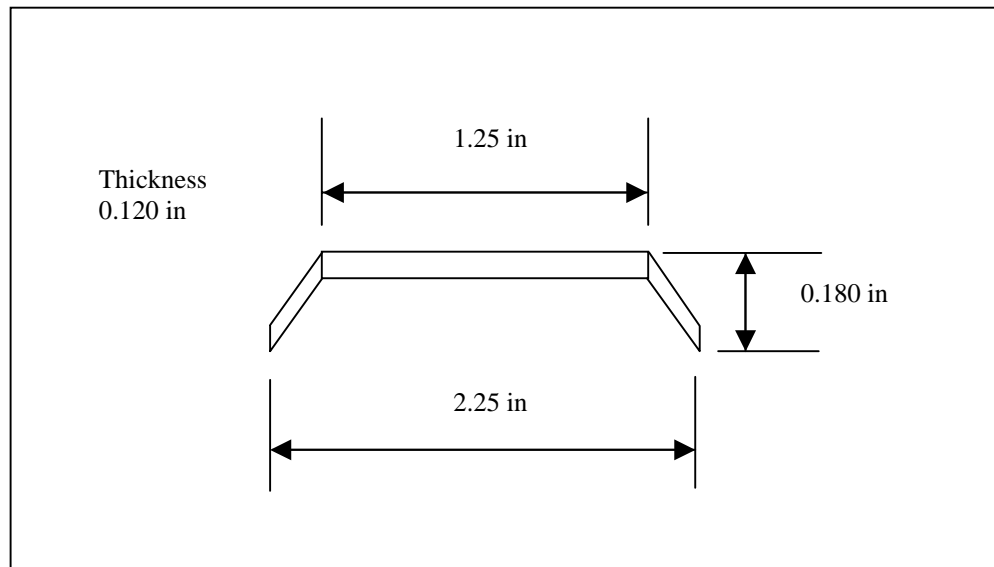


Figure 3.5 - Belleville Disc Spring Dimensions

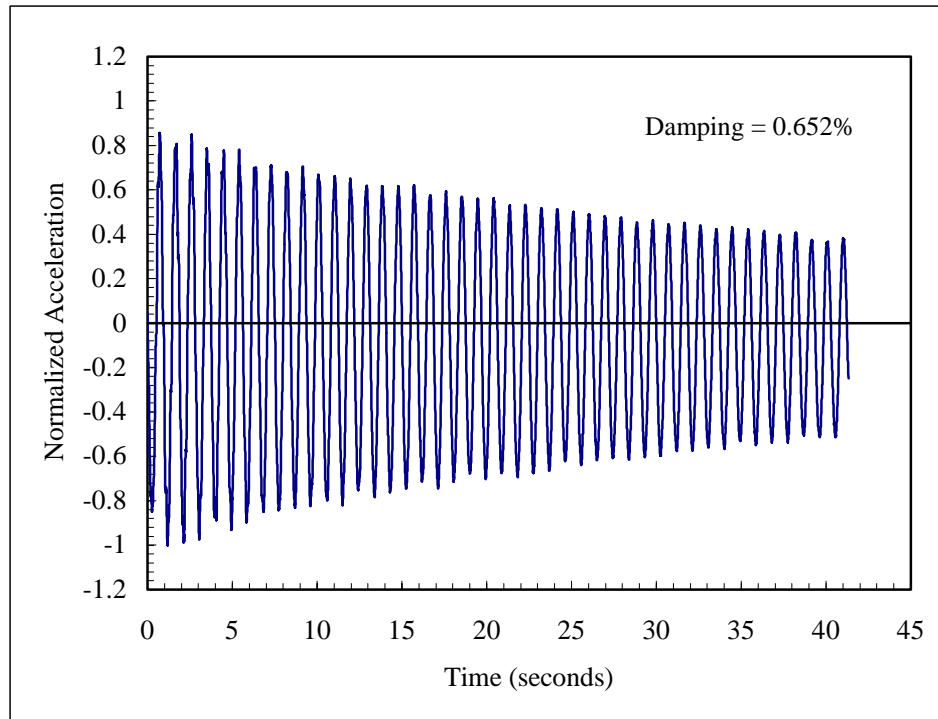


Figure 3.6 - Belleville Disc Springs Vibration Response

The second damping attempt at the arm-pole connection was to add a neoprene pad between the mast and the pole over the entire connection plate. Figure 3.7 shows the dimensions of the pad. Kalajian used a pad thickness of 0.25 in and 0.75 in. The pad was to simulate the characteristics of a spring and absorb the energy of the vibration. By observation, the neoprene pads were ineffective at damping the vertical displacements. Therefore, no data was taken for this test.

Following these two attempts at damping the mast arm at its arm-pole connection, it was determined that vibrations must be dissipated from the tip of the arm.



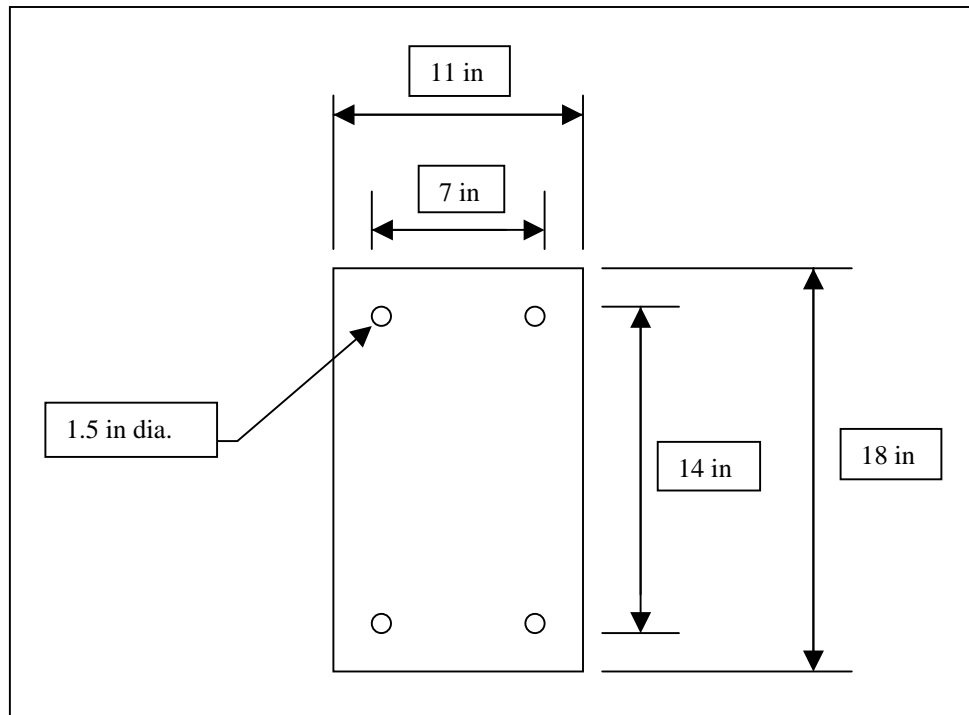


Figure 3.7 - Neoprene Pad Dimensions



Figure 3.8 - Connection where Belleville Disc Springs and Neoprene Pads were installed

### 3.5.2 Stockbridge Type Version Dampers

A Stockbridge damper consists of a flexible rod mounted at the tip of the arm with a mass attached to the tip of the rod. The concept for this device was that energy from the vibrating arm would be transferred through the flexible rod to the mass. Two types of Stockbridge dampers were tested. Figure 3.9 shows the first device made of a windsurfing batten with weights of 1 lb and 1.5 lbs. The second device is pictured in Figure 3.10 and consists of a 14 in long, 0.5 in diameter, cable with a 20 lb mass.



Figure 3.9 - Batten Damper



Figure 3.10 - Stockbridge Version Damper

The batten device would cycle between positive and negative damping, but overall was not effective in mitigating the vibrations. This can be seen in Figure 3.11. The damping presented for the batten damper can be misleading because it was calculated while the batten provided positive damping only. The Stockbridge version device just appeared to go along for the ride when the mast arm was set into a vibration mode. Figure 3.12 shows the response of the Stockbridge version device.

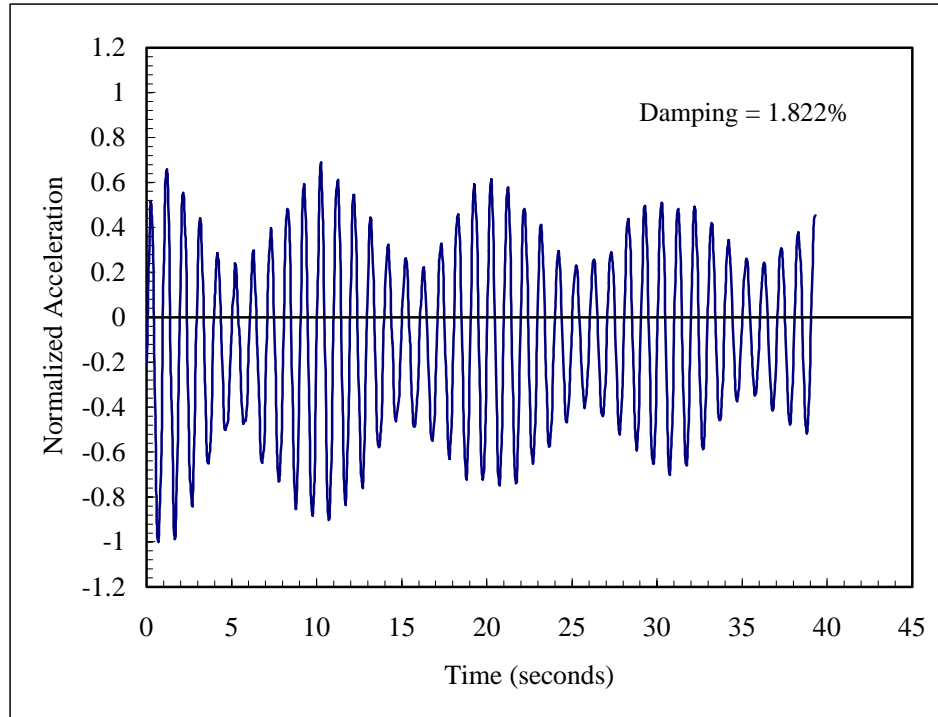


Figure 3.11 - Batten Damper Vibration Response

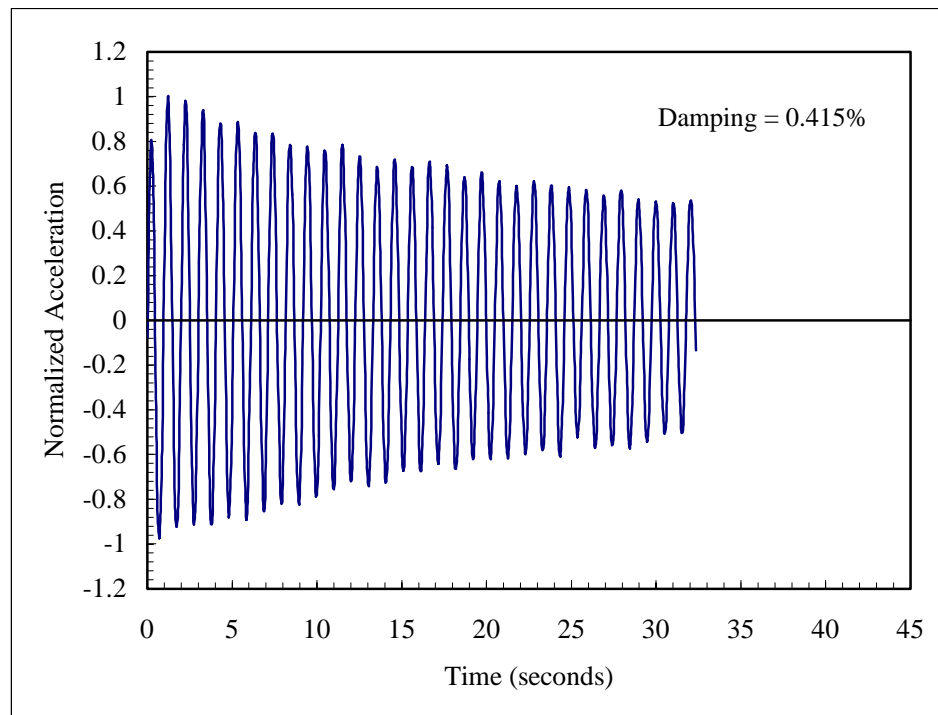


Figure 3.12 - Stockbridge Version Damper Vibration Response

### 3.5.3 Liquid Tuned Dampers

A liquid tuned damper is a device in which movement of a liquid is used to damp the vibrations of a structure. The idea is for the liquid to slosh back and forth and counteract the frequency of the structure and in turn damp out the vibrations. There were two different versions of the liquid damper tested. In each version, water was used as the damping liquid.

The first device was a 4 in-diameter, 20 ft long PVC tube. The device was attached to the traffic light fixtures using hose clamps. The PVC tube was then filled with water by the gallon and tested after the addition of each gallon. The damping increased slightly with the addition of each gallon. However, the overall damping to the structure was minimal. The second device attempted was a u-shaped 3 in-diameter PVC tube. The dimensions of the tube were 24 in long with 16 in tall ends. A u-shaped tube with dimensions of 78 in long with 24 in tall ends was also tested. Like the first device, the damping increased with addition of water, but was never very effective overall. These liquid tuned dampers and their responses can be seen in Figures 3.13, 3.14, and 3.15, 3.16, 3.17, and 3.18.

### 3.5.4 Tuned Mass Damper

A tuned mass damper is a device that matches the natural frequency of the structure and damps its vibrations. The concept behind this device is to use a spring and mass with matching frequency of the structure. There are two properties that can be varied to match the frequency of the structure, stiffness and mass. The relationship between stiffness, mass, and natural frequency is:



Figure 3.13 - 20 ft Long PVC Liquid Damper

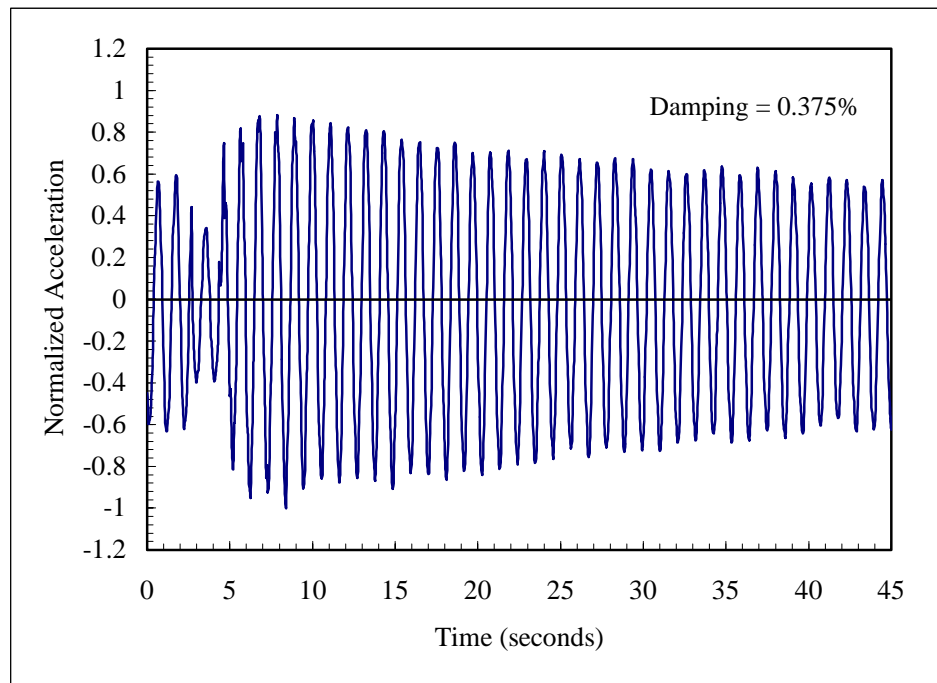


Figure 3.14 - 20 ft Long PVC Liquid Damper Vibration Response



Figure 3.15 - Short U-Tube Liquid Damper

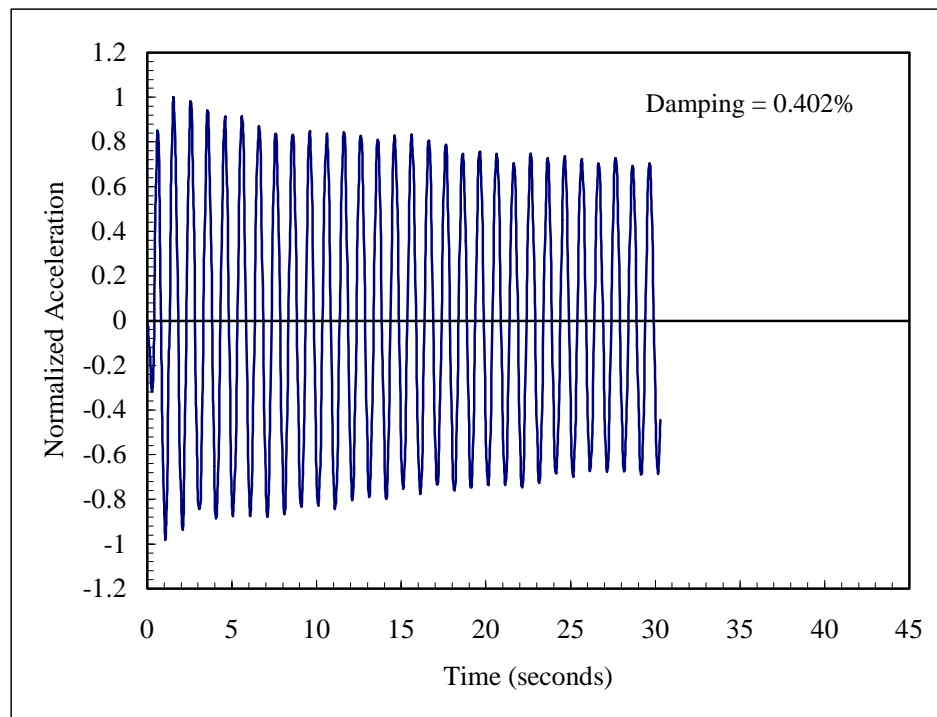


Figure 3.16 - Short U-Tube Liquid Damper Vibration Response



Figure 3.17 - Long U-Tube Liquid Damper

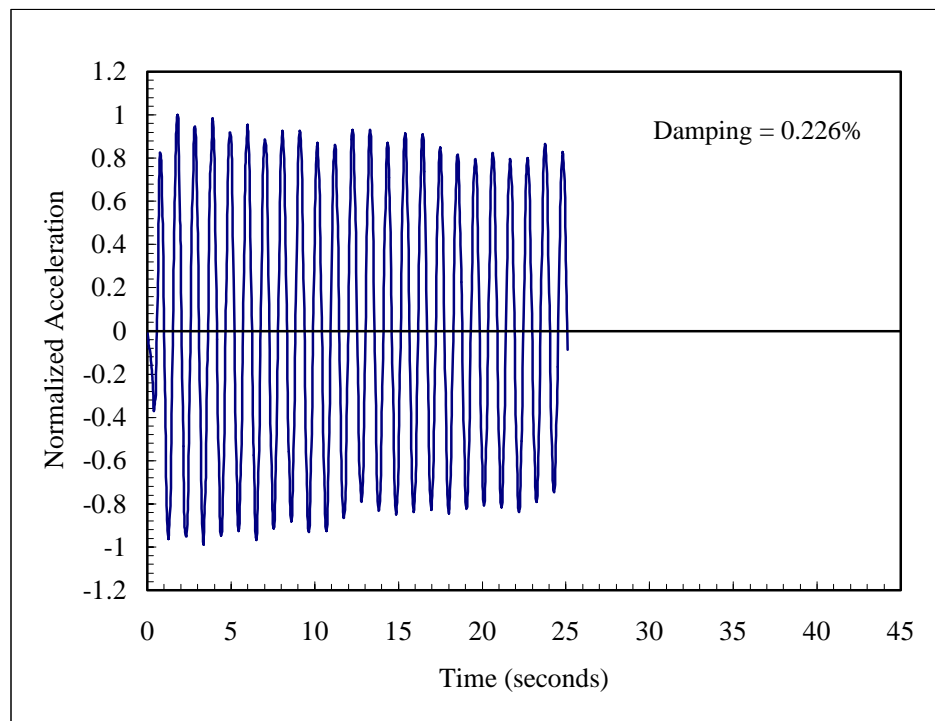


Figure 3.18 - Long U-Tube Liquid Damper Vibration Response

$$f = \frac{1}{2 \cdot \pi} \cdot \sqrt{\frac{k}{m}}$$

where  $f$  is the natural frequency,  $k$  is the stiffness, and  $m$  is the mass. Kalajian's tuned mass damper consisted of a 0.375 in-diameter rod attached to the end of the mast arm with linear ball bearings and a spring attached to the ball bearing case. A mass was then attached to the end of the spring. The stiffness of the spring was 0.7 lb/in and the mass used was 12.5 lbs. Although this spring/mass combination did not exactly match the frequency of the mast arm, it was still very effective at damping the vibrations. Figure 3.19 shows the tuned mass damper device and Figure 3.20 shows its vibration response.

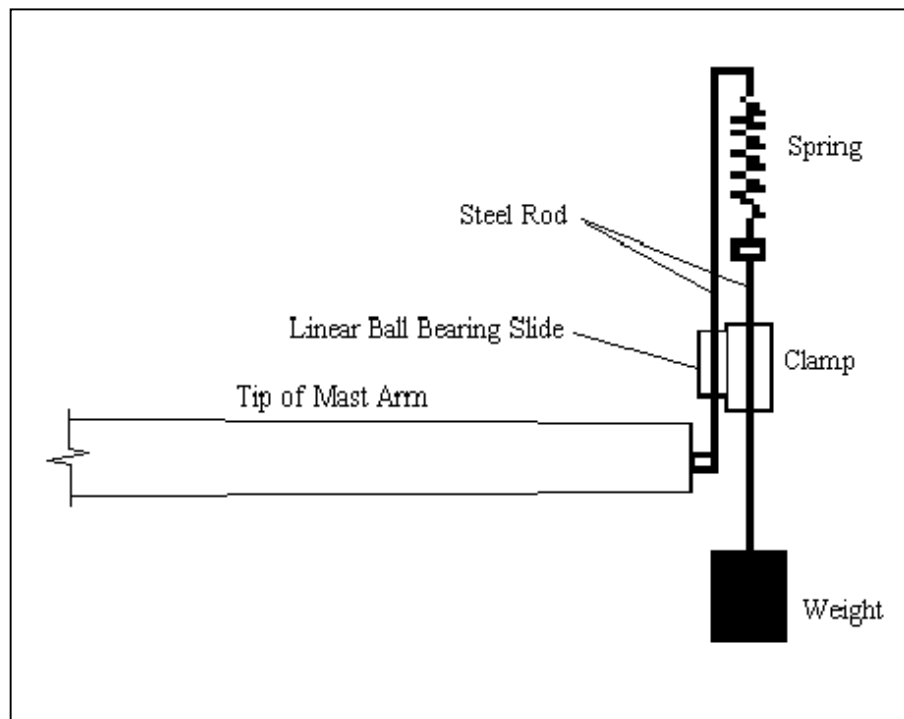


Figure 3.19 - Tuned Mass Damper



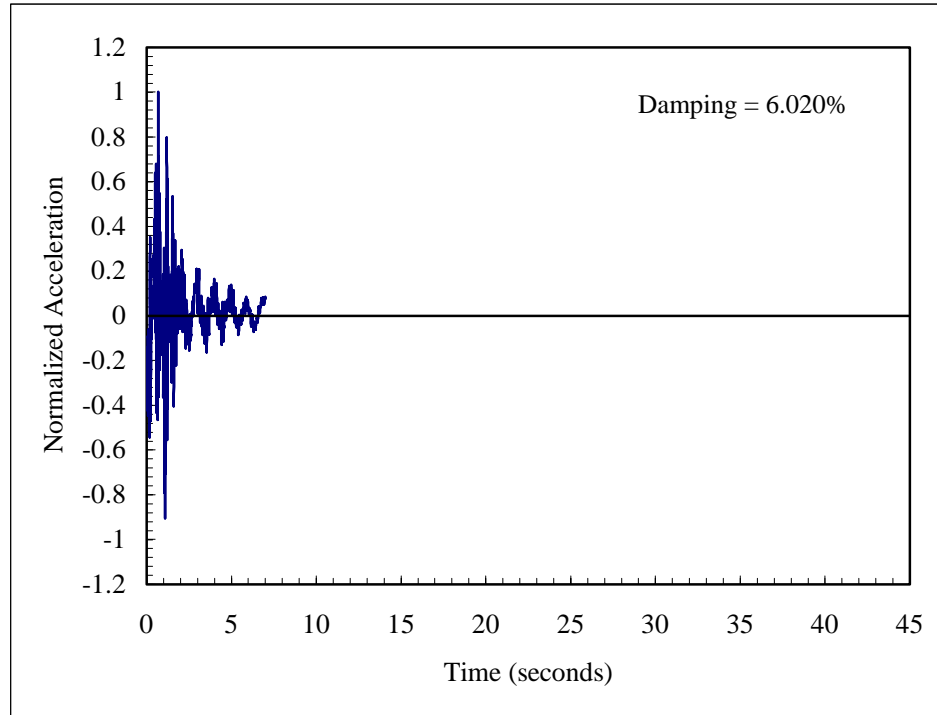


Figure 3.20 - Tuned Mass Damper Vibration Response

The problem with the tuned mass damper is that one damper does not work well on all mast arms. Each damper would have to be modified to match the frequency of the pole it is placed on. This would require adjustments to the spring/mass combination for every mast arm. As a result, this device was not considered to be an acceptable option.

### 3.5.5 Spring/Mass Friction Dampers

The idea behind this type of damping device is to adapt a tuned mass damper to a friction or viscous combination damper. There were many variations of this device tested. Some of the properties varied where diameter and material of device housing, damping liquid, mass shape, and spring type. These devices were composed of a tension spring or bungee cord attached to a mass inside a circular pipe. The mass was just

smaller than the inside diameter of the pipe to create friction between the mass and the sidewalls of the pipe. Each device, although not frequency dependent, still had to have a frequency in the range of 0.5 Hz to 1.5 Hz in order to work of different lengths of mast arms. Each spring/mass friction damper was mounted to the end of the mast arm.

The first spring/mass friction damper contained a 16 lb cylindrical mass with dimensions of 16 in long and 1.875 in diameter. The mass was connected to a bungee cord with a stiffness of 1.0 lb/in. The mass and bungee were assembled inside a 48 in long, 2 in diameter, galvanized pipe. The device was then capped at the top and bottom. This device and its vibration response are pictured in Figure 3.21 and 3.22 respectively.



Figure 3.21 - 2 in Galvanized Pipe, Bungee and Mass Damper

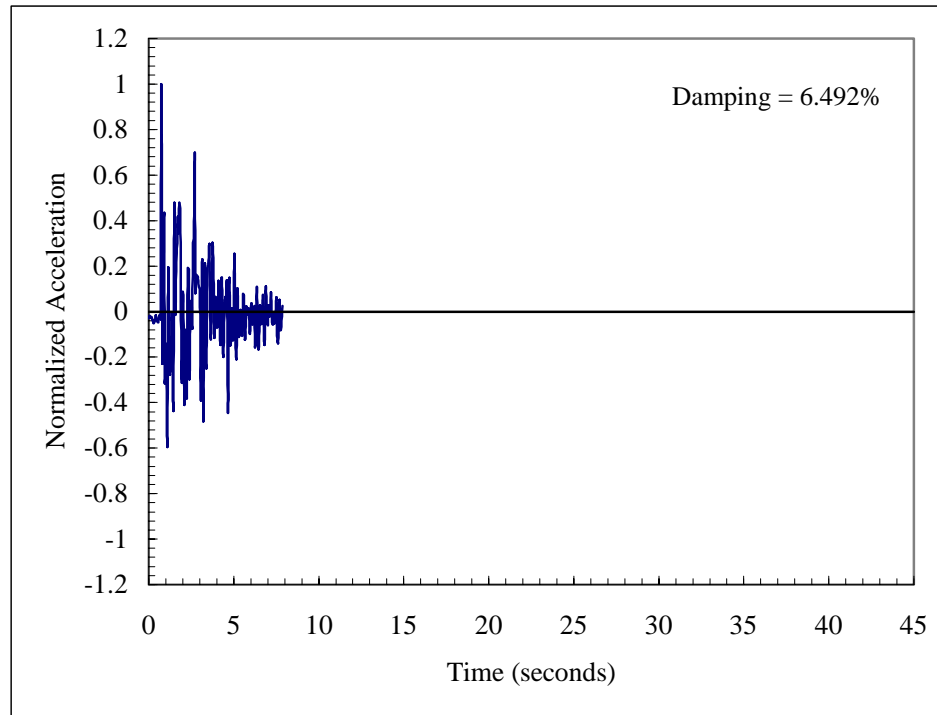


Figure 3.22 - 2 in Galvanized Pipe, Bungee and Mass Damper Vibration Response

A second device was developed with the same dimensions, but was made out of a clear PVC tube. Also, SAE 10w30 oil was added to allow a one-inch gap between the mass and oil. This was done so small displacements of the mass would impact the oil and damp quickly. This device was not as effective as the previous galvanized device. This device and its vibration response can be seen in Figures 3.23 and 3.24 respectively.

There were concerns about the long-term effects of a bungee cord, so a third device containing a spring was created. This device was composed of a tension spring with a stiffness of 1.4 lb/in, a mass of 16 lbs, and a 4 in-diameter PVC tube housing at 36 in long. The device was capped on both ends and also filled with oil to about one-inch from the bottom of the mass. This device proved to be as effective as the one with the bungee chord. The device is pictured in Figure 3.25 with its response in Figure 3.26.



Figure 3.23 - 2 in PVC Pipe, Bungee and Mass Damper with Oil

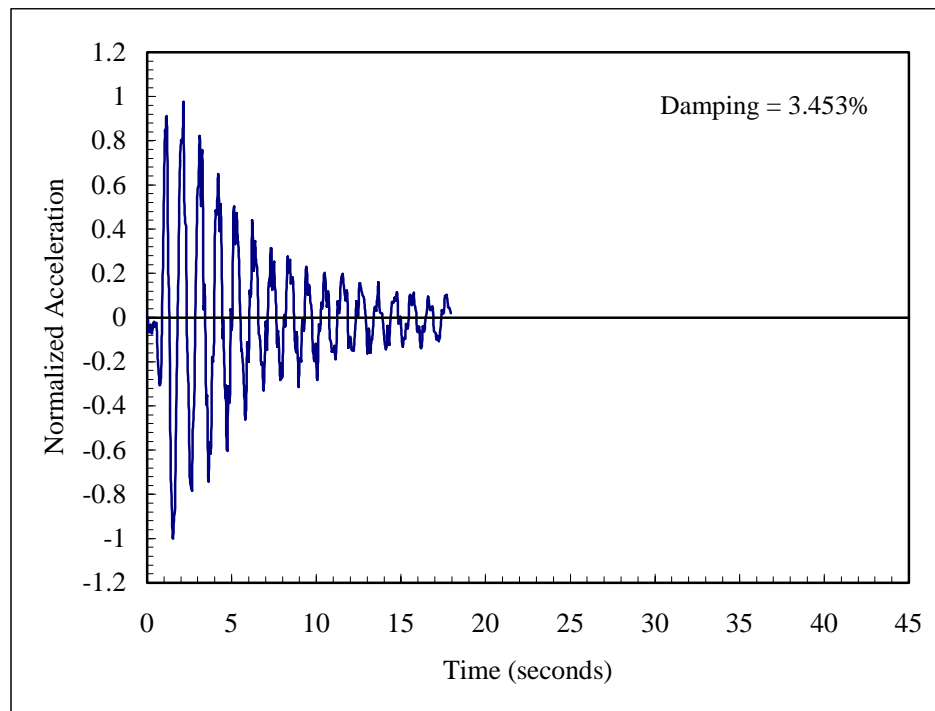


Figure 3.24 - 2 in PVC Pipe, Bungee and Mass Damper with Oil  
Vibration Response



Figure 3.25 - 4 in PVC Pipe, Spring and Mass Damper with Oil

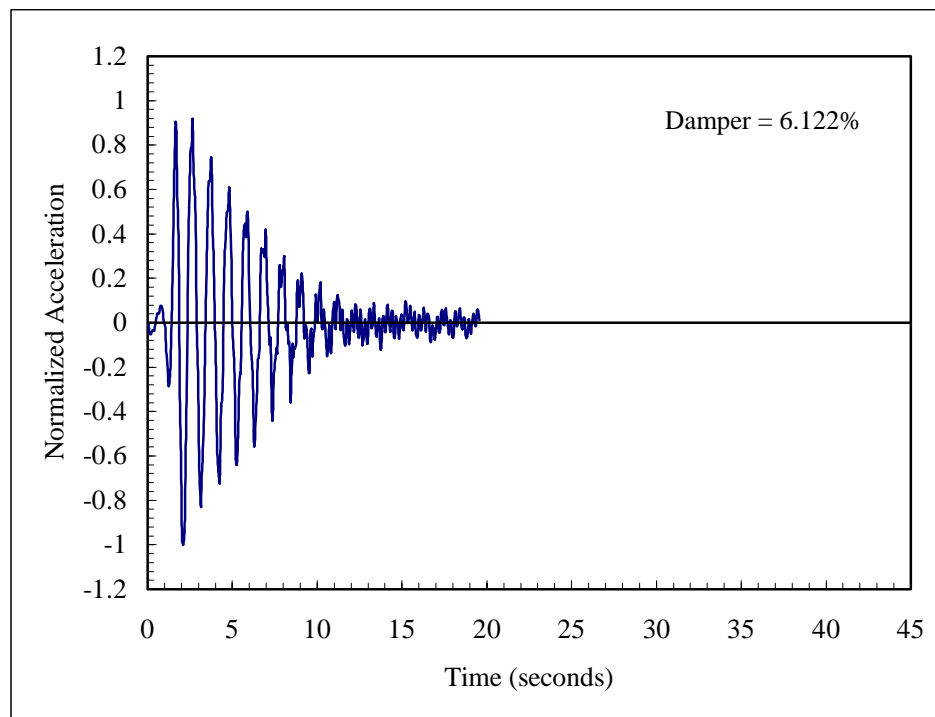


Figure 3.26 - 4 in PVC Pipe, Spring and Mass Damper with Oil  
Vibration Response

In an attempt to shorten all of the previously mentioned devices, compression springs were considered. The compression spring device contained three compression springs attached to a bottom plate with rods attached to the bottom plate and passing through linear ball bearings attached to the top plate. A 12 lb mass was added to the top plate. The springs that were used were 2.25 in diameter, 8 in long, and had spring stiffness values of 1.0 lb/in. The device housing was an 18 in long, 8 in diameter, clear PVC pipe. The bottom plate of the device was placed on a ring mounted inside the PVC just above the cap level. This device did not appear to be very effective in damping out the vibrations. The problem appeared to be that the mass was not getting enough acceleration in the device housing and therefore not enough motion to damp the vibrations. Figures 3.27 and 3.28 show the compression spring device and its vibration response respectively.

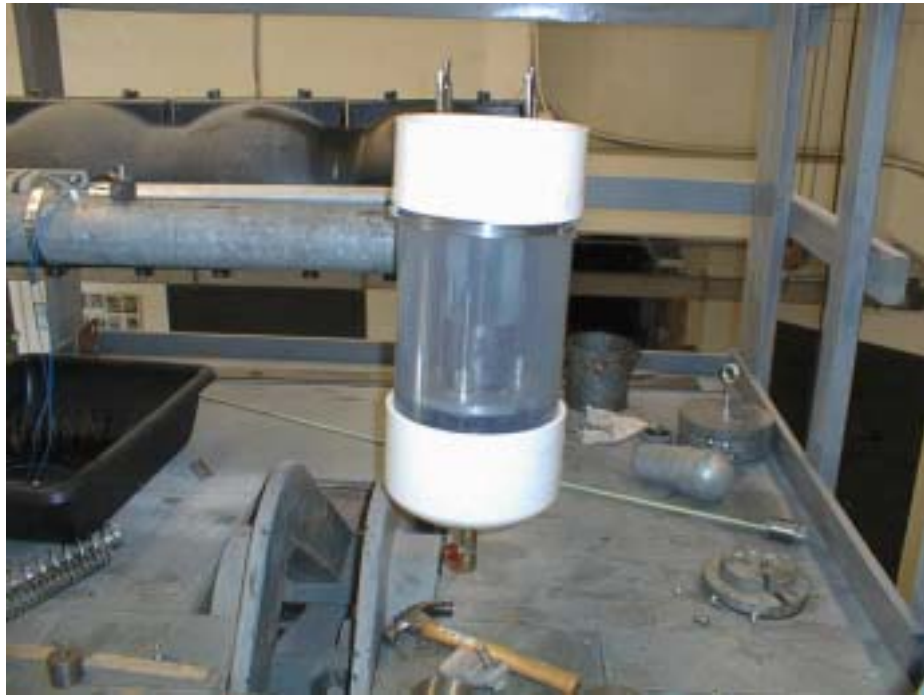


Figure 3.27 - Compression Spring Damper

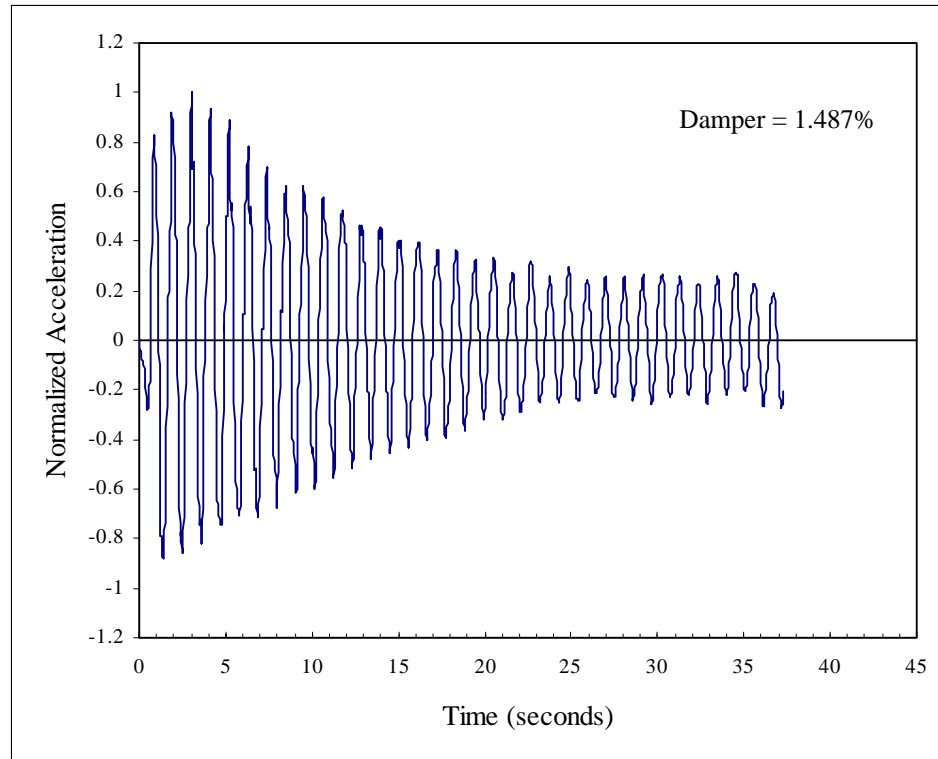


Figure 3.28 - Compression Spring Damper Vibration Response

### 3.5.6 Spring/Mass Impact Friction Dampers

The first spring/mass impact friction device was a combination of the previous tension spring and compression spring devices. A tension spring with a stiffness of 1.4 lb/in was attached to a 12 lb mass and then to a PVC cap. The compression spring device was mounted in the bottom of the device housing with three springs with a stiffness of 1.0 lbs/in each and a mass of 6 lbs. When this device was first created, an 8 in coupling was used to extend the clear PVC so that the characteristics of the damping device could be observed. This can be seen in Figure 3.29. The coupling left a gap between the two pieces of PVC where the tension spring mass would get hung up in the gap for a second. The hang-up caused the device to work exceptionally well. This can be seen in Figure

3.30. The problem with the device was its size. It needed to be scaled down so that it would not be as noticeable to passing motorists.



Figure 3.29 - Tension Spring/Mass Binding on Joint Damper

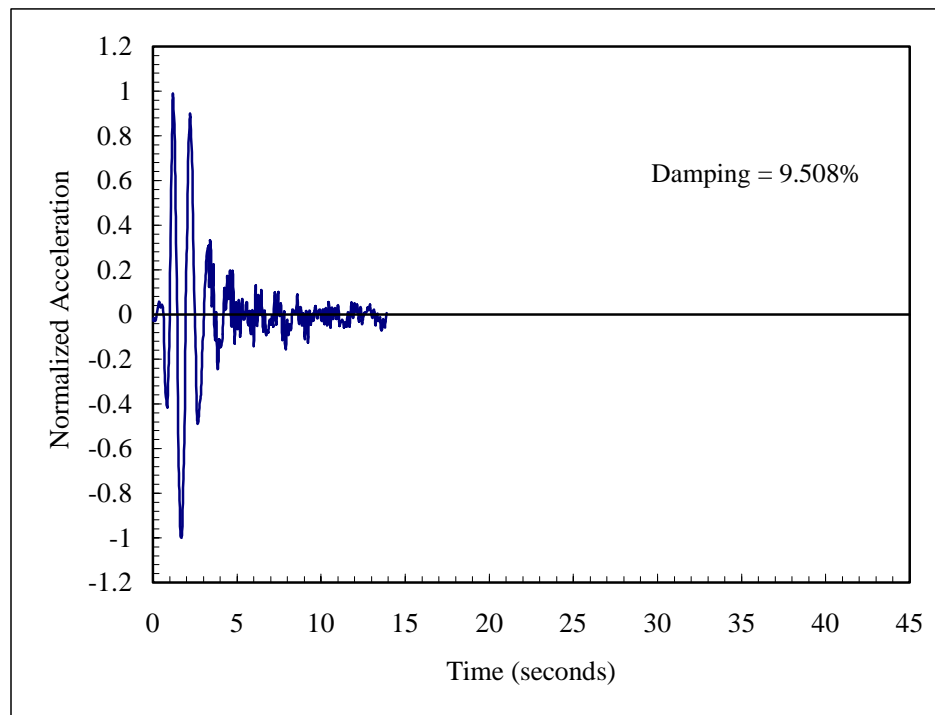


Figure 3.30 - Tension Spring/Mass Binding on Joint Damper  
Vibration Response



The next device was a smaller version of the mass binding on the joint in the walls of the housing. The device consisted of a tension spring with a stiffness of 1.4 lb/in and a 16 lb mass with a 1.875 in diameter. The housing was a 30 in long piece of 3 in PVC pipe that was reduced to a 16 in long piece of 2 in PVC pipe. The concept was for the mass to bang into the reducer and disrupt the vibrations of the arm. The device proved to be effective in mitigating the vibrations, but it was still thought to be too long at 46 in total height. This device is pictured in Figure 3.31 with its response in Figure 3.32.



Figure 3.31 - 3 in to 2 in Tapered Spring/Mass Impact Damper

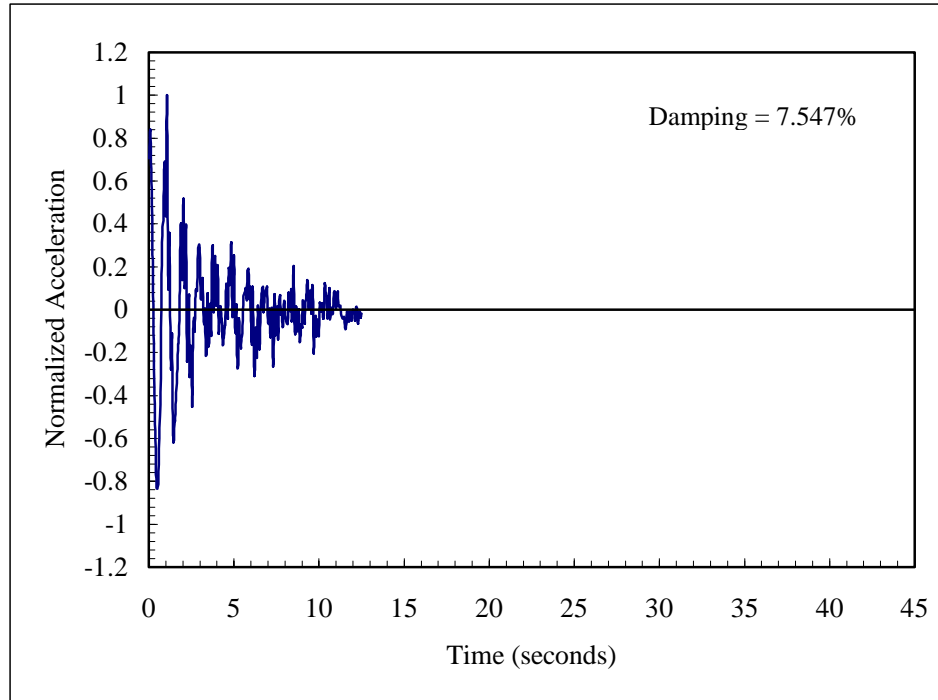


Figure 3.32 - 3 in to 2 in tapered Spring/Mass Impact Damper  
Vibration Response

Two smaller variations of the tapered device were then built. The first was a 4 in PVC pipe tapered to a 3 in PVC pipe with a reducer. The spring stiffness was 1.4 lb/in with a mass weighing 12 lbs. The mass was 3 in diameter so that it would barely fit into the reducer. The total length of this device was 25 in. The second smaller tapered device built used a 4 in to 2 in reduced housing. The spring constant was 1.4 lb/in with a mass weighing 15 lbs. The devices total length was 27 in. Both of these smaller devices are pictured in Figures 3.33 and 3.34 respectively. Their vibration responses can be seen in Figures 3.35 and 3.36.



Figure 3.33 - 4 in to 3 in Tapered Spring/Mass Impact Damper



Figure 3.34 - 4 in to 2 in Tapered Spring/Mass Impact Damper

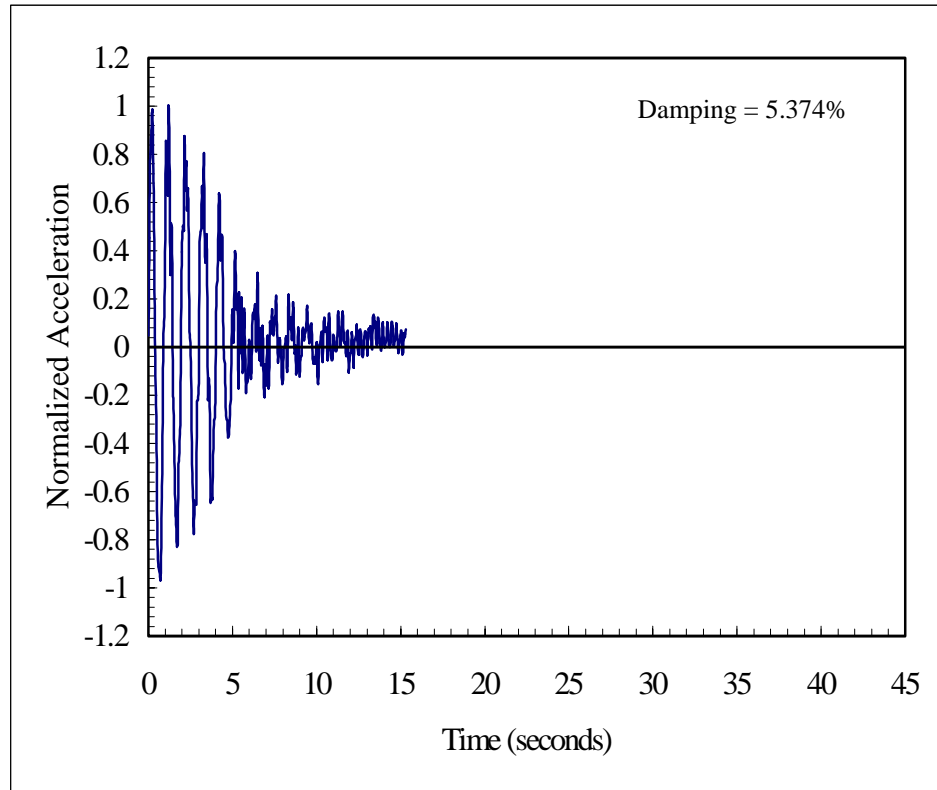


Figure 3.35 - 4 in to 3 in Tapered Spring/Mass Impact Damper

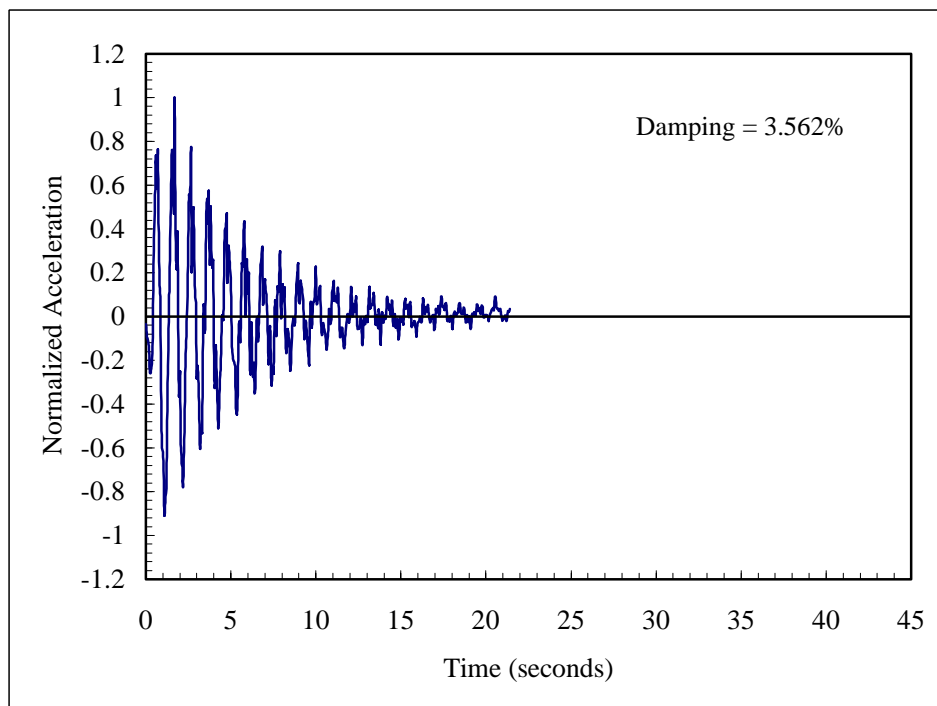


Figure 3.36 - 4 in to 2 in Tapered Spring/Mass Impact Damper Vibration Response

### 3.5.7 Woodpecker Damper

The woodpecker device involved a mass banging on the top of the pole with a compression spring used to create motion. A 0.375 in diameter stainless steel rod was attached to the pole with a bearing so that it could pivot freely. The rod used was 36 in long with a 12 lb mass attached to the end and a compression spring with a stiffness of 4.5 lb/in located at the  $\frac{3}{4}$  point of the span. A PVC collar was placed around the spring so that the spring would not buckle. This device was not effective in mitigating the vibrations. The woodpecker device is shown in Figure 3.37 and its vibration response is shown in Figure 3.38.



Figure 3.37 - Woodpecker Damper

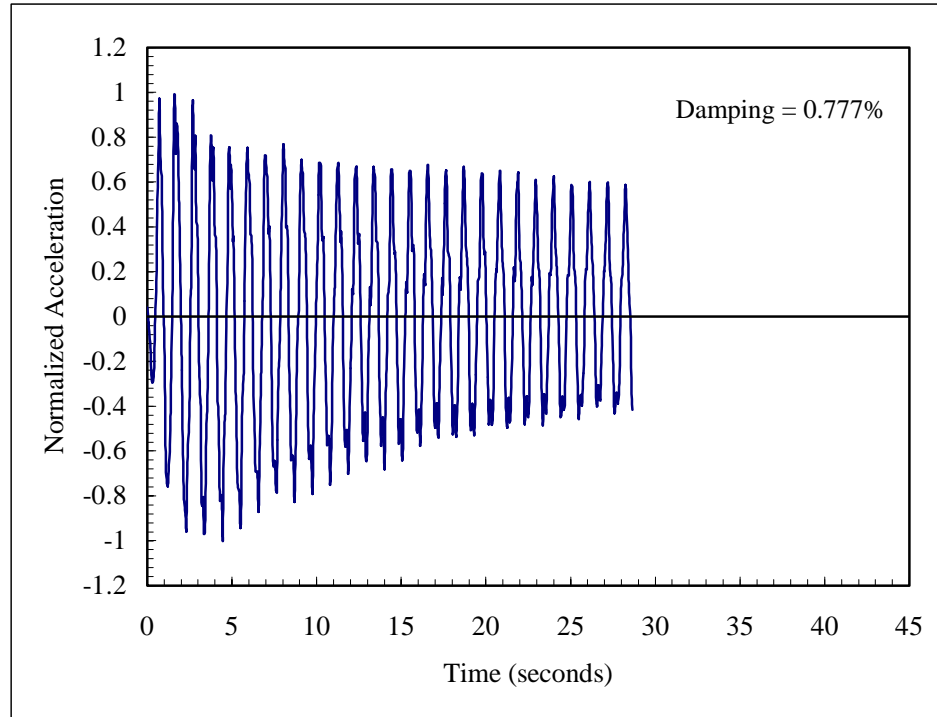


Figure 3.38 - Woodpecker Damper Vibration Response

### 3.5.8 Summary of Kalajian's Dampers

Table 3.1 contains schematic drawings of each of Kalajian's devices. The lab mast arm testing results of those devices are also provided in the table. The chosen device, as will be determined in Section 3.6, has been shaded.

### 3.6 Field Testing of Damping Devices

The objective of the field-testing was to check the damping characteristics of a variety of different poles with five of the effective devices developed in the lab. The lengths of the mast arms tested in the field were 36 ft, 40 ft, 68 ft, and 70 ft. They were located at the intersection of SW 34<sup>th</sup> St. and SW 47<sup>th</sup> Ave. in Gainesville, Florida. The

Table 3.1 - Summary of Kalajian's Dampers

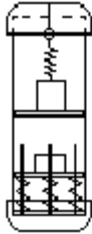
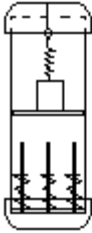
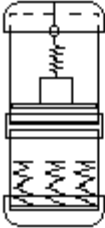


Device	Device Diagram	% Critical Damping
Tuned Mass Damper	N/A	8.71
8" PVC with Tension Mass(12lb) Banging on Compression Mass (5lb) Device Rods (10" from top of mass to top of PVC cap)		6.79
8" PVC with Tension Mass(12lb) Banging on Compression Mass (5lb) Device Rods (13-1/2" from top of mass to top of PVC cap)		5.21
8" PVC with Tension Mass(12lb) Banging on Compression Device Rods No Compression Mass (13-1/2" from top of mass to top of PVC cap)		5.02
8" PVC with Mass (12lb) Binding on Sidewalls at Joint		9.51
8" PVC Compression Springs with Mass (12lb)		1.49
4" PVC Spring/Mass/Friction Damper with Oil		6.12

Table 3.1 - continued


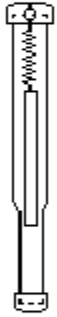

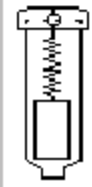
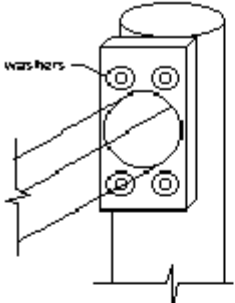
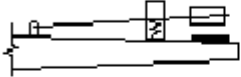

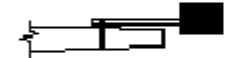
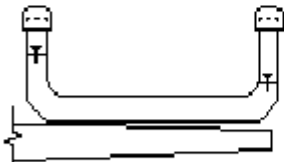
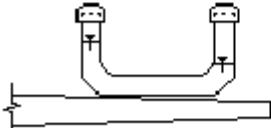
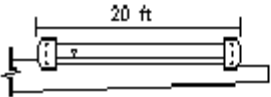
Device	Device Diagram	% Critical Damping
2" Galvanized Tube with Bungee/Mass without Oil		6.49
2" PVC Tube with Bungee/Mass and Oil		3.45
PVC Taper Damper 3" to 2" with Mass and Spring		7.55
PVC Taper Damper 4" to 3" with Spring Embedded in 12.5 lb Mass		5.37
PVC Taper Damper 4" to 2" with Spring and 15 lb Mass (Optimal Device)		3.56
Steel Taper Damper 4" to 2" with Spring and 15 lb Mass (Optimal Device)		4.01



Table 3.1 - continued

Device	Device Diagram	% Critical Damping
Belleville Disc Springs	 <p>The diagram shows a vertical cylindrical component with four circular openings on its front face, arranged in a 2x2 grid. Two lines labeled 'washers' point to the top two openings. The component is mounted on a base with a vertical line extending downwards.</p>	0.65
Woodpecker Damper	 <p>The diagram shows a horizontal assembly with a central rectangular block and a smaller block to its right, connected by a thin rod. The assembly is mounted on a base with a vertical line extending downwards.</p>	0.78
Green Batten with Mass (damps but then excites again)	 <p>The diagram shows a horizontal assembly with a central rectangular block and a larger, solid black rectangular mass to its right, connected by a thin rod. The assembly is mounted on a base with a vertical line extending downwards.</p>	1.82
Stockbridge 12" long cable and Mass	 <p>The diagram shows a horizontal assembly with a central rectangular block and a larger, solid black rectangular mass to its right, connected by a thin rod. The assembly is mounted on a base with a vertical line extending downwards.</p>	0.42
Liquid Tuned Damper LONG- U-shaped Water Tube 3" PVC (78" long bottom tube 24" high)	 <p>The diagram shows a U-shaped tube with two vertical legs. The bottom horizontal section is longer than the vertical legs. The tube is mounted on a base with a vertical line extending downwards.</p>	0.23
Liquid Tuned Damper SHORT-U-shaped Water Tube 3" PVC (24" long bottom tube 16" high)	 <p>The diagram shows a U-shaped tube with two vertical legs. The bottom horizontal section is shorter than the vertical legs. The tube is mounted on a base with a vertical line extending downwards.</p>	0.40
Liquid Tuned Damper 20 ft Water Tube 3" PVC (1,5,10 gallons)	 <p>The diagram shows a long horizontal tube with two vertical legs at each end. A dimension line above the tube indicates a length of 20 ft. The tube is mounted on a base with a vertical line extending downwards.</p>	0.38

mast arms were accessed using a lift truck from Gainesville Regional Utilities. The accelerometers were attached to the tips of the arms with wax, similar to the lab testing, and then connected to the computer. Each mast arm and device combination was given a small, medium, and large displacement in the vertical direction and allowed to oscillate. This was done to determine if the magnitude of the displacement had an effect on the damping of the arm. After the field tests were completed, the data was analyzed and the percent critical damping was calculated for each device on each mast arm tested. The results of the lab and field-testing are compared below in Tables 3.2 and 3.3.

Table 3.2 - Mast Arm Frequency Results for Lab and Field Testing

Frequency (Hz)				
36ft Pole	40ft Pole	68ft Pole	70ft Pole	Lab Pole
1.198	1.149	0.719	0.71	0.94

Table 3.3 - Percent Critical Damping Results for Lab and Field Testing

Device	Critical Damping				
	36ft Pole	40ft Pole	68ft Pole	70ft Pole	Lab Pole
Free Vibration	0.279%	0.181%	0.356%	0.620%	0.272%
2in PVC Pipe, Bungee and Mass Damper with Oil	2.176%	1.128%	1.226%	NA	3.453%
4in PVC Pipe, Spring and Mass Damper with Oil	1.717%	1.277%	1.355%	NA	6.122%
3in to 2in Tapered Spring/Mass Impact Damper	2.972%	NA	NA	0.790%	7.547%
4in to 3in Tapered Spring/Mass Impact Damper	2.946%	NA	NA	2.422%	5.374%
4in to 2in Tapered Spring/Mass Impact Damper	3.575%	NA	NA	2.835%	3.562%

### 3.7 Conclusion

The device Kalajian chose to be the most suitable in damping the vibrations of the various lengths of mast arms was the 4 in to 2 in Tapered Spring/Mass Impact Damper. This device was selected because it produced a consistent percent critical damping on each pole tested (approximately 3%). It was also reported to have 1.1% critical damping, in the horizontal direction, for the lab mast arm. Kalajian finished his project by constructing a steel prototype of his selected device. Steel was used so the device would be able to withstand outdoor conditions. The device was also galvanized to prevent rusting and corrosion.

The purpose of the research presented in this report was to extend the research performed by Kalajian. The goals of this extension were as follows:

1. Determine why Kalajian's device was effective and further its development.
2. Try to improve both the vertical and horizontal damping.
3. Simulate wind-induced vibrations during the testing of dampers.
4. Select a final device and observe its performance on a mast arm known for its susceptibility to wind-induced vibrations.
5. Develop a specification for the final damping device design and implementation.

The remaining chapters of this report contain the procedures and results for obtaining these goals.

CHAPTER 4  
DATA ACQUISITION AND INSTRUMENTATION

4.1 Data Required

For each mast arm tested, it was necessary to obtain displacement data in both the vertical and horizontal direction. This not only demonstrates how much the mast arm is moving, but can also be used to calculate the structures' natural frequency, and percent critical damping. Field-testing took place in Tampa, Florida, that also needed data for the wind force and direction as it acted on the mast arm structure.

4.2 Data Acquisition

A laptop computer equipped with a PCMCIA data acquisition card was used to record the mast arm tests. The program used to record the data was Virtual Bench 1.0, by National Instruments. The data acquisition systems components were as follows:

Computer:	Micron 166 MHz Pentium processor 48MB EDO DRAM 2 type-II PCMCIA slots
Data Acquisition Card:	National Instruments DAQ
Connecting Components:	68-pin shielded terminal block 68-wire cable (3 ft. long)
Software:	National Instruments NIDAQ data acquisition drivers

### 4.3 Displacement Instrumentation

Use of a Wire-LVDT (Linear Variable Differential Transducer) was initially considered for measuring displacements at the tip of the mast arm structures (See Figure 4.1). The LVDT is accurate to the nearest thousandth of an inch. Although it would produce extremely precise measurements, the sensor had many drawbacks when being applied to a mast arm.



Figure 4.1 - Wire-LVDT

Mast arm structures can move up to twelve inches vertically or horizontally from their at rest positions. Transducers would need to be located both below and to the side of the cantilever's tip. Also, the instruments would have to be held completely fixed with respect to the moving mast arm structure. Constructing a base for the LVDT devices to

mount to was not practical for field-testing. However, a wire-LVDT was used in the lab for calibration purposes on other sensors.

The second attempt for measuring displacements was to attach an inclinometer at the tip of the mast arm (See Figure 4.2). The angle of rotation at the tip of the cantilever would be used to back calculate its displacement at that point. A liquid-capacitive based inclinometer and a pendulous-mass based inclinometer were both tested on the lab mast arm.



Figure 4.2 - Inclinometer attached to tip of lab mast arm

A Wire-LVDT was fixed with respect to the structure and also attached to the tip of the mast arm, as seen in Figure 4.1. The LVDT was used to verify the calculated displacements from the inclinometer data. Displacements matched very well under static loading of the mast arm. However, the displacement results from the LVDT and inclinometer differed when the pole was put into free vibration. This discrepancy was

due to the inclinometer's inability to respond quickly enough to the mast arms oscillations. Since both inclinometers were gravity based, they were not able to measure the horizontal displacements of the mast arm either.

Finally, PCB brand general-purpose piezo-electric accelerometers were selected to calculate the displacements at the tip of the cantilever. The acceleration data was integrated twice to calculate the mast arms' displacements. Accelerometers are accurate, portable, and can be attached in almost any orientation with wax. This was ideal for both lab and field-testing. Two accelerometers were attached to a tri-axial mounting block and fixed to the mast arms with wax. The two sensors were oriented such that one would measure a pole's vertical motion and the other would measure its horizontal motion. Figure 4.3 shows the accelerometers on the lab mast arm.



Figure 4.3 - Accelerometers attached to tip of lab mast arm

#### 4.4 Calibration of Accelerometers

The accelerometers were connected to their own power supply units with wires. The power supplies were located at the data acquisition area. Originally, the accelerometer output went directly to the data acquisition where it was recorded. However, the accelerometers were so sensitive that the high frequency impact of the dampers caused the signal to be unrecognizable. So, a unity-gain second-order low-pass filter, built by David P. Arnold, was added in line between the power supply unit and the data acquisition. Figure 4.4 shows the power supplies and the filter.



Figure 4.4 - Accelerometer Power Supplies and Filter

The filter removed all frequencies above 4.7 Hz, allowing for a cleaner and more accurate signal to be recorded. For comparison, two accelerometers were placed on the mast arm tip, side by side, and in the vertical direction. One accelerometer went through the filter before going to the data acquisition, while the other one was connected directly to the data acquisition. The pole was given an initial displacement in the vertical direction with



a damping device attached. Figures 4.5 and 4.6 are graphs displaying the normalized acceleration vs. time of the filtered and non-filtered acceleration data respectively.

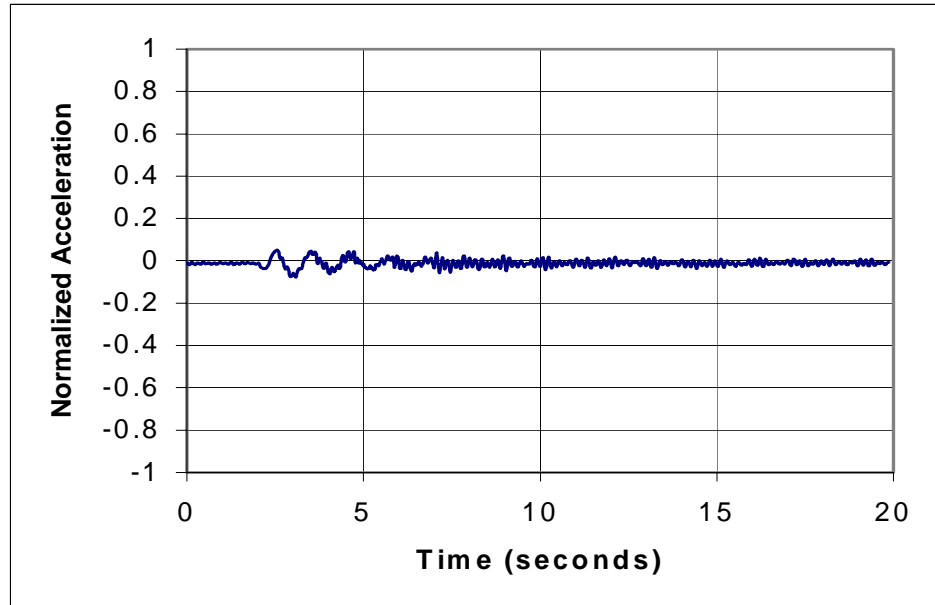


Figure 4.5 - Filtered Acceleration Data

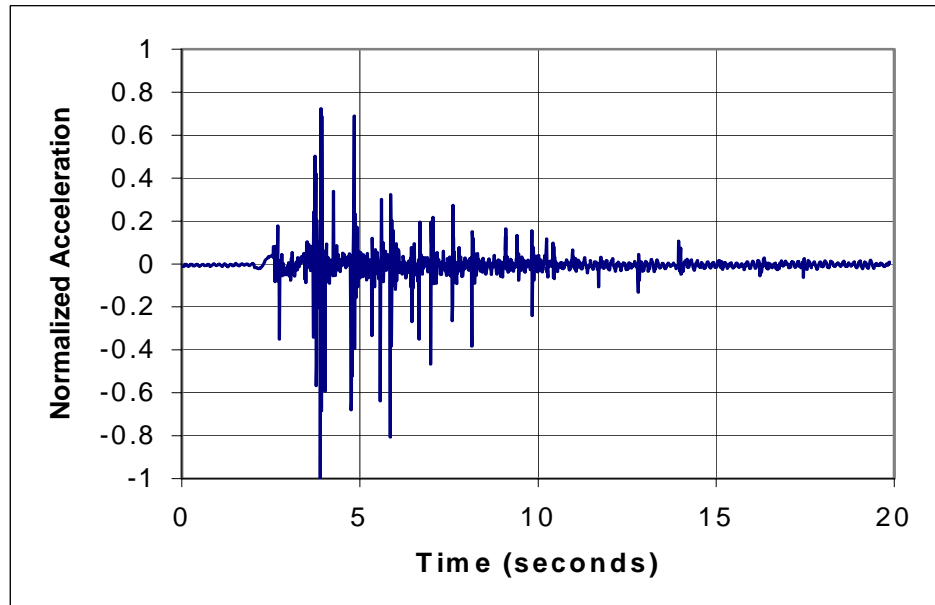


Figure 4.6 - Non-Filtered Acceleration Data

A wire-LVDT, as in Figure 4.1, was once again fixed relative to the mast arm and attached to the tip at the same location of the accelerometers. The LVDT displacements were used to compare the displacements calculated from the acceleration data. Once a set of acceleration data was recorded, it was integrated twice with the trapezoidal rule to obtain displacements. However, the acceleration data still contained some noise (higher frequencies), thus causing the calculated displacement data to blow up. Two steps were necessary in order to solve this problem. First, a Fast Fourier Transform (FFT) was performed on the acceleration data before it was integrated and all frequencies above the natural frequency of the structure were removed mathematically. Sample graphs of the acceleration data before and after the FFT filtering can be seen in Figures 4.7 and 4.8 respectively. Next, a centering function, written by Dr. Gary Consolazio, was applied to both the velocity and displacement data following each integral. Figures 4.9 and 4.10 show the effects of the displacement data blowing up and the application of the centering function to that data respectively. Once properly filtered, centered, and integrated, the acceleration data produced displacements within 1/2 in of the LVDT displacements. It is important to note that this 1/2 in discrepancy was due to the intense banging of the damping device, and was a worst-case error. A large majority of the tests had displacement discrepancies, between the acceleration data and LVDT data, well below 1/10 in consistently. The LVDT and accelerometer-calculated displacement data for the free vibrations without dampers were identical. Therefore, the accelerometers were determined to be reliable sensors for acquiring displacements of the tested mast arms. The MathCad worksheet used to manipulate all the recorded data, including the wind data in the next section, is located in Appendix A.

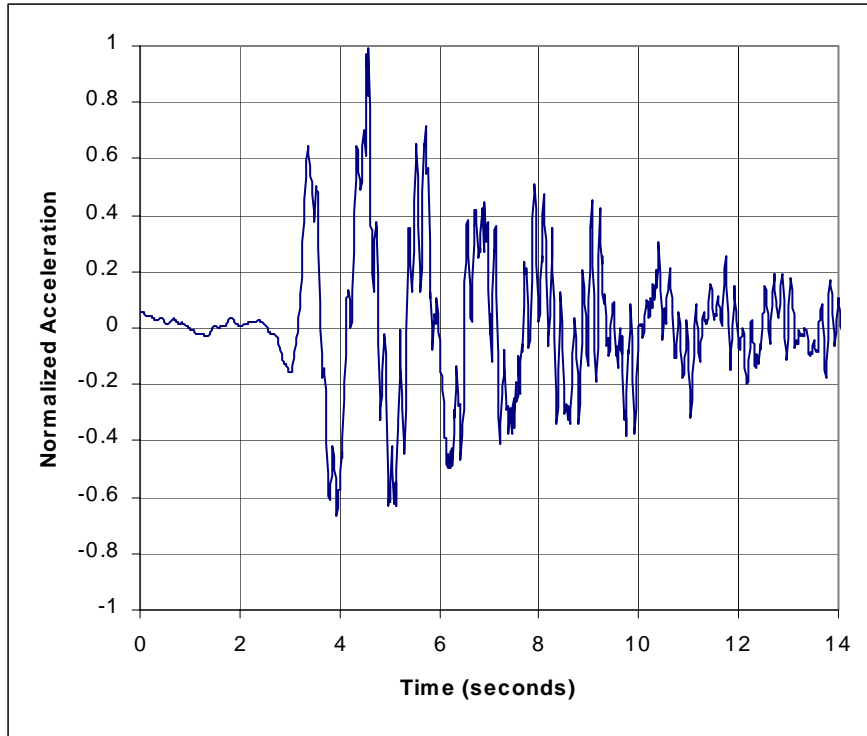


Figure 4.7 - Acceleration Data Before FFT Filtering

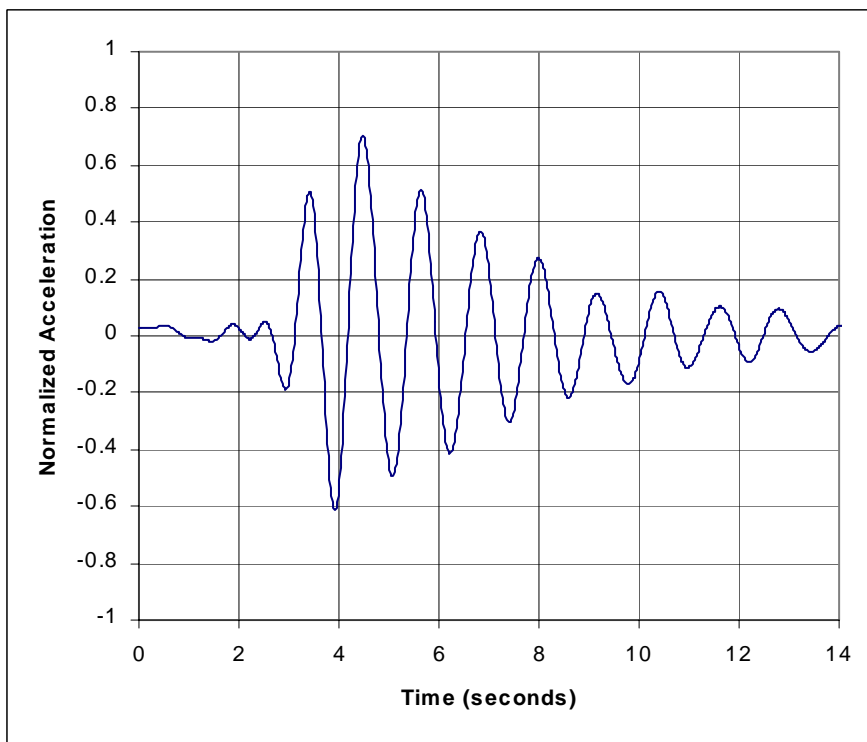


Figure 4.8 - Acceleration Data After FFT Filtering

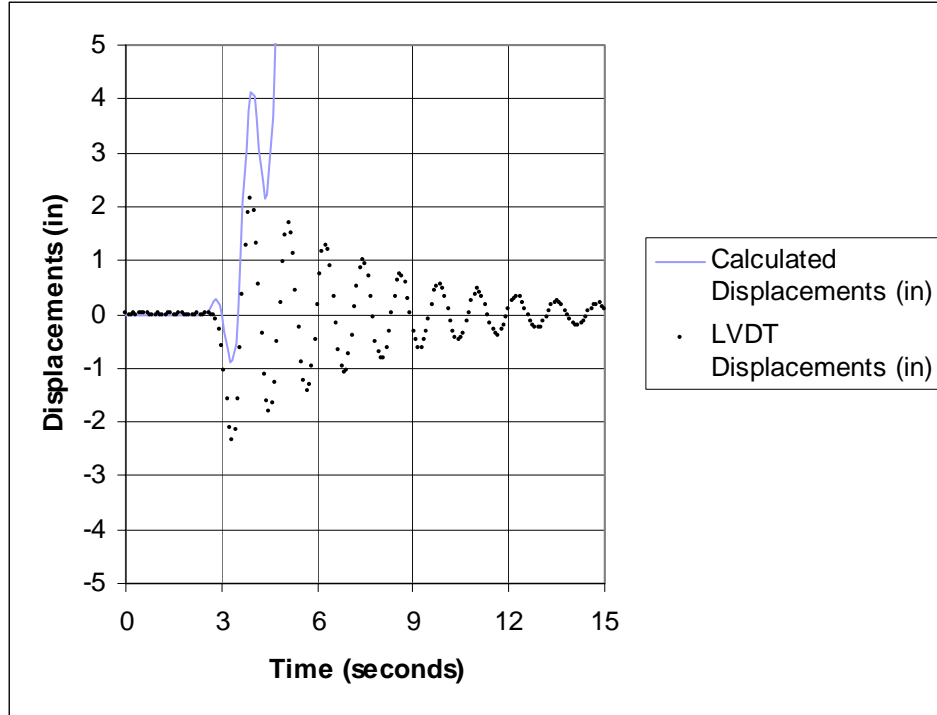


Figure 4.9 - Displacement Data Comparison without utilizing the Centering Function

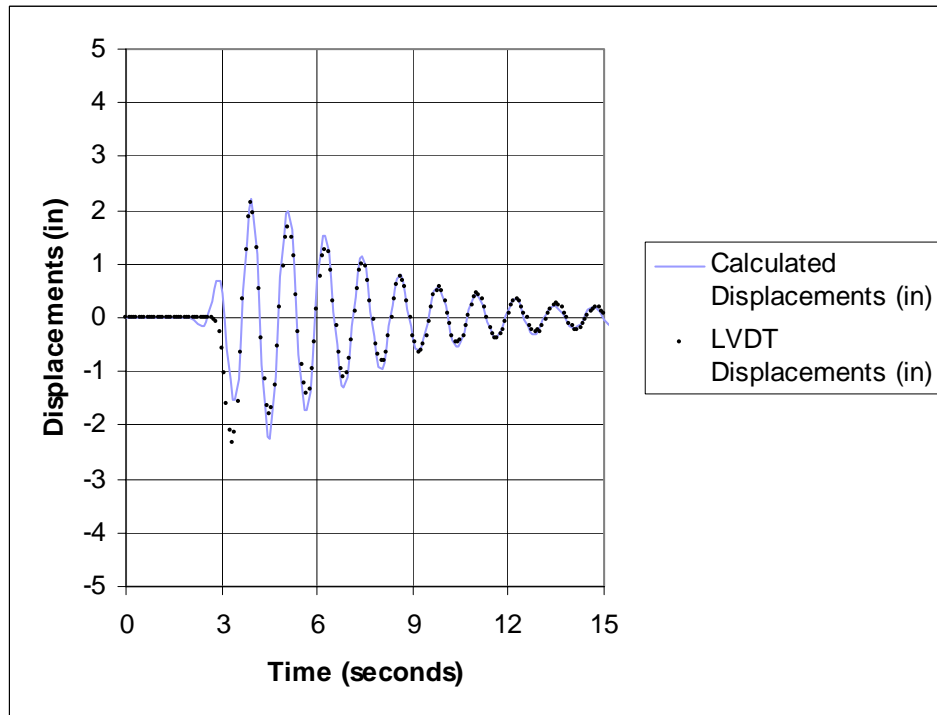


Figure 4.10 - Displacement Data Comparison utilizing the Centering Function

#### 4.5 Wind Instrumentation

Wind speed and direction data were needed to help understand what forces existed during the testing of a mast arm structure in Tampa. The R.M. Young Wind Sentry 3001 anemometer and vane was selected to acquire this data during the field-testing. The anemometer generates an AC sine wave signal induced by a rotating magnet on a three-cup wheel shaft. The wind speed can be measured by recording the anemometer's sine wave, extracting the sine wave's frequency, and applying it to the factory calibration. The vane is made up of a precision conductive plastic potentiometer. It requires an excitation of 2.5 Volts. As the vane spins, its output ranges from 0 Volts to 2.5 Volts. Wind direction can be determined as long as the direction of zero voltage is known. The anemometer and vane are pictured in Figure 4.11.



Figure 4.11 - Anemometer and Vane

#### 4.6 Instrument Effects on Mast Arm Structures

One concern that came up before the field-testing took place was whether or not the instrumentation and their wires would have an effect on the mast arm's natural damping and frequency. So, the entire setup was placed on to the lab mast arm and tested under free vibration. This was compared to the results of the mast arm without the wires attached along the structure to its base. There was a 0.59% change in the systems frequency and a 4.27% change in its natural damping. Therefore, it was concluded that the instruments had minimal effects on the mast arm's natural response characteristics.

## CHAPTER 5 PRELIMINARY MAST ARM TESTING

### 5.1 Introduction

Four mast arm structures were used throughout this research. They include the University of Florida lab mast arm, two of the arms tested by Kalajian in Gainesville, Florida, and one structure in Tampa, Florida. The first three structures were selected for their close proximity to the University and their range of frequencies. As reported by Kalajian, these three structures contain a good range of the natural frequencies that cantilevered mast arms possess. The Tampa mast arm has been observed, by the FDOT, to oscillate on a regular basis. Therefore, it was selected in order to test the final damping device on a pole that would be susceptible to wind-induced vibrations.

The purpose of this chapter is to define the four tested mast arms, discuss how they were tested, present their natural vibration results, and compare those results to computer modeling.

### 5.2 Mast Arms

The 37 ft lab mast used was fully described in Chapter 3. The cantilevered structures tested in Gainesville were 70 ft long and 40 ft long. Both structures were located at the intersection of SW 34<sup>th</sup> St. and SW 47<sup>th</sup> Ave. Dimensions of the longer pole and a photograph of it can be seen in Figures 5.1 and 5.2 respectively. The same can be seen for the short pole in Figures 5.3 and 5.4 respectively. The details of the mast arm

in Tampa are located in Figures 5.5 and 5.6. This mast arm was 66 ft long and located at the intersection of Ulmerton Rd. and Egret Blvd.

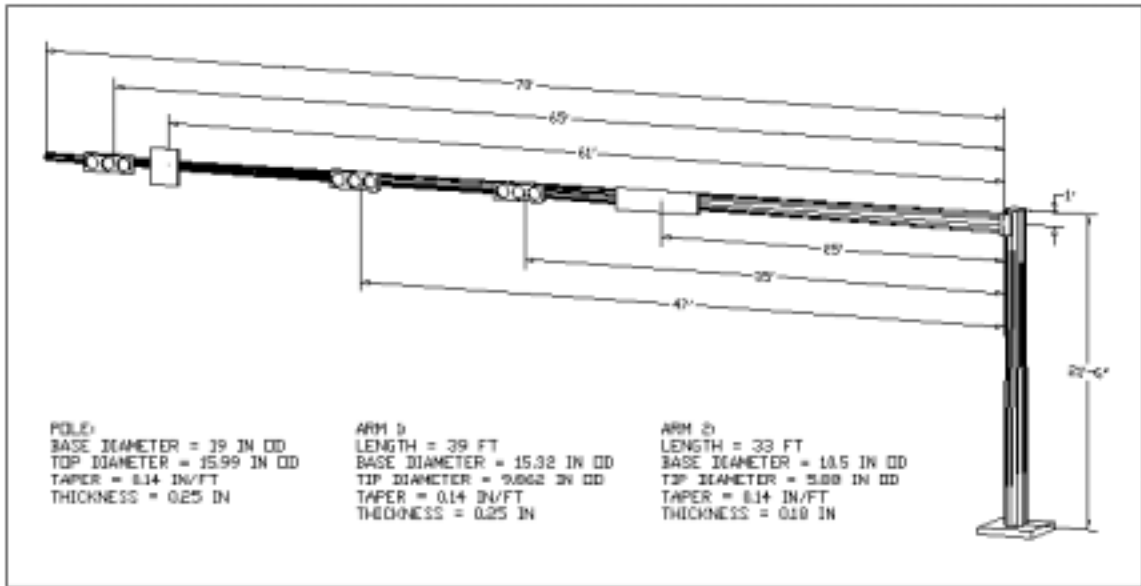


Figure 5.1 - Gainesville Long (70ft) Mast Arm Dimensions



Figure 5.2 - Gainesville Long (70ft) Mast Arm



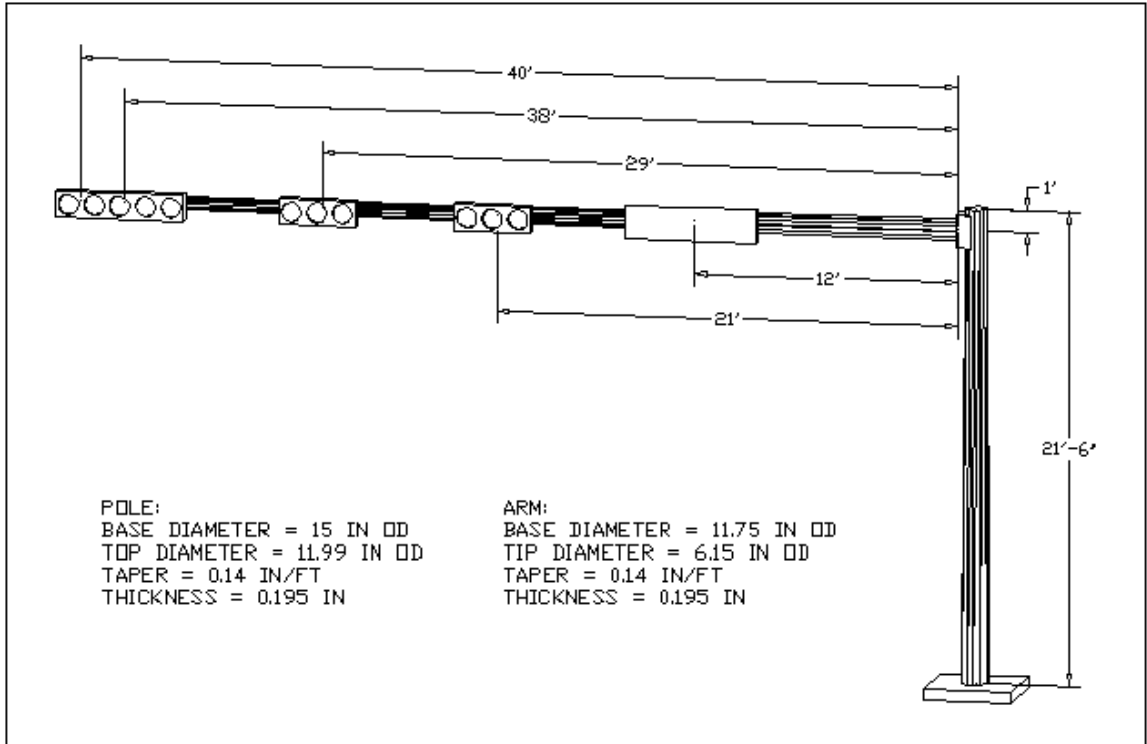


Figure 5.3 - Gainesville Short (40ft) Mast Arm Dimensions



Figure 5.4 - Gainesville Short (40ft) Mast Arm

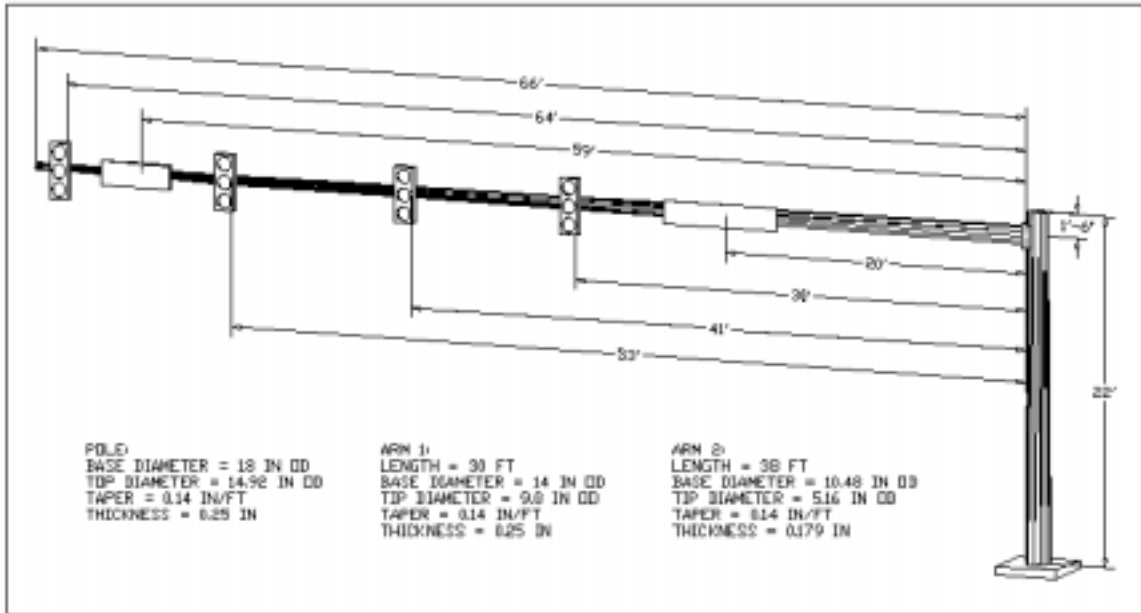


Figure 5.5 - Tampa Mast Arm Dimensions



Figure 5.6 - Tampa Mast Arm

### 5.3 Testing Procedures

The lab mast arm, Gainesville mast arms, and Tampa mast arm were each tested in a similar manner. First, the arms were instrumented with the vertical and horizontal accelerometers at their tips. Once the data acquisition was in place, each structure was given six different types of initial displacement and allowed to oscillate freely without a damping device attached. The poles were given a small and large vertical displacement, horizontal displacement, and diagonal displacement. The diagonal displacement was performed so its vertical and horizontal components could be compared to the vertical and horizontal displacements respectively. The small and large displacements were performed to determine if the percent critical damping of the mast arm was dependent on amplitude. Next, the dampers were attached, and the process was repeated. All this data resulted in each mast arms' percent critical damping and natural frequency with and without a damper attached.

The percent critical damping used in this entire research was determined with the method of logarithmic decrement. Critical damping is the rate at which the amplitude, of an oscillating structure, decreases relative to time. Percent critical damping,  $\xi$ , is approximately equal to:

$$\xi = \frac{1}{2 \cdot \pi} \cdot \frac{1}{n} \cdot \ln\left(\frac{y_1}{y_2}\right)$$

In this equation,  $y_1$  is the first peak in a set of decaying data,  $y_2$  is the second peak in that set of decaying data, and  $n$  is the number of cycles occurring between  $y_1$  and  $y_2$ . The Mathcad worksheet used to perform these calculations is located in Appendix A.

Although knowing the percent critical damping of a mast arm with and without a damper attached is useful in selecting a device, the previous free vibration testing is not representative of the type of wind loading that occurs in the field. None of the four wind phenomena, mentioned in Chapter 2, are capable of inducing a large initial displacement on a mast arm like the previous test. Vibrations of cantilevered structures are initiated from at rest states and build up amplitude due to sustained wind loading or wind gusts. The best way to test wind-induced vibrations in a laboratory setting would be to use a wind tunnel on a scale model of a mast arm. Even if the University of Florida Civil Engineering department had a wind tunnel for testing, it still would not be easy to generate the wind loading phenomena mentioned in Chapter 2. In attempting to simulate wind-induced vibrations, it was necessary to excite the mast arms with some sort of sinusoidal loading. This need was fulfilled with the development of an eccentric mass and motor device.

The eccentric mass and motor device contained a motor with an extended shaft. The shaft had a threaded rod attached perpendicular to it with a 5 lb mass attached to the end of the rod. This vibration excitation device can best be understood by observing the photographs of it attached to the lab mast arm in Figures 5.7 and 5.8.

The idea behind the eccentric mass and motor device was to rotate the mass about the shaft at approximately the same frequency as the mast arm structure. It was believed that this would excite the arm from its at rest position and continue to increase its amplitude of displacements. The main concern with this vibration excitation device was that it might not produce oscillations in the vertical direction, and instead in the horizontal direction. Fortunately, the device performed predominately in the vertical



Figures 5.7 - Eccentric Mass and Motor Device (Photo 1)



Figure 5.8 - Eccentric Mass and Motor Device (Photo 2)

horizontal direction. Fortunately, the device performed predominately in the vertical direction. It was then used in the testing of the lab mast arm and the two mast arms in Gainesville. The structure in Tampa was tested for its natural wind-induced oscillations, and therefore did not need the eccentric mass and motor device for excitation.

#### 5.4 Computer Modeling

Once the free vibration testing of all four mast arms was complete, it was necessary to check the validity of the data before continuing with the testing of the damping devices. A dynamic analysis was performed for each structure using the geometric properties given in Section 5.2. The computer software used was SSTAN (Structural analysis program written by Dr. Marc Hoit, University of Florida). The analyses calculated the natural frequencies for the first four modes of each structure as well as the shape of each mode. Of the four modes, two were in the vertical direction (perpendicular to the ground) and two were in the horizontal direction (parallel to the ground). These computer generated natural frequencies were then compared to those determined from the free vibration testing of each cantilevered mast. The results are located in Table 5.1. Appendix B contains a sample SSTAN input file from the lab mast arm structure.

The results from Table 5.1 proved that the natural frequencies from the mast arm free vibration tests were valid. However, there were some slight percent differences between the dynamic analyses and the mast arm tests. One possible source of error is that the finite element models used average cross sections for each foot of the tapered structure instead of modeling the actual tapered dimensions. Also, the weights used for

Mode	Lab Mast Arm		Short Gainesville Mast Arm		Long Gainesville Mast Arm		Tampa Mast Arm	
	Frequency (Hz)	Percent Difference	Frequency (Hz)	Percent Difference	Frequency (Hz)	Percent Difference	Frequency (Hz)	Percent Difference
Vertical 1st Mode	Actual	1.029	1.15	2.09%	0.724	3.18%	0.67	8.81%
	SSTAN	1.053	1.126		0.747		0.729	
Horizontal 1st Mode	Actual	0.927	1.055	1.33%	0.676	4.88%	0.623	11.40%
	SSTAN	0.989	1.041		0.709		0.694	
Vertical 2nd Mode	Actual	NA	NA	NA	2.828	3.50%	2.47	14.82%
	SSTAN	NA	NA	NA	2.927		2.836	
Horizontal 2nd Mode	Actual	NA	NA	NA	2.784	2.84%	2.472	12.18%
	SSTAN	NA	NA	NA	2.863		2.773	

**Table 5.1 - Comparison of Computer Model and Free Vibration Mast Arm Testing Results**

the signal and sign attachments were either taken from actual design calculations or from FDOT standard design weights, and may not have been the true loads on the structures. The mast arms over 40 ft are made up of two segments along their cantilevered portions. These segments contain a 2 ft splice and are held together by a bolt. The additional cross sectional area at the splice was not considered in the dynamic analysis. Finally, the base of each mast arm was modeled as though it were completely fixed. If the base connection had any give at all, the computer model would be in error. Given these chances for error in the finite element modeling, the percent differences in Table 5.1 were considered to be acceptable.

### 5.5 Results

Since the free vibration test results were determined to be valid and the natural response characteristics of each mast arm were known, the new damping devices were ready to be tested. The next chapter will introduce the new dampers and present their results.



## CHAPTER 6 DAMPING DEVICES AND RESULTS

### 6.1 Introduction

As explained in Chapter 3, the purpose of a damping device is to decrease the number and amplitude of wind-induced oscillation cycles of a mast arm. The challenge in this project was to develop a device that would be effective on all types and lengths of mast arm structures. It was also necessary to concentrate on the horizontal damping provided by the damper as well as the vertical damping. The target percent critical damping was 5% for each direction. This chapter will introduce the devices and present their results in the order of their development. Unlike Kalajian's results, the free vibration responses in this chapter will be shown in graphs of the mast arms' normalized displacements vs. time.

### 6.2 Kalajian's Selected Damping Device

This research began with the damping device selected in Kalajian's project. His 4 in to 2 in tapered spring/mass impact damper (four-inch tapered damper) was fabricated with a steel shell instead of the original PVC shell. This device was composed of a 4 in ID steel pipe, 27 in long, a spring with a stiffness of 1.4 lb/in, and a mass of 15 lbs. The mass was a 3.5 in diameter cylinder at 5.5 in long. The total weight of the device was approximately 40 lbs. It was tested on the lab mast arm in order to observe the vertical damping. A picture of this device and its vibration response are located in Figure 6.1 and

6.2 respectively. By observation, the horizontal damping of Kalajian's tapered device appeared to be ineffective on the lab mast arm, therefore no readings were taken in the horizontal direction.



Figure 6.1 - 4 in Tapered Impact Damper

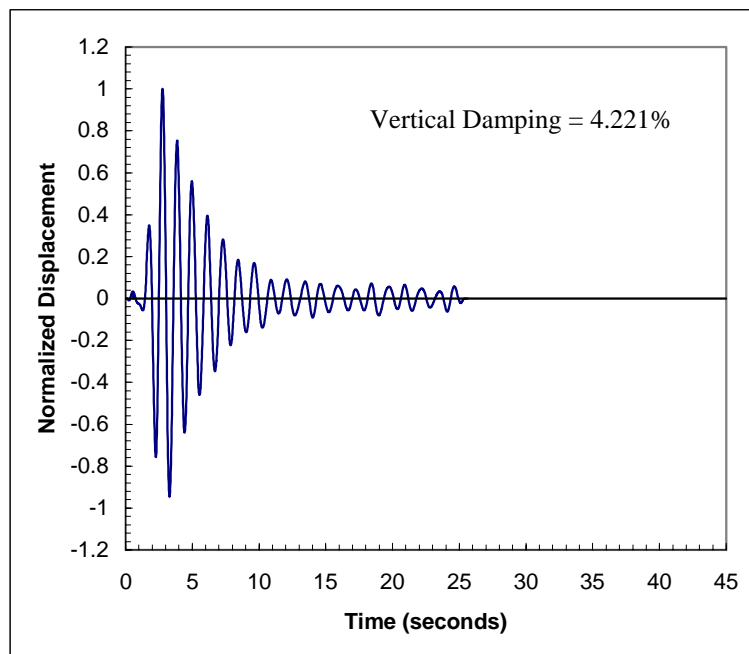


Figure 6.2 - 4 in Tapered Impact Damper Vibration Response

### 6.3 Round Impact Damper

At this point, the four-inch tapered damper's effectiveness was believed to be due to the impact action of the device. However, its horizontal damping needed to be improved. The idea for the round damping device was to maintain the vertical impacting while allowing the mass more horizontal movement for better horizontal damping. The round device was an 18 in OD pipe with a 0.25 in thickness and a length of 6 in. A 16 lb spherical shot put with a 4.5 in diameter was used as the mass. The round device can best be understood by observing the pictures in Figures 6.3 and 6.4. This device mounted directly to the tip of the pole as seen in Figure 6.5.

Unfortunately, the round impact damper was ineffective in the vertical direction and in some cases seemed to induce vibration. Since mitigating the vertical displacement was the main concern in this research, no readings were taken for this device. However, the horizontal damping appeared to work very well. Therefore, the idea of allowing more space for the mass to move horizontally was applied to upcoming devices.



Figure 6.3 - Round Impact Damper with Cover Plate



Figure 6.4 - Round Impact Damper without Cover Plate

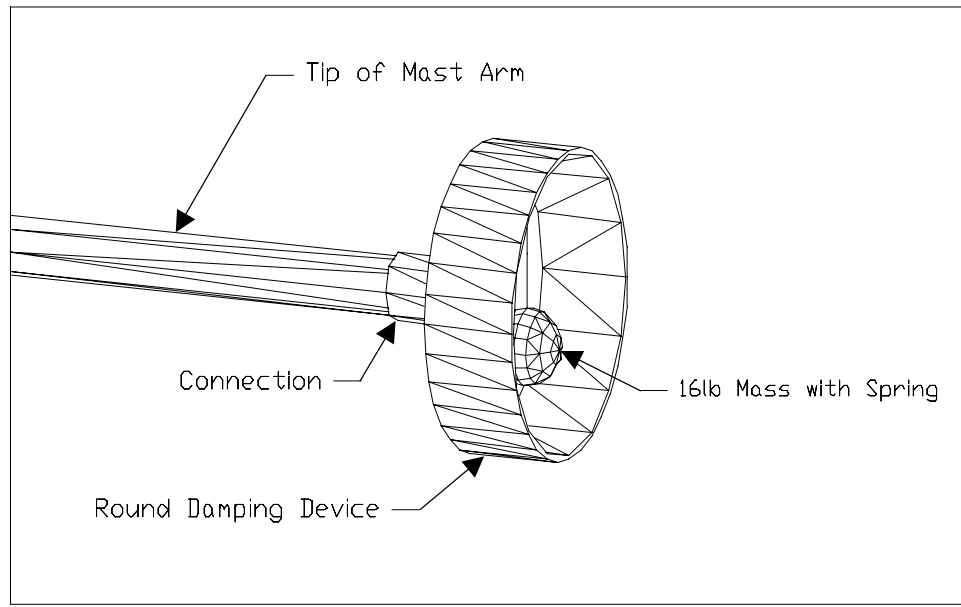


Figure 6.5 - Round Impact Damper without Cover Plate, and Connected to the Tip of a Mast Arm

#### 6.4 Eight-Inch Tapered Impact Damper

The eight-inch tapered impact device was made out of an 8 in ID diameter, 18 in long, with a 1/2 in wall thickness, steel pipe. A 4.5 in diameter spherical shot put, weighing 16 lb, was used as the mass. The mass was attached to a spring that was connected to the cap. The device's total weight was approximately 80 lbs. This damper is pictured in Figure 6.6.

No data was collected for the eight-inch tapered impact device. The device was observed on the lab mast arm and performed poorly in both the vertical and horizontal directions. The impacting seemed to have virtually no effect on the poles' oscillations. This made it apparent that the impacting effect of the four-inch tapered damper was not the sole reason for its performance.



Figure 6.6 - Eight-Inch Tapered Impact Damper

#### 6.5 Long Four-Inch Tapered Impact Damper

Since both the round damper and the eight-inch tapered impact dampers were ineffective, the research turned back to Kalajian's four-inch tapered device. The round damper and eight-inch tapered impact damper both had heights of 18 in, while the four-inch tapered device was 27 in tall. And, all three devices used masses within a pound of each other. If the same masses were used in all three devices, the springs in the two ineffective devices would have to be either stiffer or shorter, than the spring in the four-inch tapered device, to fit in their 18 in tall shells. A shorter or stiffer spring would lead to a different damper frequency. This prompted a review of Kalajian's damper to see if it was tuned to the lab mast arm. Using the natural frequency equation presented in

Chapter 3, it was determined that the four-inch tapered impact damper had a vertical frequency of 0.955 Hz. The lab mast arm's vertical frequency was 1.029 Hz. Although the four-inch damper and the lab mast arm frequencies were not identical, they were close, and this suggested the damper was semi-tuned to the structure.

A longer version of the four-inch tapered impact damper was then constructed to allow for a variety of spring lengths and stiffness, and mass weights. The purpose of this device was to be able to test a variety of damper frequencies on the lab mast arm and the two Gainesville mast arms. The idea was to determine what range of damper frequencies would be effective on each of these structures. The shell of this device was 4 in ID with a 0.25 in wall thickness and a length of 40 in. A threaded rod was placed through the cap of the device to adjust the height of each spring/mass combination to where the at-rest position of the mass was one inch from bottom of the damper. When the gap of the mass was too big or too small, the device was not properly activated. By observation, a one-inch gap for the mass was the most effective for small, medium, and large initial displacements of the structure. A cross-sectional drawing and picture of this device, attached to the lab mast arm, are in Figures 6.7 and 6.8 respectively.

For the first series of tests, the weight of the mass was held constant at 15 lbs and the spring lengths and stiffness were varied. The frequency of each spring/mass combination was calculated with the natural frequency equation from Chapter 3. Then, an accelerometer and the data acquisition were used to perform a free vibration test of each spring/mass combination and the actual natural frequency was determined. A comparison of the calculated and actual frequencies for the different spring/mass combinations is located in Table 6.1.

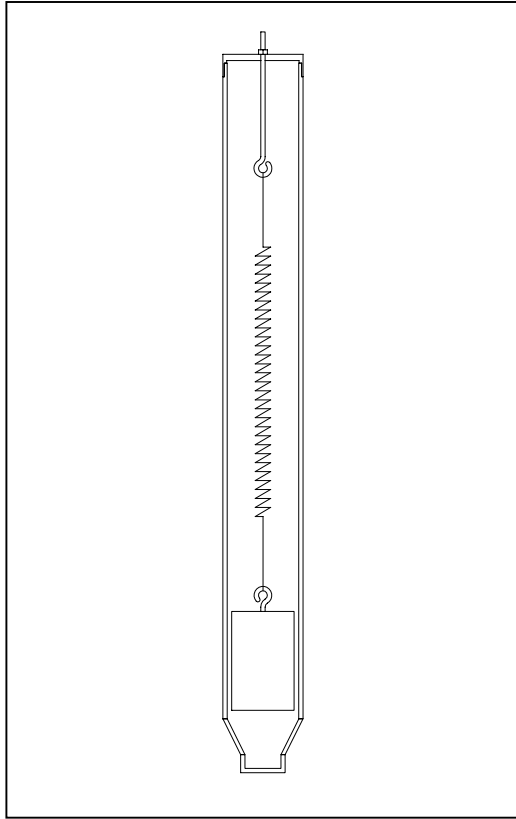


Figure 6.7 - Cross Section Drawing of Long 4 in Tapered Impact Damper



Figure 6.8 - Long 4 in Tapered Impact Damper

Table 6.1 - Spring/Mass Natural Frequency Comparisons  
(Mass held constant at 15 lbs)

Spring #	Stiffness (lb/in)	Calculated Frequency (Hz)	Actual Frequency (Hz)		Average Actual Frequency (Hz)	Percent Difference
1	1.2	0.885	0.875	0.882	0.878	0.7%
2	1.4	0.956	0.990	0.988	0.989	3.5%
3	1.045	0.826	0.849	0.845	0.847	2.6%
4	2.4	1.251	1.252	1.238	1.245	0.5%
5	6.7	2.091	2.141	2.146	2.144	2.5%
6	0.69	0.671	0.681	0.677	0.679	1.2%

Since the Gainesville long mast arm, the lab mast arm, and the Gainesville short mast arm had natural frequencies of 0.724 Hz, 1.029 Hz, and 1.150 Hz respectively, the above mentioned spring/mass combinations were acceptable for determining the range of damper frequencies that would work the best on each pole. The testing procedure, for the different damper setups on these three mast arms, was similar to the free vibration testing mentioned in Chapter 5. A small and large initial displacement was given in the vertical, horizontal, and diagonal direction for each pole combined with each of the long four-inch tapered dampers' setups. The average vertical and horizontal percent critical damping values were then calculated. Figures 6.9, 6.10, and 6.11 are graphs of the percent critical damping vs. the damper period for the Gainesville short mast arm, the lab mast arm, and the Gainesville long mast arm respectively.

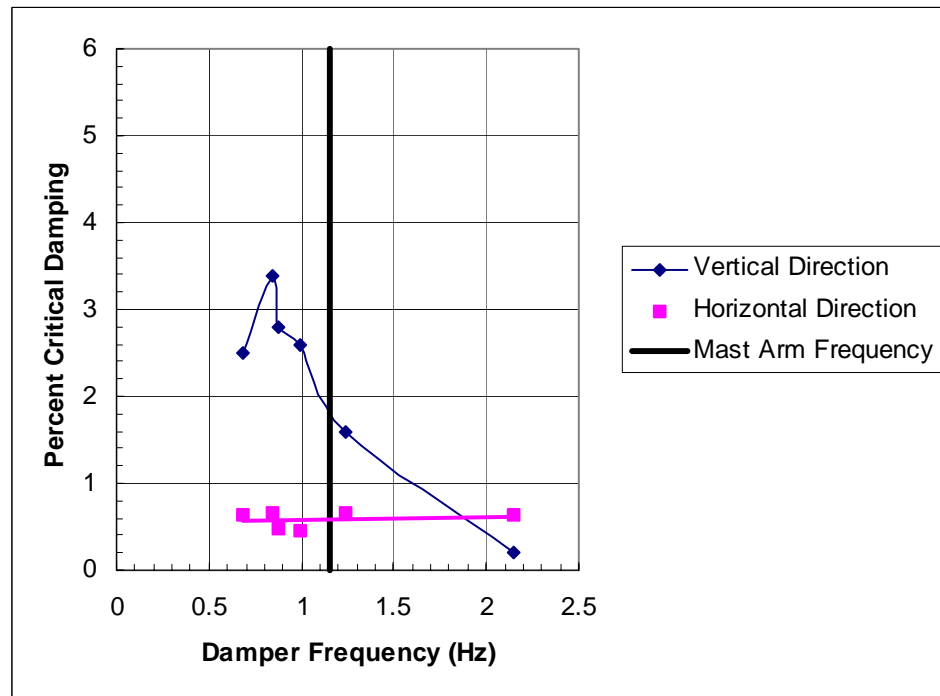


Figure 6.9 - Long 4 in Tapered Impact Damper on Gainesville Short Mast Arm (Variable Springs with Constant Mass (15 lb))



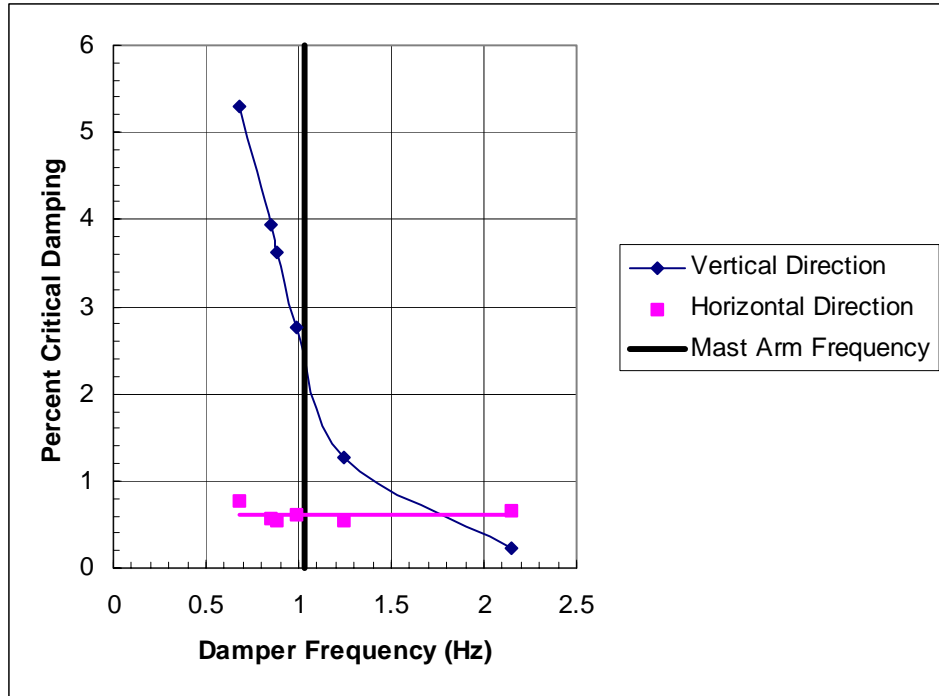


Figure 6.10 - Long 4 in Tapered Impact Damper on Lab Mast Arm (Variable Springs with Constant Mass (15 lb))

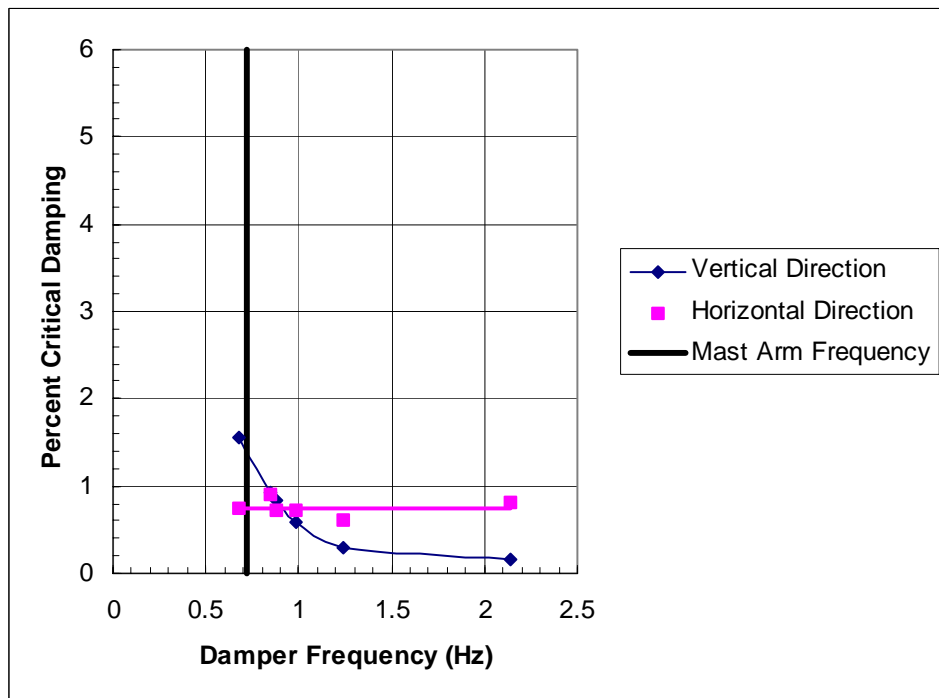


Figure 6.11 - Long 4 in Tapered Impact Damper on Gainesville Long Mast Arm (Variable Springs with Constant Mass (15 lb))

The plots of percent critical damping vs. damper frequency for the lab and Gainesville mast arms indicated that the damping device does need to be semi-tuned to the structure. Although the horizontal damping remained constant, the effective range of the frequencies for the device's vertical direction damping seemed to be approximately 0.75 to 1 times the frequency of the pole it was attached to. The plots clearly show that the damper is less effective when its spring/mass frequency is greater than the pole that it is connected to. This explains why the round and eight-inch tapered dampers were ineffective on the lab mast arm. They contained stiffer springs than the four-inch tapered device, thus making their frequencies higher than the lab mast arm's.

The second series of tests, with the long four-inch tapered damper, involved changing the weight of the mass while maintaining the damper frequency. The damper frequency was held constant by adjusting the spring/mass combination. Once again, the mass was placed one inch from the bottom of the damper during its at-rest position. This procedure was done for three separate cases. These cases are defined in Table 6.2. Figures 6.12, 6.13, and 6.14 show the results of testing for the three cases respectively.

Table 6.2 - Spring/Mass Combinations for Long 4 in Tapered Impact Damper (Variable Mass Testing)

Case #	Mast Arm Tested	Stiffness (lb/in)	Mass (lb)	Calculated Frequency (Hz)
1	Lab	1.2	15	0.88
		1.4	17.5	0.88
		2.4	30	0.88
2	Lab	1.045	15	0.83
		1.4	20	0.83
		2.4	34	0.83
3	Gainesville Long	1.045	15	0.83
		2.4	34	0.83

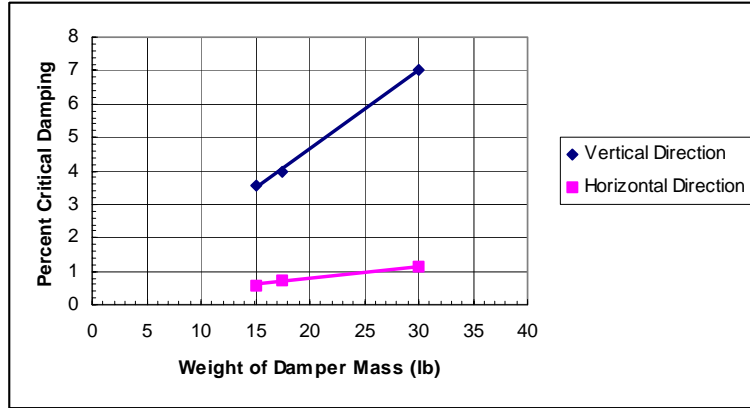


Figure 6.12 - Variable Mass Testing for Long 4 in Tapered Impact Damper (Case 1)

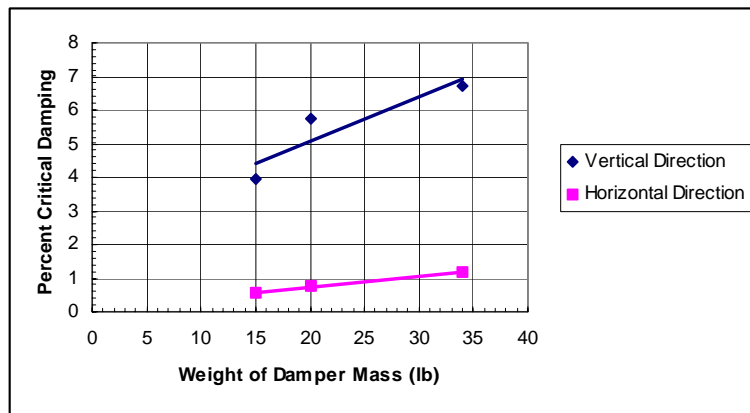


Figure 6.13 - Variable Mass Testing for Long 4 in Tapered Impact Damper (Case 2)

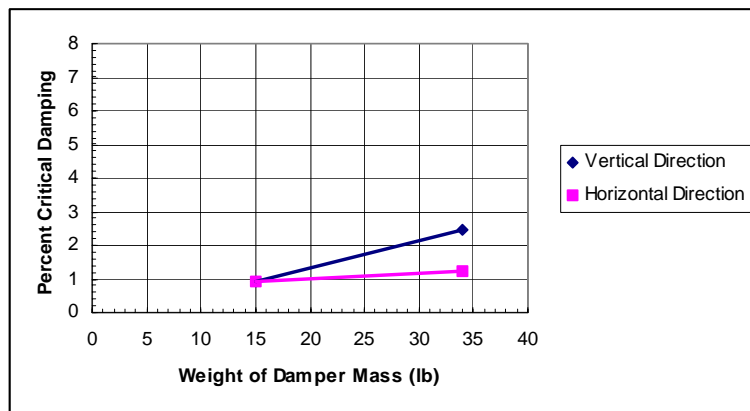


Figure 6.14 - Variable Mass Testing for Long 4 in Tapered Impact Damper (Case 3)

The results of the variable mass testing indicated that as the weight of the mass inside the damper gets heavier, the percent critical damping in the vertical direction of the mast arm increases almost linearly. Although it was not as significant, the horizontal damping also increased linearly with an increase of the mass's weight.

This concluded the testing of the long four-inch tapered impact damper. However, the only good information given for the horizontal damping was that it increases with a heavier mass in the device. This prompted further testing to improve the critical damping of the mast arms in their horizontal directions. First, the natural frequency of the spring/mass combination in the horizontal direction was compared to that of the lab mast arm. Second, a larger diameter shell was used to allow for a bigger gap between the mass and the damper's side walls.

### 6.6 Horizontal Damping Test

The natural frequency,  $f$ , of a mass hanging from a string is dependent on the length,  $L$ , from the top of the string to the centroid of the mass, and gravity,  $g$ .

$$f = \frac{1}{2 \cdot \pi} \cdot \sqrt{\frac{g}{L}}$$

This equation was used to determine what spring lengths would be necessary for a damper to match the lab and Gainesville mast arms. Table 6.3 shows these results.

Table 6.3 - Spring Lengths Required to Match Damper and Mast Arm Horizontal Frequencies

Mast Arm	Horizontal Frequency (Hz)	Required L (in)
Gainesville Short	1.055	8.8
Lab	0.927	11.4
Gainesville Long	0.676	21.4

Since the damper's frequency needed to be smaller than that of the mast arm it was placed on in order to increase vertical damping, the same concept was applied to the horizontal damping. This test started by attaching a 6 in ID pipe to the tip of the lab mast arm. The pipe was 48 in long and had a wall thickness of 0.25 in. A cap was then placed on top of the pipe with a string hanging down the center of the pipe. A 15 lb mass was then hung from the string to provide an array of lengths, from the top of the string to the centroid of the mass, ranging from 8 in to 40 in. The mast arm device was given an initial horizontal displacement for each setup and the horizontal percent critical damping was determined. The results are presented graphically, in two different forms, in Figures 6.15 and 6.16.

The results of the horizontal damping test were similar to the vertical damping test in that the percent critical damping increased when the damper's frequency was less than the mast arm it was tested on. The most effective range for the lab mast arm was when the frequency of the damper was 0.5 to 0.7 times the arm's horizontal frequency. This resulted in a range of spring lengths from 20 in to 35 in.

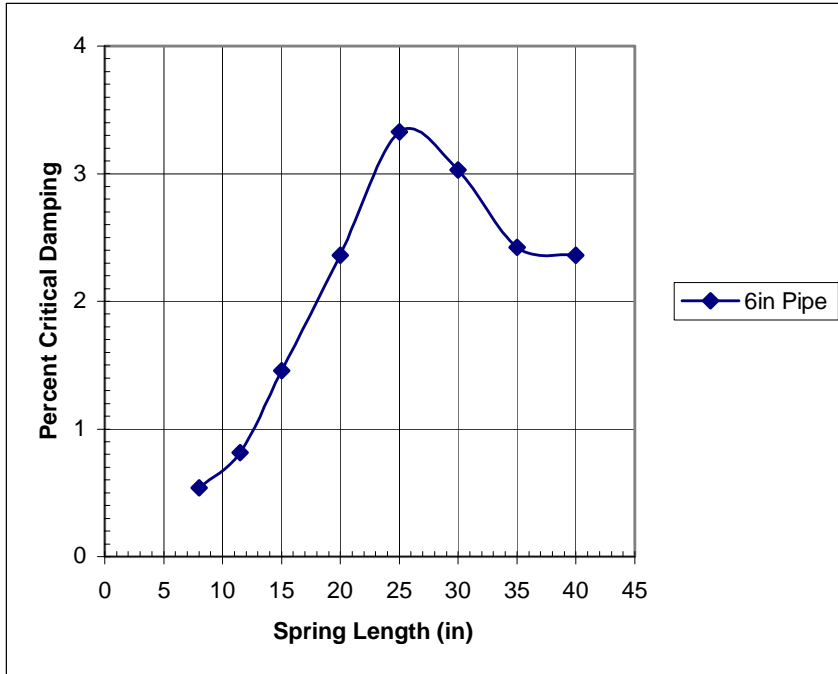


Figure 6.15 - Results of 6 in Pipe with Various Spring Lengths and Constant Mass (15lb)

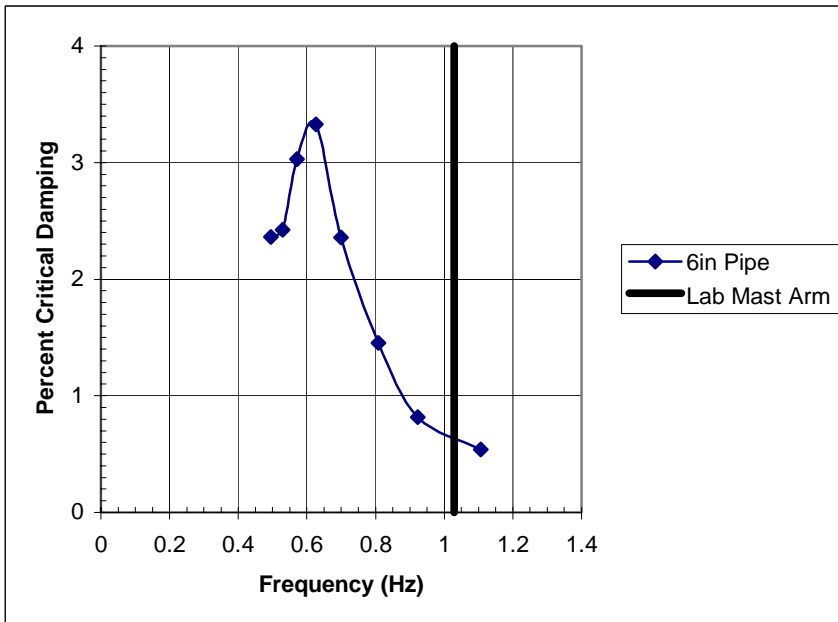


Figure 6.16 - Results of 6 in Pipe with Various Frequencies (Using Constant Mass (15 lbs) and Variable Spring Lengths)

### 6.7 Semi-Tuned Tapered Impact Damper – Final Design

The idea behind the semi-tuned tapered impact damper was to combine every effective damping aspect of the previous dampers into one final design. The parameters in the device's design were as follows:

1. Damper's vertical frequency approximately 0.7 Hz.
2. Damper's horizontal frequency approximately 0.6 Hz (L=25 in to 30 in).
3. Use six-inch steel pipe for the shell with a taper at the bottom.
4. Use four-inch diameter mass.
5. Prepare two devices with total weights of 40 lbs and 80 lbs.
6. Minimize shell weight and maximize internal mass weight.
7. Limit device's overall length to 4 ft.

As is indicated in the above parameters, two devices were designed and built.

Both devices were made of 6 in ID steel pipe with a wall thickness 1/8 in. The thin wall was used to help minimize the total weight of the shell. The first device was 3 ft long and contained a spring with a stiffness of 0.69 lb/in and a 4.2 in long, 4 in diameter, 15 lb cylindrical mass. The total weight of this device was 43 lbs. Figures 6.17 and 6.18 show a cross-sectional drawing and a photo of the 3 ft tapered impact damper attached to the tip of the lab mast arm. The weight of this device was considered to be safe for implementing on existing structures and therefore was tested on the all four mast arms from this research. The results of all the free vibration responses and eccentric mass and motor responses, with and without the 3 ft tapered impact damper, are located in Figures 6.19 through 6.32.

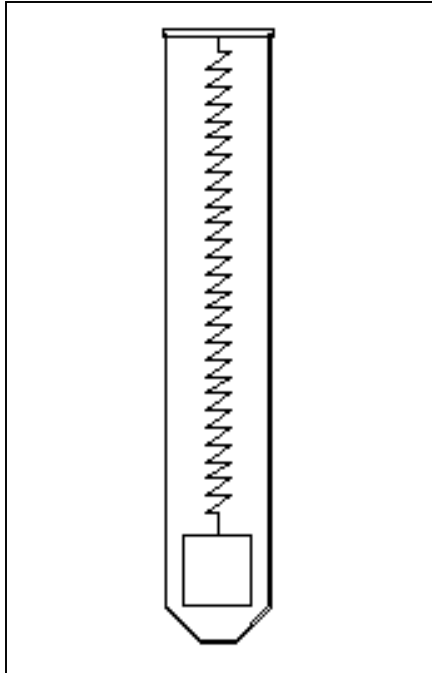


Figure 6.17 - Cross Section Drawing of 3 ft Tapered Impact Damper



Figure 6.18 - 3 ft Tapered Impact Damper



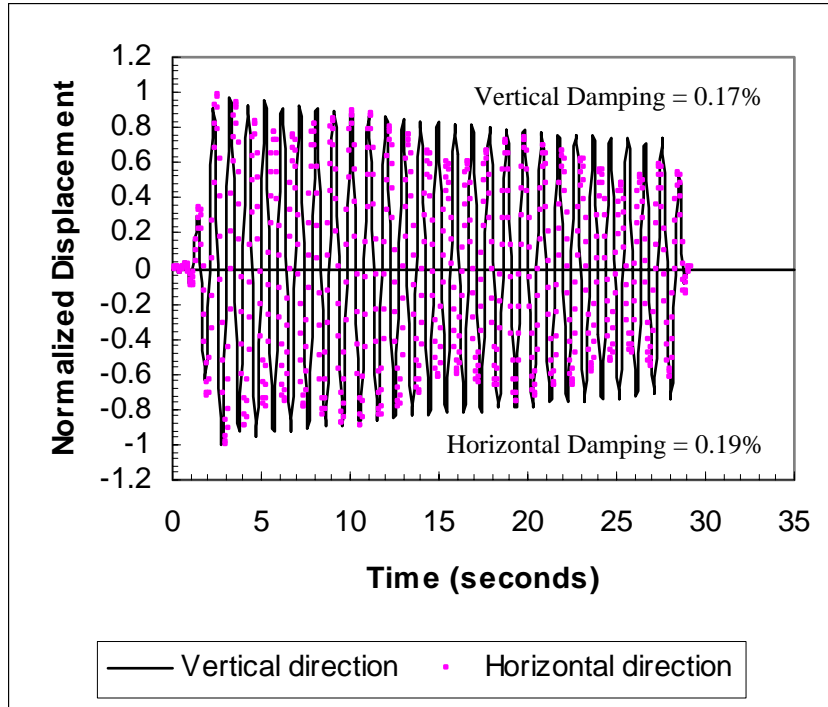


Figure 6.19 - Free Vibration of the Lab Mast Arm

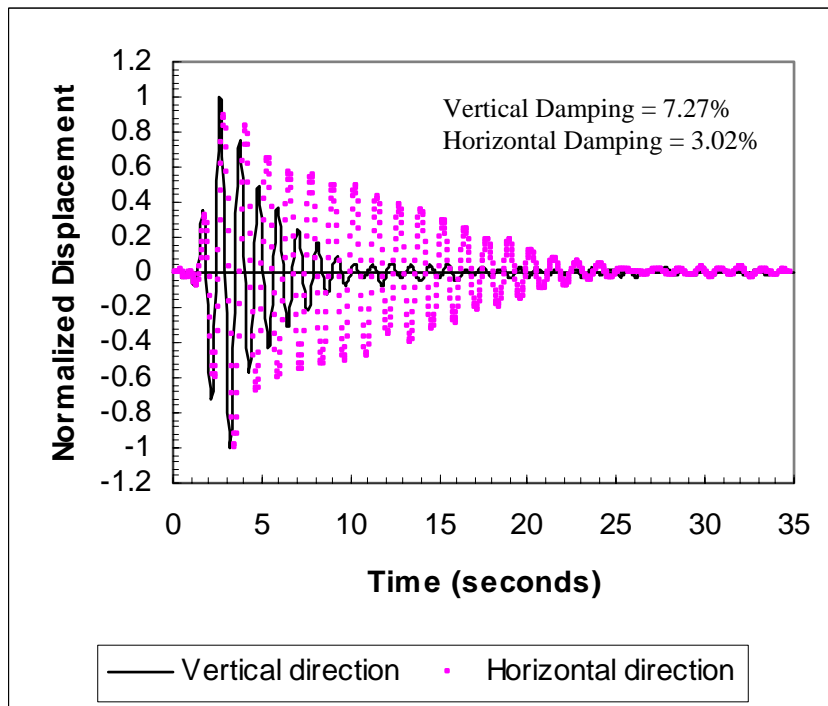


Figure 6.20 – Free Vibration of the Lab Mast Arm with 3 ft Tapered Impact Damper

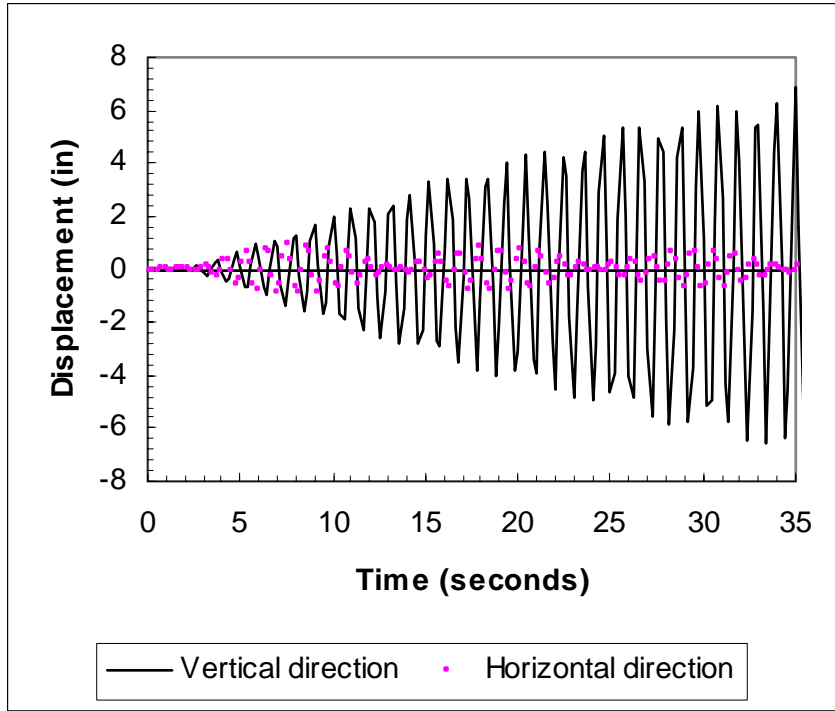


Figure 6.21 - Eccentric Mass and Motor Vibration of the Lab Mast Arm

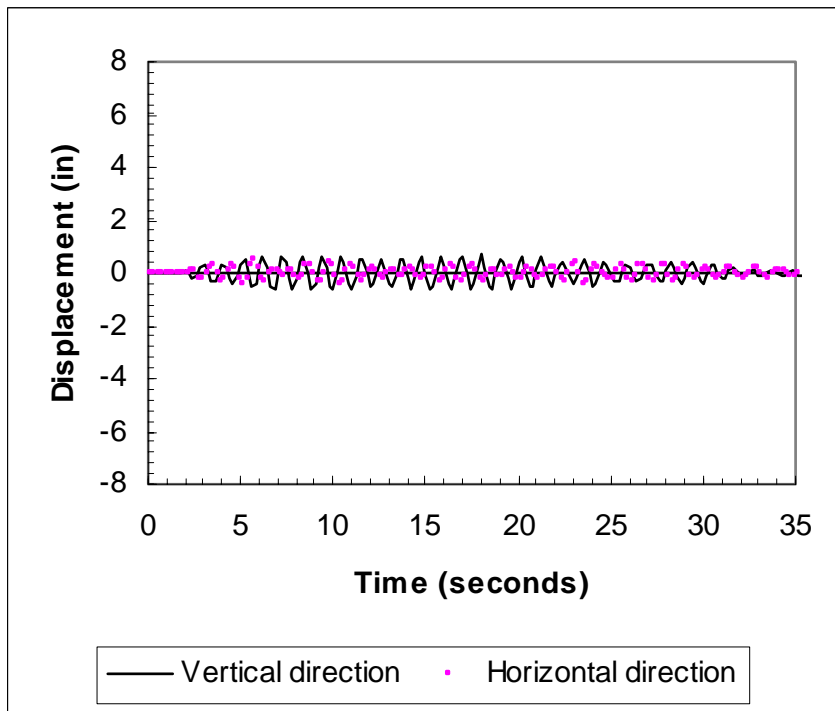


Figure 6.22 - Eccentric Mass and Motor Vibration of the Lab Mast Arm with 3 ft Tapered Impact Damper

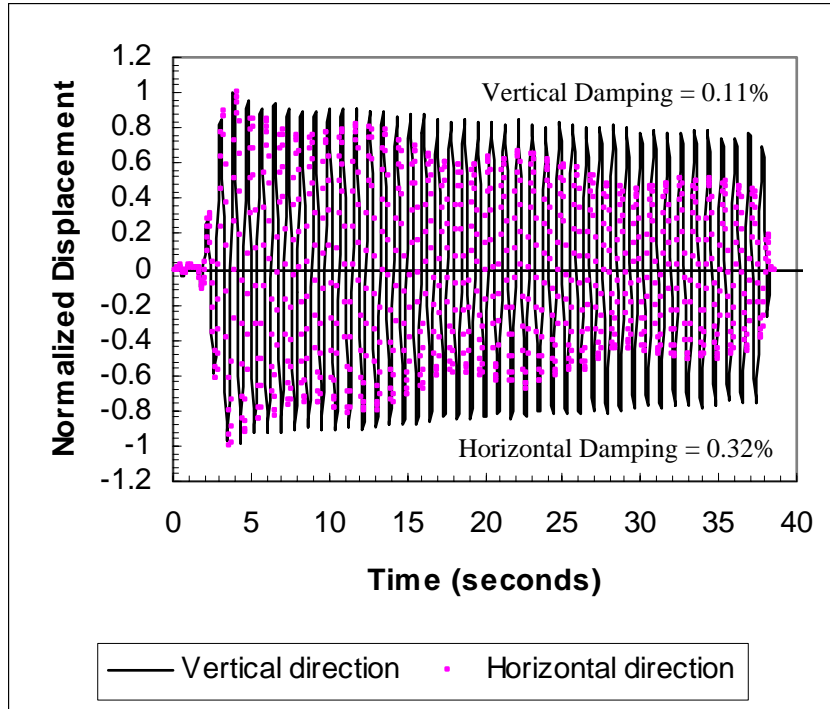


Figure 6.23 - Free Vibration of the Gainesville Short Mast Arm

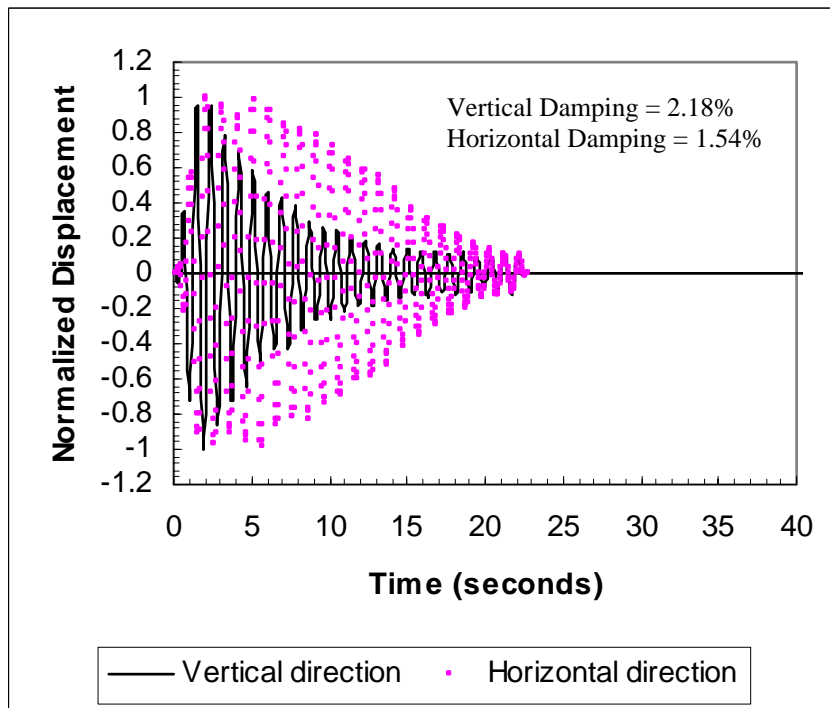


Figure 6.24 - Free Vibration of the Gainesville Short Mast Arm with 3 ft Tapered Impact Damper

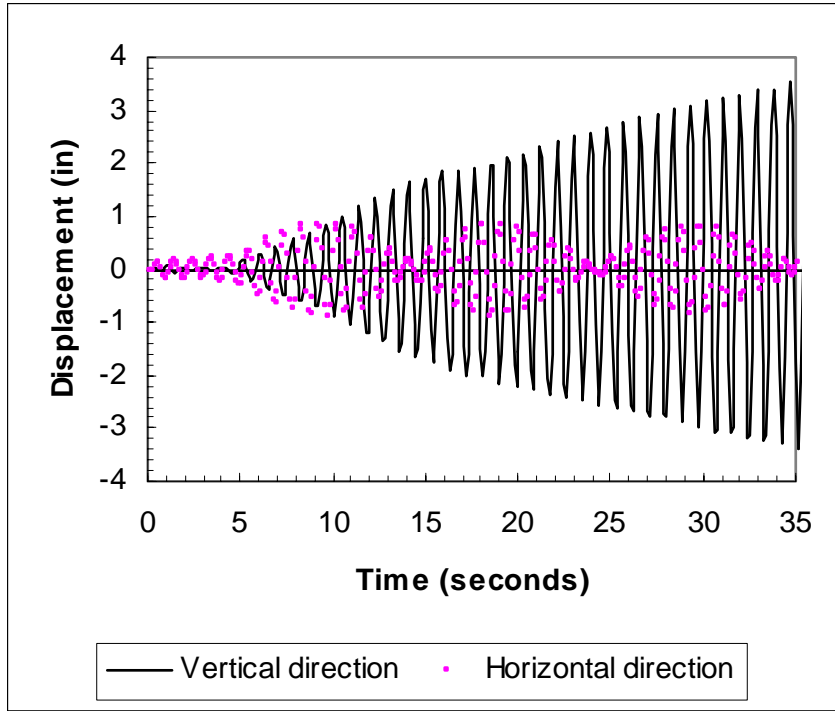


Figure 6.25 - Eccentric Mass and Motor Vibration of the Gainesville Short Mast Arm

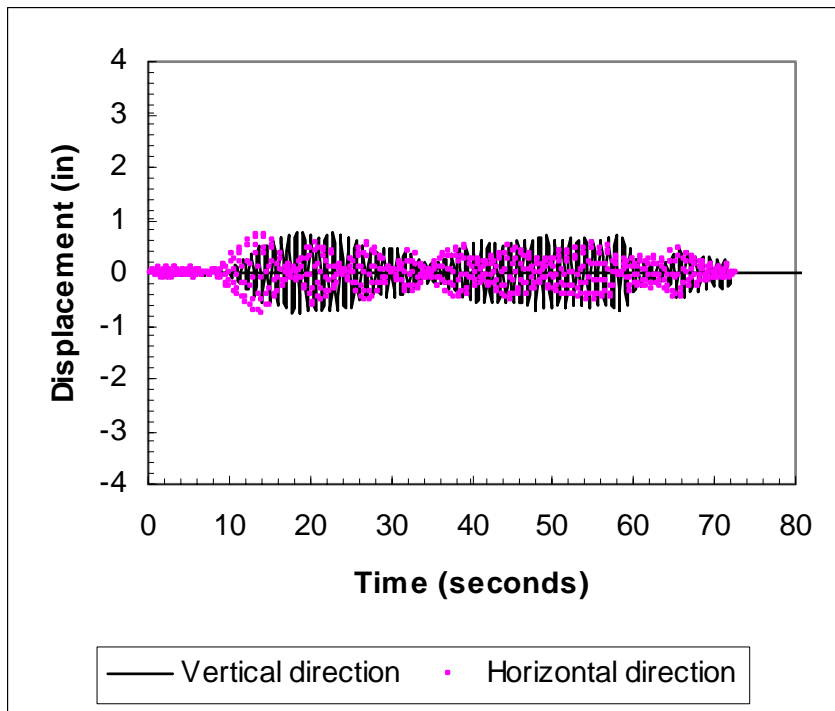


Figure 6.26 - Eccentric Mass and Motor Vibration of the Gainesville Short Mast Arm with 3 ft Tapered Impact Damper

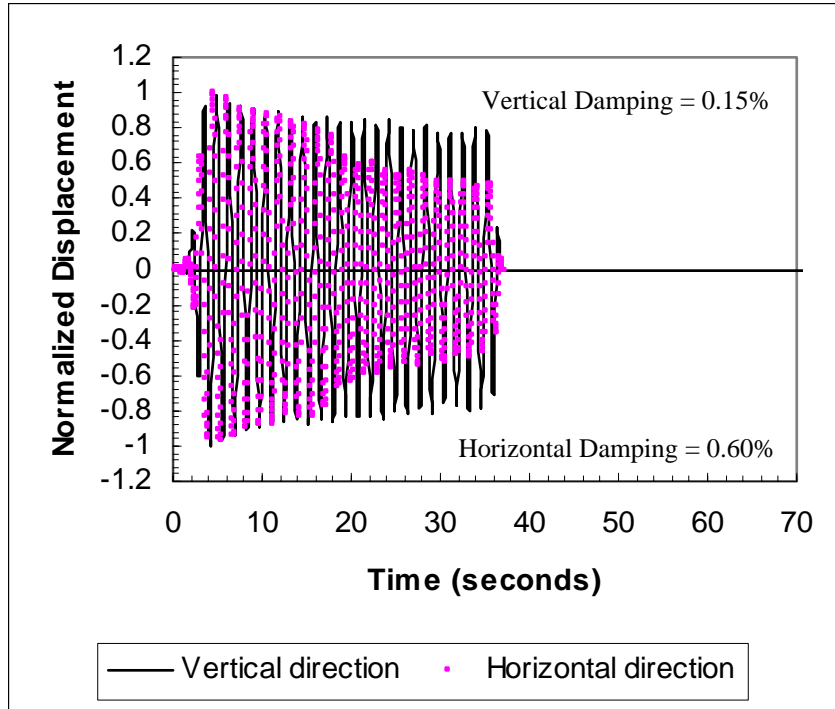


Figure 6.27 - Free Vibration of the Gainesville Long Mast Arm

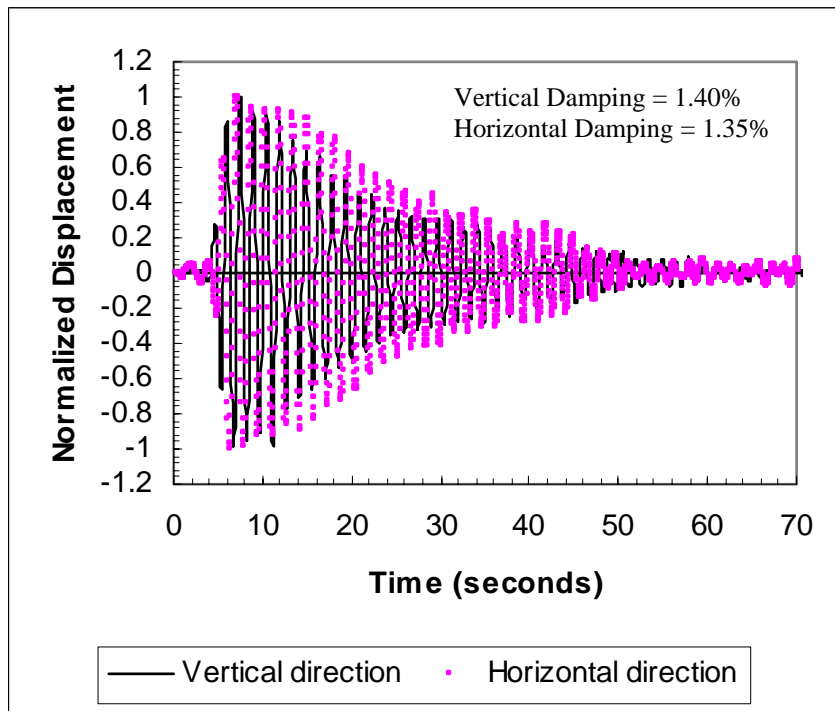


Figure 6.28 - Free Vibration of the Gainesville Long Mast Arm with 3 ft Tapered Impact Damper

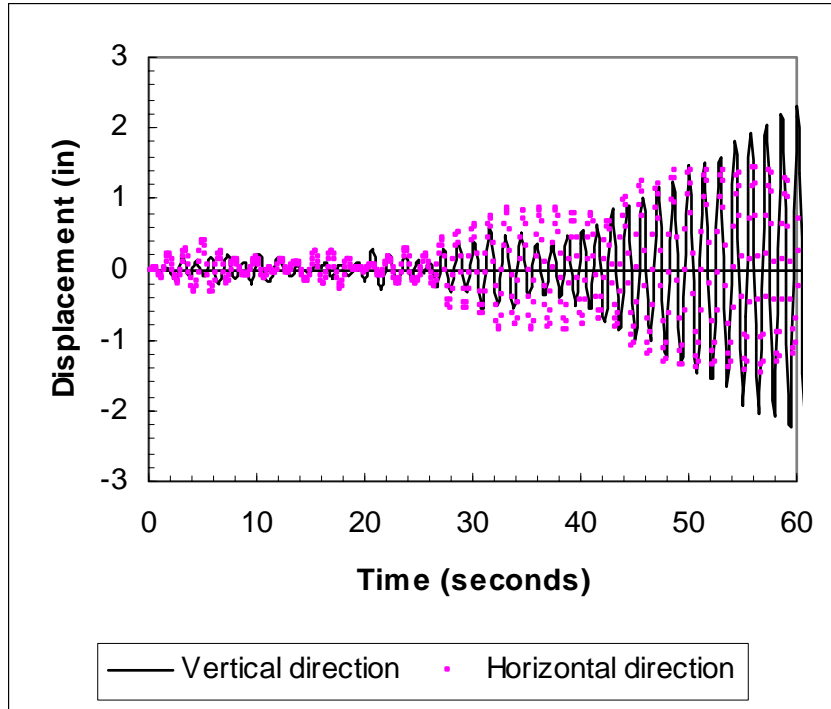


Figure 6.29 - Eccentric Mass and Motor Vibration of the Gainesville Long Mast Arm

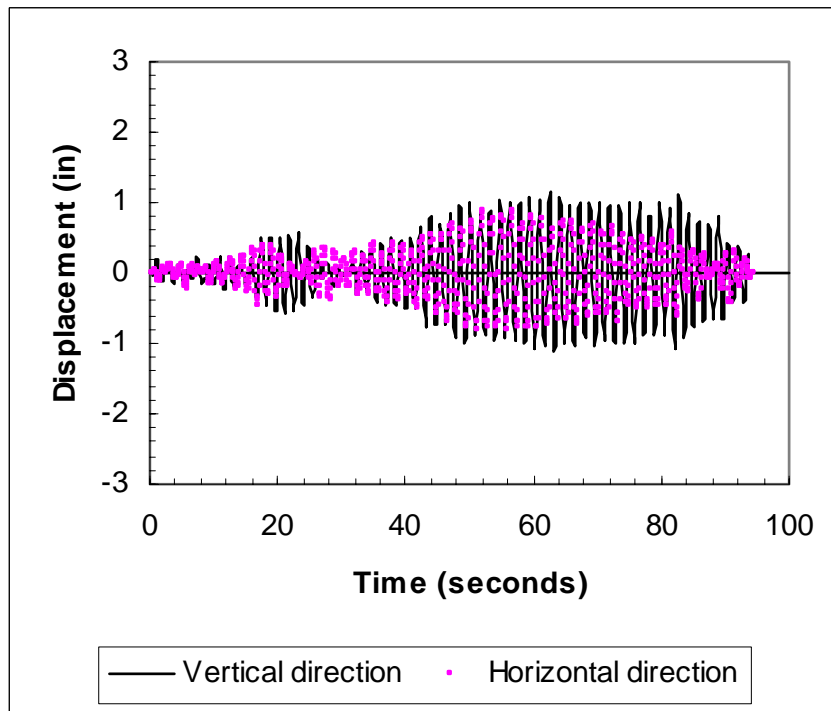


Figure 6.30 - Eccentric Mass and Motor Vibration of the Gainesville Long Mast Arm with 3 ft Tapered Impact Damper

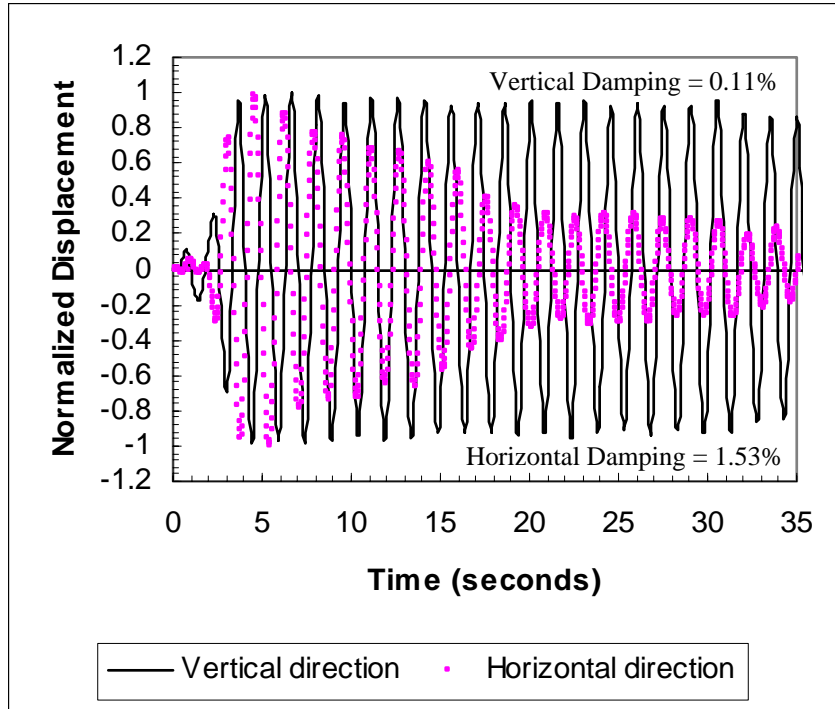


Figure 6.31 - Free Vibration of the Tampa Mast Arm

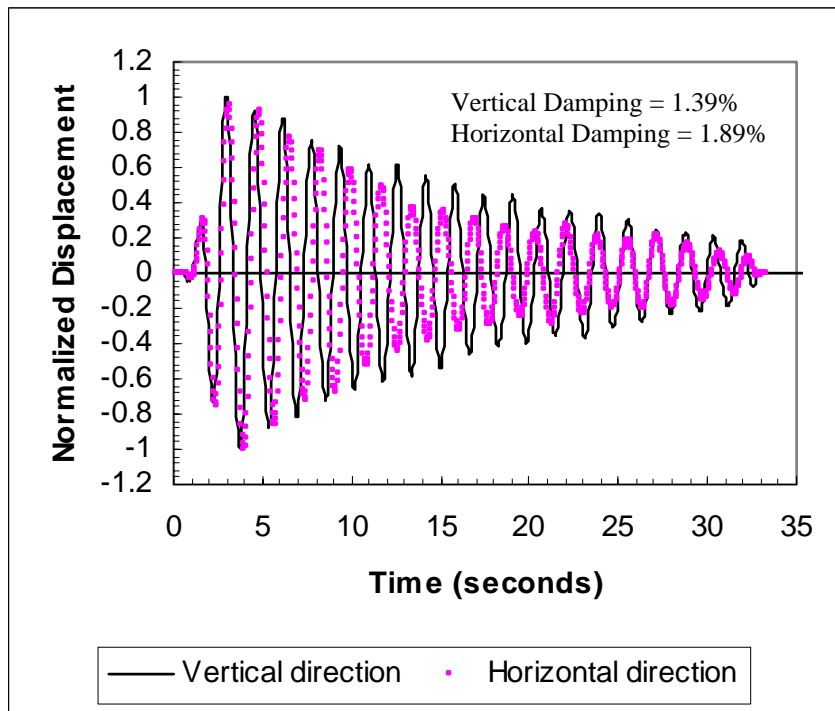


Figure 6.32 - Free Vibration of the Tampa Mast Arm with 3 ft Tapered Impact Damper

The second device was 4 ft long and contained a spring with a stiffness of 2.1 lb/in and a 12 in long, 4 in diameter, 43 lb cylindrical mass. The total weight of this device was 79 lbs. Although this device is too heavy to be added to existing mast arm structures, it could be placed on new structures that are designed for its weight. Using the mast arm design program offered by the FDOT, it was determined that an 80 lb device would increase the moment at the base of the long Gainesville mast arm by 8% and the short Gainesville mast arm by 15%. This moment increase was deemed excessive and therefore the 79 lb device was only tested on the lab mast arm. A drawing and picture of the 4 ft semi-tuned tapered damper are in Figures 6.33 and 6.34 respectively. The free vibration and eccentric mass and motor testing results for this damper are presented in Figures 6.35 and 6.36 respectively.

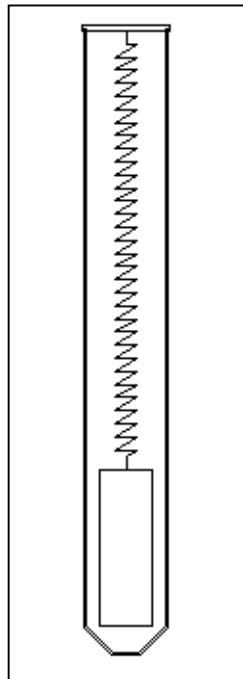


Figure 6.33 - Cross Section Drawing of 4 ft Tapered Impact Damper



Figure 6.34 - 4 ft Tapered Impact Damper



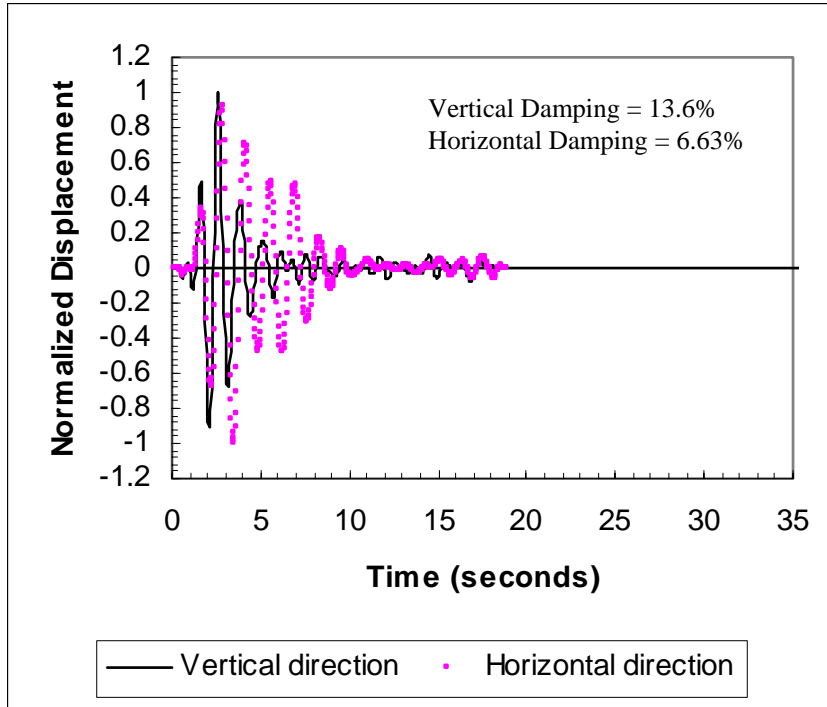


Figure 6.35 - Free Vibration of the Lab Mast Arm with 4 ft Tapered Impact Damper

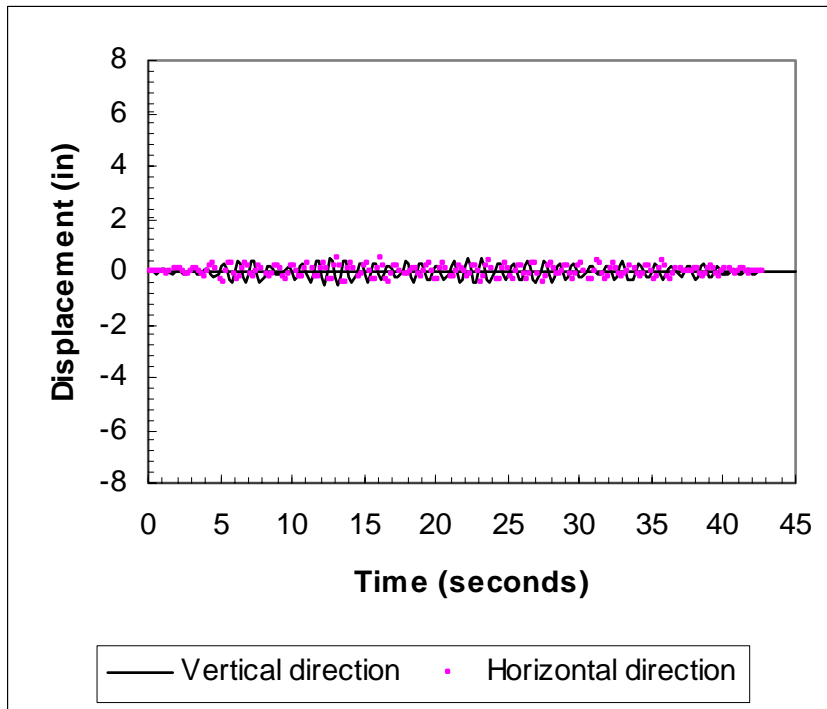


Figure 6.36 - Eccentric Mass and Motor Vibration of the Lab Mast Arm with 4 ft Tapered Impact Damper

Tables 6.4 and 6.5 give a brief summary of all the results of the semi-tuned tapered dampers. The first one shows the percent critical damping values determined and the other indicates total movement of the mast arms under the influence of the eccentric mass and motor device.

Table 6.4 - Summary of Percent Critical Damping Values for Each Tested Mast Arm

Mast Arm	Free Vibrations		3 ft Tapered Impact Damper		4 ft Tapered Impact Damper	
	Vertical	Horizontal	Vertical	Horizontal	Vertical	Horizontal
Lab	0.166%	0.189%	7.28%	3.02%	13.6%	6.63%
Short Gainesville	0.111%	0.316%	2.18%	1.54%	NA	NA
Long Gainesville	0.146%	0.604%	1.40%	1.35%	NA	NA
Tampa	0.107%	1.528%	1.39%	1.89%	NA	NA

Table 6.5 - Summary of Total Displacements Allowed by the Dampers Under the Influence of the Eccentric Mass and Motor Device

Mast Arm	3 ft Tapered Impact Damper		4 ft Tapered Impact Damper	
	Vertical (in)	Horizontal (in)	Vertical (in)	Horizontal (in)
Lab	1.40	0.96	1.12	1.01
Short Gainesville	1.58	1.53	NA	NA
Long Gainesville	2.28	1.75	NA	NA

The target percent critical damping for this research was 5% for both the vertical and horizontal directions. Both semi-tuned tapered dampers exceeded this value on the lab mast arm, with the exception of the 3 ft device's horizontal direction. The 4 ft device performed exceptionally well. However, the values were consistently lower than 5% with the 3 ft damper on the Gainesville and Tampa mast arms. They averaged at about 1.5% critical damping for each arm. But, these low numbers were not as bad as they first

seemed. The results of the eccentric mass and motor vibrations showed that both devices restricted the mast arms' movements to an average of 1.5 in in the vertical and horizontal directions. With this in mind, it appears that the target 5% critical damping value was overkill.

### 6.8 Conclusion

The 3 ft semi-tuned tapered impact damper was selected as the best method for mitigating vibrations in the tested structures. This device was semi-tuned to the range of frequencies seen in the majority of mast arm cantilevers. The damper's spring/mass combination will allow it to be the only damper necessary for all signal structures.

The 3 ft semi-tuned tapered impact damper performed well due to its mass and spring mechanics. As a mast arm oscillates upward in the vertical direction the mass would extend the spring allowing it to impact and rest on the bottom of the damper's shell. This provided a downward force from the mass onto the cantilever as it attempted to move upward. Then, as the mast arm switches directions to move vertically downward, the spring pulls the mass away from the bottom of the damper shell with its built up tensile forces. This allows the cantilever to oscillate downward with only the effects of gravity on it. The weight of the mass is absorbed by the spring. The horizontal damping was effective due to the mast arm having to overcome the mass in the damper as it impacted and pushed against the side-walls of the shell.

Once an optimal damper was selected, it was time to place it on a pole that was known to be susceptible to wind-induced oscillations. The mast arm in Tampa had been reported by the FDOT to undergo significant movement on a regular basis. Chapter 7

describes the field-testing procedures and results for the natural vibration testing of the mast arm in Tampa.

CHAPTER 7  
FIELD TESTING IN TAMPA, FL

7.1 Introduction

The field-testing in Tampa, Florida took place at the intersection of Ulmerton Rd. and Egret Blvd. The mast arm on the SE corner was reported by the FDOT to undergo significant visible movement on a regular basis. The 66 ft cantilever spanned a three-lane road that contained heavy automobile and truck traffic at speeds of 45 to 55 mph. The site was also in a flat and windy area. The surrounding environment was very conducive to wind-induced oscillations of the structure. A plan view of the intersection is located in Figure 7.1.

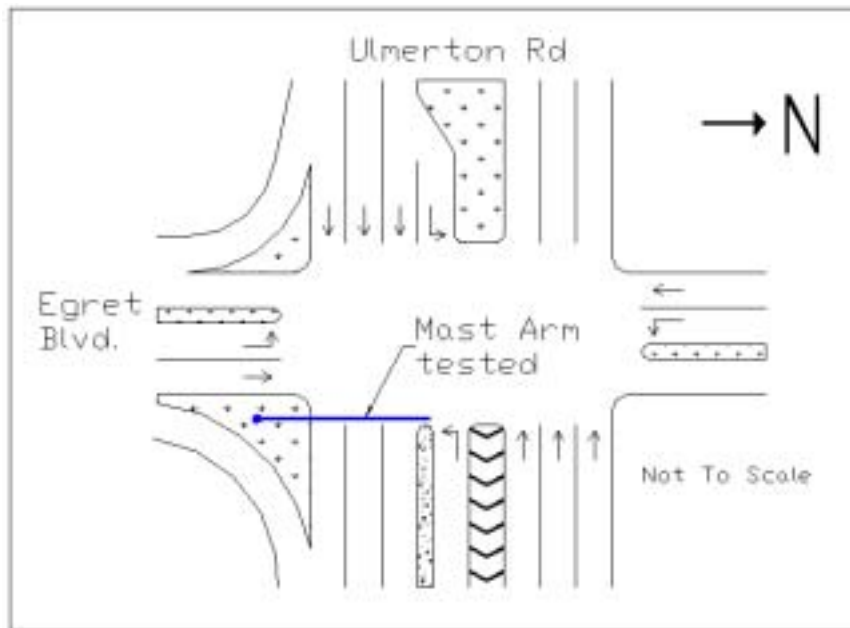


Figure 7.1 - Plan View of Tampa Mast Arm Intersection

## 7.2 Procedure

The first step for the Tampa testing was to instrument the mast arm. Two accelerometers were needed at the tip of the arm and the anemometer and vane were needed at the top of the pole. The accelerometers were housed in a waterproof metal box that was connected to the tip of the cantilever. Accelerometer wires were then attached along the structure from the box to the base of the pole. Wires were also connected from the anemometer and vane to the base of the pole. The mast arm base was located on a built up grassy island. The data acquisition was placed there during testing in order to connect the sensor wires. Figure 7.2 shows the instrumentation setup.

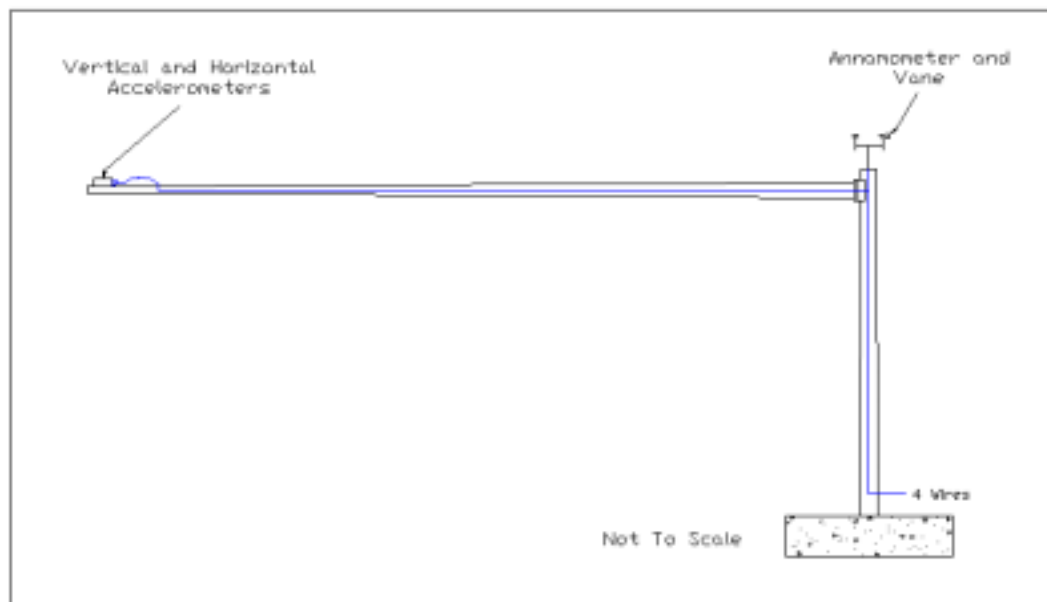


Figure 7.2 - Instrumentation Setup for Tampa Mast Arm

Once the instrumentation was in place, data readings were taken from the mast arm without a damper placed on it. This was done to get an idea of how much the

structure moved under its natural conditions. Several random data sets were recorded on four separate days. These data sets were approximately two minutes long each. The wind direction, wind speed, and mast arm tip displacements were then obtained from the data. Next, the 3 ft semi-tuned tapered impact damper was attached to the tip of the mast arm. Similar data readings were taken to see how much the structure moved with the damping device in place.

### 7.3 Results

The data of most interest was when the winds were either out of the west or east. The winds from the west were in the direction of traffic (impacted the front of the structure), while the winds from the east were into the traffic (impacted the back of the structure). Results will be presented from winds impacting the front and back of the mast arm in the 90-degree range on each side of the mast arm indicated in Figure 7.3.

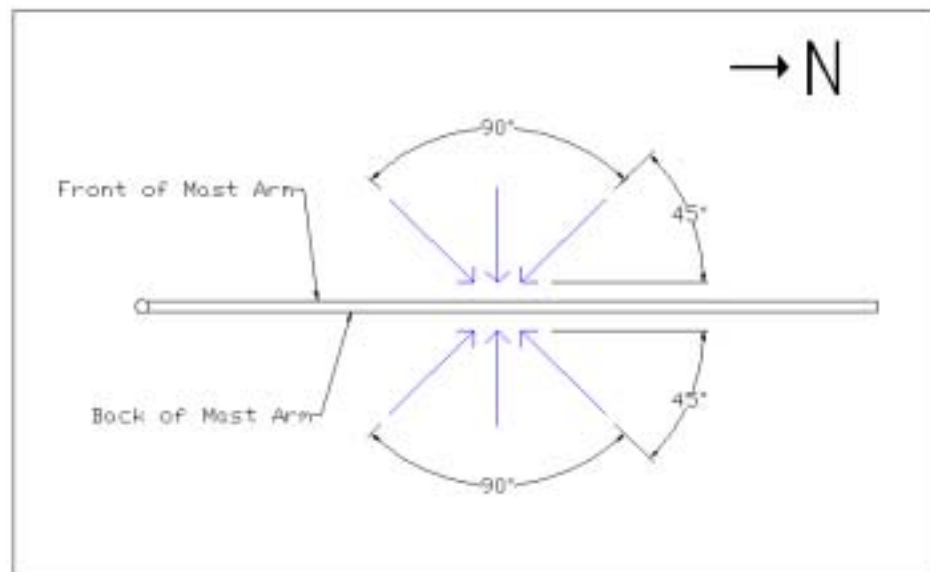


Figure 7.3 - Range of Wind Directions for Test Results

Figures 7.4 through 7.7 present the displacement vs. wind speed data for the Tampa mast arm with and without the 3 ft tapered impact damper attached.

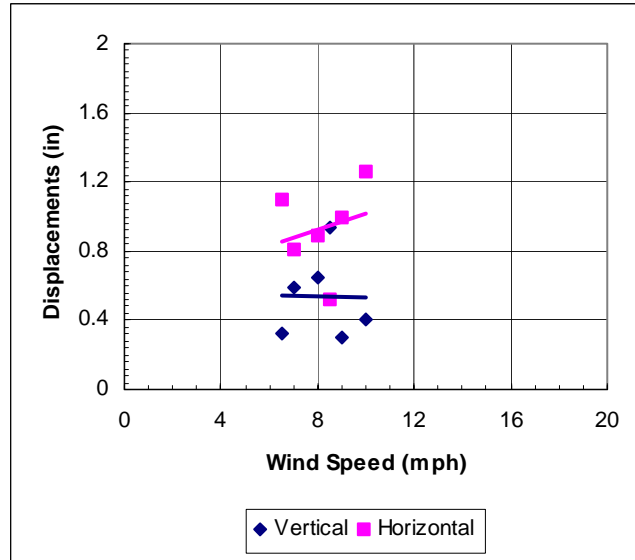


Figure 7.4 - Natural Vibration Displacements of the Tampa Mast Arm (Winds on the Front)

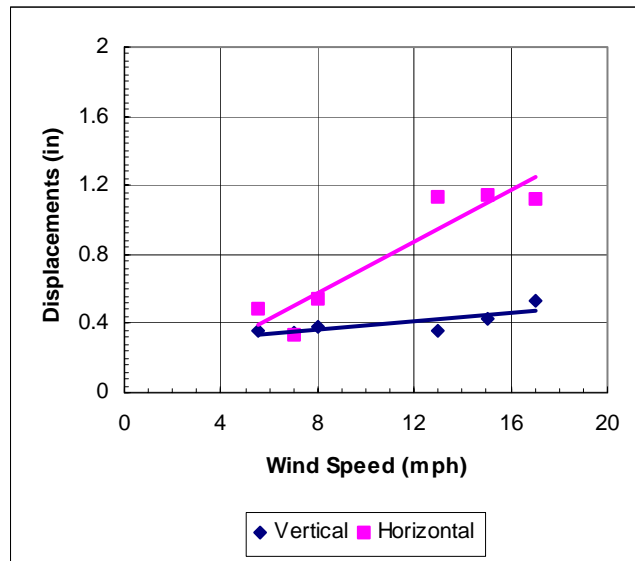


Figure 7.5 - Natural Vibration Displacements of the Tampa Mast Arm with the 3 ft Tapered Impact Damper (Winds on the Front)



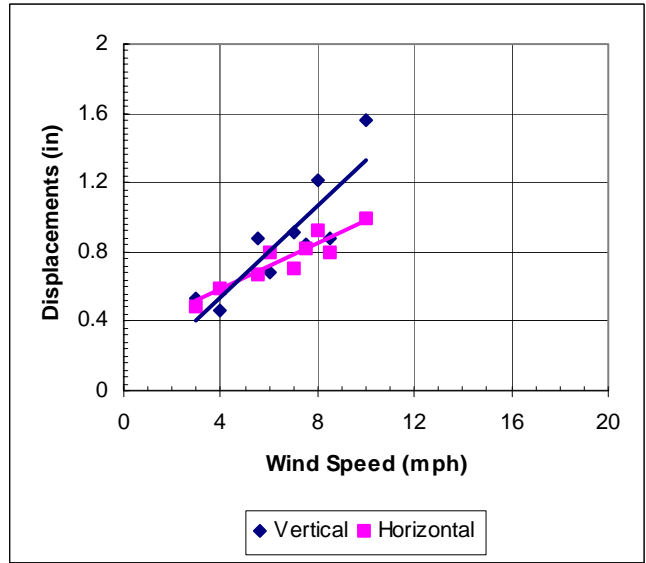


Figure 7.6 - Natural Vibration Displacements of the Tampa Mast Arm (Winds on the Back)

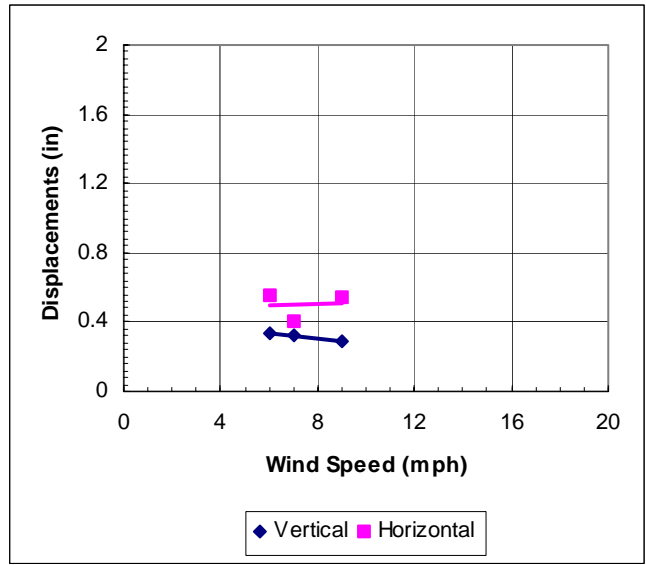


Figure 7.7 - Natural Vibration Displacements of the Tampa Mast Arm with the 3 ft Tapered Impact Damper (Winds on the Back)

#### 7.4 Conclusion

The results from the Tampa natural vibration testing were somewhat limited but very useful nonetheless. The winds only exceeded 10 mph during one of the days of testing. The remaining days produced informative data, but did not offer a wide range of wind speeds. Therefore, the ability of the damper to resist large displacements (ie. greater than 8 in) is still unknown.

The vibrations of the mast arm without the damper attached proved to occur predominately in the horizontal direction with the wind on the front of the structure, but occurred in both the vertical and horizontal directions with the wind on the back of the structure. It is important to recall that Kaczinski et al. [5] reported similar results for cantilevered mast arm structures. They indicated that these structures are more susceptible to galloping and slight vortex shedding when winds are from the rear, the signals are mounted vertically, and when backplates are used on the signals. These conditions all existed on the Tampa structure at one point. If the vertical and horizontal displacement lines in Figure 7.6 were to be extrapolated to higher wind speeds, it is possible the Tampa mast arm could and does experience large movements in both directions as a result of these conditions. The horizontal natural vibration movement from the frontal winds was predominately due to the combination of wind and truck gusts.

The 3 ft tapered damper performed exceptionally well in the vertical direction of motion. It restricted the mast arm to approximately 0.4 in displacement with wind conditions on both the front and back of the structure. If the vertical displacement lines in Figures 7.5 and 7.7 were to be extrapolated to greater wind speeds, an increase in

allowed displacements would not be expected. The damper limited the horizontal motion when winds were on the back of the structure, but did not perform as well with wind on the front of the structure. Although, the horizontal displacements with the damper were lower than those without the damper, they still tended to increase with increased wind speed. However, the pole's movement slowed much quicker, when the winds ceased, with the damper in place than it did without it.

Overall, the 3 ft tapered impact damper performed very well. One test day produced wind gust measurements as high as 25 mph, with an average wind speed of 17 mph (See Figure 7.5). The remaining three mast arms at the Tampa intersection were observed to move considerably, while the test structure was held to approximately 0.5 in vertically and 1.2 in horizontally. This researcher estimated the other three structures to each be moving 4 to 6 in vertically and 2 to 4 in horizontally. Therefore, it is believed that the 3 ft tapered impact damper is effective in preventing excessive displacements in mast arm structures as well as reducing the amount of wind-induced oscillations.

## CHAPTER 8 SUMMARY, CONCLUSIONS, AND RECOMMENDATIONS

### 8.1 Summary

The purpose of this research was to develop a damping device to mitigate wind-induced vibrations in cantilevered mast arm signal structures. A mast arm was constructed at the University of Florida structures laboratory. The lab mast arm and two existing mast arms in Gainesville, Florida were used to test the developed damping devices. The final damper design was tested on a mast arm in Tampa, Florida due to its susceptibility and history of wind-induced oscillations.

This research started with a literature review based on the types of wind phenomena that cause wind-induced vibrations in mast arm structures. It was determined that vortex shedding, galloping, natural wind gusts, and truck-induced wind gusts can all be responsible for the movement of these cantilevered structures. Vortex shedding was probably the least likely cause of oscillations due to the tapered geometry of most horizontal cantilevers. However, it is possible that vertically mounted lights could experience vortex shedding enough to initiate galloping. Galloping was probably the main cause of excessive vibrations. The galloping phenomena can occur with winds from virtually any direction. Natural wind gusts were not thought to be the main cause of fatigue failure, but they are significant enough to be considered. Finally, truck-induced wind gusts cause relatively small and quick vibrations. However, some roads have high volumes of truck traffic and can inflict numerous oscillation cycles on a structure.

Next, the FDOT report by Michael A. Kalajian was reviewed. Kalajian's report was the base for the research performed in this paper. Several types of damper's were built and tested by Kalajian. Some of his dampers included adaptations to Stockbridge dampers, liquid dampers, spring/mass tuned dampers, double spring/mass system dampers, and a woodpecker damper. Kalajian's final device was a 4 in to 2 in tapered impact damper. This device was the starting point for the research in this paper.

The first two devices developed were an attempt to maintain the vertical percent critical damping of Kalajian's device, while increasing the horizontal percent critical damping. They were a round impact damper and an eight-inch tapered impact damper. However, due to the height of each device, neither one was effective in the vertical direction. But the round device was effective in the horizontal direction. From here a longer version of the 4 in to 2 in tapered impact damper was built to better understand what range of damper frequencies were effective on certain mast arms. Also, a six-inch diameter pipe was used to test what horizontal frequencies (spring lengths) were most effective on certain poles. Parameters were then set forth for an optimal device to be designed from. From these parameters, two devices were built weighing 40 lbs and 79 lbs. The 79 lb device was determined to be overkill in design and unsafe for implementing of existing mast arm structures. The 40 lb device (3 ft tapered impact damper) became the selected device for this research.

The selected damper provided approximately 1.5 percent of critical damping, in the vertical and horizontal directions, on the primary mode of each existing structure tested. It also restricted the vertical and horizontal movement of the lab and Gainesville mast arms to 1.5 in when subjected to the eccentric mass and motor device (sinusoidal

vibration excitation device). The selected damper was also placed on the Tampa mast arm and tested against natural wind vibrations. It restricted vertical movement of the cantilever to approximately 0.4 in with wind gusts up to 25 mph and sustained winds up to 17 mph. The damper only slightly reduced the arm's movement in the horizontal direction but was very effective in bringing it to a stop quickly after wind gusts. Overall, it is believed that the 3 ft tapered impact damper would be effective in preventing excessive displacements in cantilevered mast arm structures as well as reduce the amount of wind-induced oscillations.

The fabrication drawings that will be used in the specification for the 3 ft tapered impact damper are located in Appendix C.

## 8.2 Conclusions

The results of this study indicated the following:

- the dominant frequencies present in the mast arm structures are in the approximate range of 0.6 Hz and 1.4 Hz.
- natural frequencies of mast arm structures can be determined within approximately 5% accuracy using a line model dynamic analysis.
- the spring/mass combination in a damper for mast arm structures needs to be semi-tuned to approximately 0.7 Hz for optimal vertical damping.
- the spring length in a damper for mast arm structures needs to be between 25 in and 30 in for optimal horizontal damping.
- a one inch gap between the damper's mass and shell during its at rest state provides optimal percent critical damping.

- A high percent critical damping does not insure the most optimal damper.
- the fatigue failures occurring in mast arm structures can be reduced with the implementation of the 3 ft tapered impact damper.
- the 3 ft tapered impact damper successfully increased the percent critical damping of the tested mast arms and reduced the wind-induced displacements on the Tampa mast arm.

### 8.3 Recommendations

Although the selected device performed well at mitigating wind-induced vibrations, it still needs to be tested under higher wind speed conditions. The device will also need to be galvanized in its final state to protect it against the elements. The damper is not loud at the device when it impacts, but it can be heard at the base of the pole. The noise needs to be eliminated while maintaining the effectiveness of the damper. Finally, a standard signal attachment bracket was used to mount the damper to the test mast arms. However, a final attachment bracket will need to be specified.

## LIST OF REFERENCES

1. Cook, R.A., Bloomquist, D., Agosta, A.M., Taylor, K.F., Wind Load Data for Variable Message Signs, Report No. FL/DOT/RMC/0728-9488, Engineering and Industrial Experiment Station, University of Florida, Gainesville, FL, 1996.
2. Fouad, H.F., Calvert, E.A, Nunez, E., Structural Supports for Highway Signs, Luminaires, and Traffic Signals, NCHRP Report 411, National Academy Press, Washington D.C., 1998.
3. Harris, C.M., Shock and Vibration Handbook, Fourth Edition, McGraw-Hill, New York, NY, 1996.
4. Hartog, J.P. Den, Mechanical Vibrations, Third Edition, McGraw-Hill, New York, NY, 1947.
5. Kaczinski, M.R., Dexter, R.J., Van Dien, J.P., Fatigue-Resistant Design of Cantilevered Signal, Sign and Light Supports, NCHRP 412, National Academy Press, Washington D.C., 1998.
6. Kalajian, M.A., Design of Mechanical Damping System for Mast Arm Traffic Signal Structures, University of Florida, Gainesville, FL, 1998.
7. Kolousek, V., Wind Effects on Civil Engineering Structures, Elsevier, New York, NY, 1984.
8. McDonald, J.R., Mehta, K.C., Oler, W.W., Pulipaka, N., Wind Load Effects on Signs, Luminaries, and Traffic Signal Structures, Wind Engineering Research Center, Texas Tech University, Lubbock, Texas, 1995.
9. Sachs, P., Wind Forces in Engineering, Second Edition, Pergamon Press, Oxford, England, 1978.
10. Smith, J.W., Vibrations of Structures - Applications in Civil Engineering Design, Chapman and Hall, New York, NY, 1988.



## APPENDIX A SAMPLE DATA MANIPULATION MATHCAD WORKSHEET

Read in the given data ...

time := READPRN("Time.prn.txt")

V\_accel := READPRN("VA.prn.txt")

H\_accel := READPRN("HA.prn.txt")

Anemometer := READPRN("Anemometer.prn.txt")

Vane := READPRN("Vane.prn.txt")

Determine the time step ...

$$h := \frac{\max(\text{time})}{\text{last}(\text{time}) - 1} \quad h = 0.01 \quad (\text{sec})$$

Use smoothing in the worksheet? ...

no := 0      yes := 1      smoothing\_active := yes

Plot all the given data ...

ndata := last(V\_accel)      ndata = 3313

end := max(time)      end = 33.12

i := 1..ndata

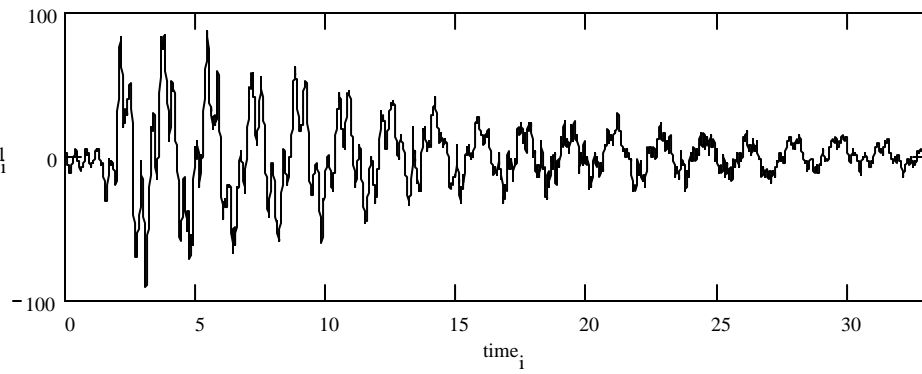
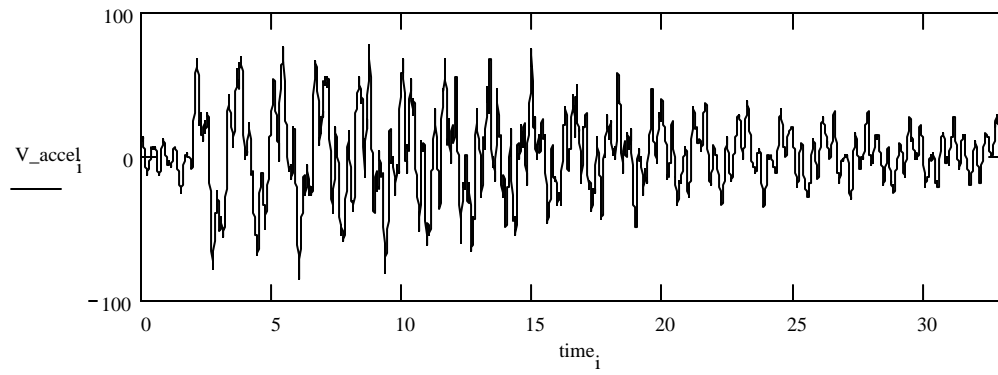
$$V\_accel_i := \frac{V\_accel_i}{1.58}$$

*Note: The 1.58 value is due to a voltage amplification in the accelerometer filter*

$$H\_accel_i := \frac{H\_accel_i}{1.58}$$

*Note: The 1.58 value is due to a voltage amplification in the accelerometer filter*

time\_i := i·h



Pad the data for a Fast Fourier Transform ...

```
nfft(ndata) :=
  a ← 1
  b ← 2a
  while ndata > b
    a ← a + 1
    b ← 2a
  b
```

$nfft := nfft(ndata)$        $nfft = 4096$

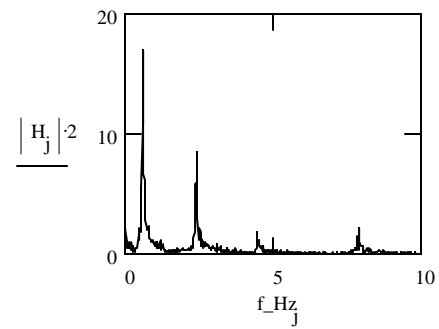
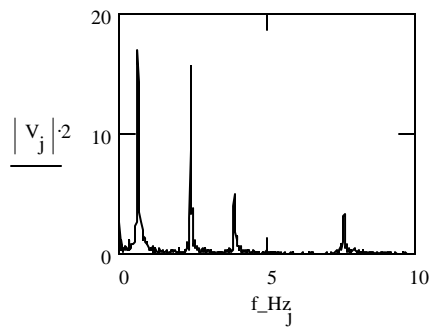
$itmp := 1, 2.. ndata$        $V\_accel_{itmp} := V\_accel_{itmp}$        $H\_accel_{itmp} := H\_accel_{itmp}$

$itmp := ndata + 1.. nfft$        $V\_accel_{itmp} := 0$        $H\_accel_{itmp} := 0$

Perform a Fast Fourier Transform & filter the data at 1.5 Hz ...

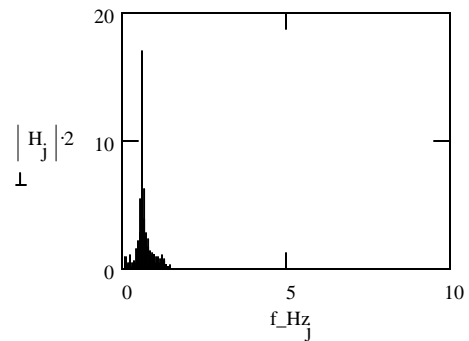
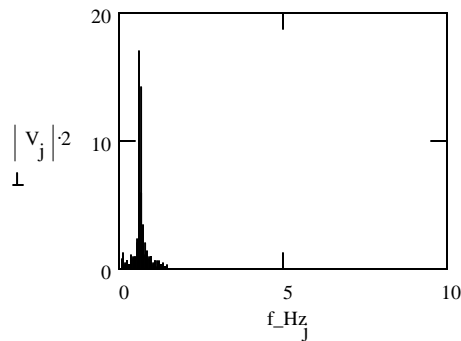
```
i := 1, 2.. nfft      time_i := i·h      V := FFT(V_accel)      H := FFT(H_accel)      j := 1.. last(V)
```

```
T-bar : T_ := nfft·h      Freq.  $\omega$  in rad/sec :  $\omega_{\text{rad}_s_j} := \frac{2 \cdot \pi \cdot j}{T_}$       Freq.  $\omega$  in Hz :  $f_{\text{Hz}_j} := \frac{j}{T_}$ 
```



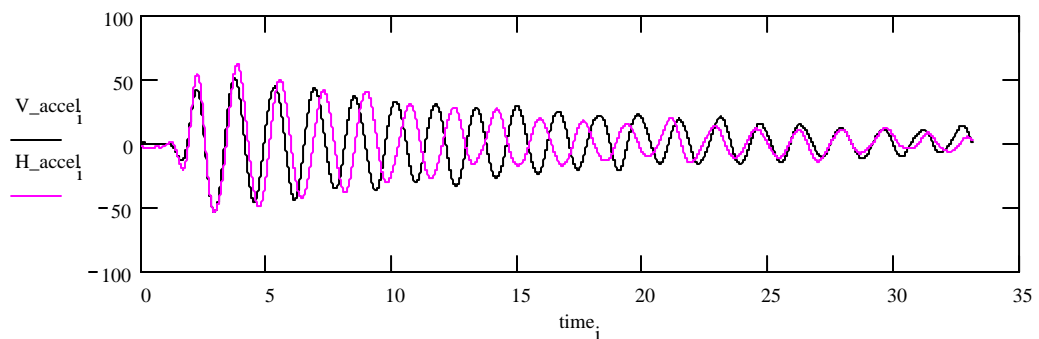
```
filter(val, index, limit) := if(index > limit, 0, val)
```

```
V_j := filter(V_j, f_Hz_j, 1.5)      H_j := filter(H_j, f_Hz_j, 1.5)
```



```
V_accel := IFFT(V)      H_accel := IFFT(H)      i := 1.. ndata
```

Plot the filtered data ...



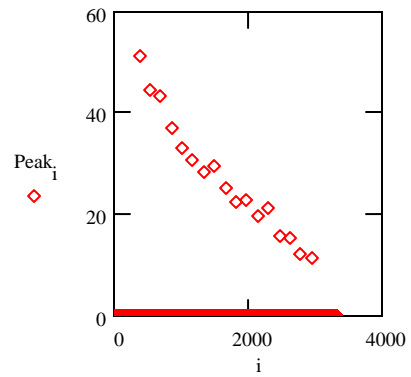
Determine the Vertical period of the system based on the vertical acceleration data ...

$$u''_i := V\_accel_i \quad u''_i := \begin{cases} u''_i & \text{if } u''_i \geq 0 \\ 0 & \text{otherwise} \end{cases}$$

```
start(u'') := j ← 1
              while u''_j ≠ max(u'')
                j ← j + 1
              j
start := start(u'')
start = 373
```

```
Peaks(u'') := for j ∈ 1..(start - 1)
               Peak1_j ← 0
               Peak2_j ← 0
               for j ∈ start..ndata
                 Peak1_j ← u''_j if u''_j < u''_{j-1}
                           0 otherwise
               for j ∈ (start - 1)..ndata
                 Peak2_j ← u''_j if Peak1_j > Peak1_{j-1}
                           0 otherwise
               Peak2
```

```
Peak := Peaks(u'')
k := 3000..ndata
Peak_k := 0
```



```
i1(Peak) := i1 ← 1
            while Peak_{i1} = 0
              i1 ← i1 + 1
            i1
```

```
i2(Peak) := i2 ← 0
            for tempi ∈ 1..ndata
              i2 ← i2 if Peak_{tempi} = 0
              i2 ← tempi otherwise
            i2
```

```
c(Peak) := c ← 0
           for i ∈ 1..ndata
             c ← c if Peak_i = 0
             c ← c + 1 otherwise
           c
```

```
i1 := i1(Peak)    i1 = 374
i2 := i2(Peak)    i2 = 2960
c := c(Peak)      c = 17
```

$$V\_Period := \frac{time_{i2} - time_{i1}}{c - 1}$$

$$V\_Frequency := \frac{1}{V\_Period}$$

V\_Period = 1.616

V\_Frequency = 0.619

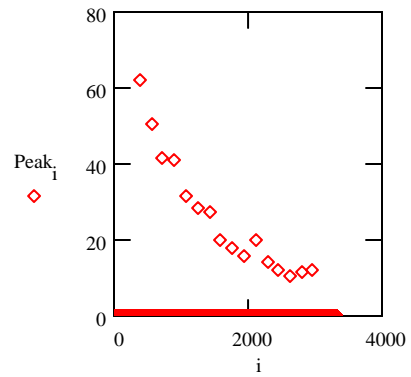
Determine the Horizontal period of the system based on the horizontal acceleration data ...

$$u''_i := H\_accel_i \quad u''_i := \begin{cases} u''_i & \text{if } u''_i \geq 0 \\ 0 & \text{otherwise} \end{cases}$$

```
start(u'') := | j ← 1
               | while u''_j ≠ max(u'')
               |   j ← j + 1
               | j
start := start(u'')      start = 384
```

```
Peaks(u'') := | for j ∈ 1..(start - 1)
               |   Peak1_j ← 0
               |   Peak2_j ← 0
               | for j ∈ start..ndata
               |   Peak1_j ← | u''_j if u''_j < u''_{j-1}
               |               | 0 otherwise
               | for j ∈ (start - 1)..ndata
               |   Peak2_j ← | u''_j if Peak1_j > Peak1_{j-1}
               |               | 0 otherwise
               | Peak2
```

```
Peak := Peaks(u'')      k := 3000..ndata      Peak_k := 0
```



```
i1(Peak) := | i1 ← 1
              | while Peak_{i1} = 0
              |   i1 ← i1 + 1
              | i1
```

```
i2(Peak) := | i2 ← 0
              | for tempi ∈ 1..ndata
              |   | i2 ← i2 if Peak_{tempi} = 0
              |   | i2 ← tempi otherwise
              | i2
```

```
c(Peak) := | c ← 0
            | for i ∈ 1..ndata
            |   | c ← c if Peak_i = 0
            |   | c ← c + 1 otherwise
            | c
```

```
i1 := i1(Peak)      i1 = 385
i2 := i2(Peak)      i2 = 2970
c := c(Peak)        c = 16
```

$$H\_Period := \frac{time_{i2} - time_{i1}}{c - 1}$$

$$H\_Frequency := \frac{1}{H\_Period}$$

H\_Period = 1.723

H\_Frequency = 0.58

Define smoothing function ...

$$uv''_i := V\_accel_i \quad uh''_i := H\_accel_i$$

$$w\_smooth(vy, b, h) := \left| \begin{array}{l} npnt \leftarrow \text{if} \left[ \left[ \left( \frac{b}{h} \right) \cdot \frac{1}{2} \right] - \text{floor} \left[ \left( \frac{b}{h} \right) \cdot \frac{1}{2} \right] < 0.5, \text{floor} \left[ \left( \frac{b}{h} \right) \cdot \frac{1}{2} \right], \text{ceil} \left[ \left( \frac{b}{h} \right) \cdot \frac{1}{2} \right] \right] \\ n \leftarrow \text{last}(vy) \\ \text{for } i \in \text{ORIGIN}.n \\ \quad \left| \begin{array}{l} n\_half \leftarrow 0 \\ n\_half \leftarrow (i - \text{ORIGIN}) \text{ if } i < npnt \\ n\_half \leftarrow npnt \text{ if } (i - \text{ORIGIN} \geq npnt) \cdot (i \leq (n - npnt)) \\ n\_half \leftarrow (n - i) \text{ if } i > (n - npnt) \\ \text{sum} \leftarrow 0.0 \\ \text{for } j \in (i - n\_half)..(i + n\_half) \\ \quad \text{sum} \leftarrow \text{sum} + vy_j \\ f_i \leftarrow \frac{\text{sum}}{1 + 2 \cdot n\_half} \end{array} \right. \\ f \end{array} \right.$$

$$smooth(vy, b, h) := \left| \begin{array}{l} f \leftarrow w\_smooth(vy, b, h) \text{ if } \text{smoothing\_active} = \text{yes} \\ \text{for } i \in \text{ORIGIN}. \text{last}(vy) \text{ otherwise} \\ \quad f_i \leftarrow 0 \\ f \end{array} \right.$$

Define trapezoid rule function ...

$$\text{trapezoid}(f, h) := \left| \begin{array}{l} fint_1 \leftarrow 0 \\ \text{for } i \in \text{ORIGIN}+1.. \text{last}(f) \\ \quad fint_i \leftarrow fint_{i-1} + \frac{h}{2} \cdot (f_{i-1} + f_i) \\ fint \end{array} \right.$$

Integrate the acceleration and velocity data to obtain displacements ...

$$uv' := \text{trapezoid}(uv'', h)$$

$$uh' := \text{trapezoid}(uh'', h)$$

$$uv'_{\text{center}} := \text{smooth}(uv', V\_Period, h)$$

$$uh'_{\text{center}} := \text{smooth}(uh', H\_Period, h)$$

$$uv'_i := uv'_i - uv'_{\text{center}_i}$$

$$uh'_i := uh'_i - uh'_{\text{center}_i}$$

$$uv := \text{trapezoid}(uv', h)$$

$$uh := \text{trapezoid}(uh', h)$$

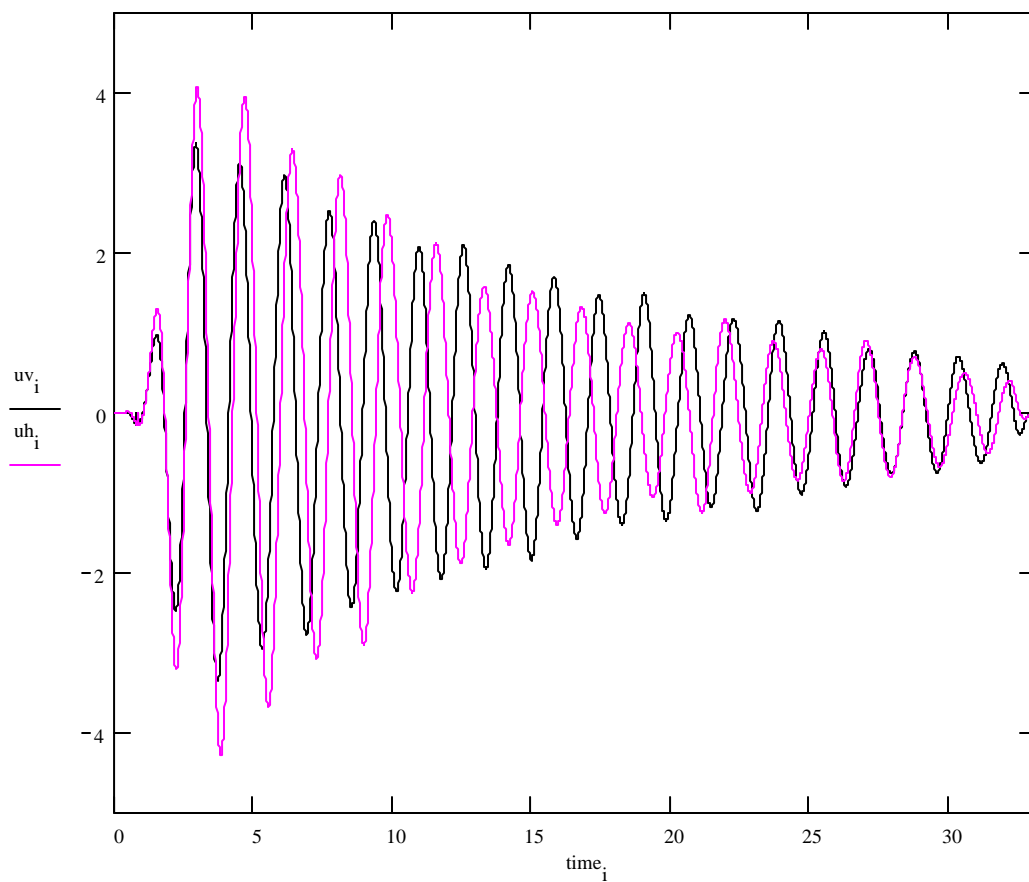
$$uv_{\text{center}} := \text{smooth}(uv, V\_Period, h)$$

$$uh_{\text{center}} := \text{smooth}(uh, H\_Period, h)$$

$$uv_i := uv_i - uv_{\text{center}_i}$$

$$uh_i := uh_i - uh_{\text{center}_i}$$

Plot the calculated displacement data ...



Plot the peaks of the displacement for percent critical damping calculations ...

$$uv\_temp_i := \begin{cases} uv_i & \text{if } uv_i \geq 0 \\ 0 & \text{otherwise} \end{cases}$$

$$start(uv\_temp) := \begin{cases} j \leftarrow 1 \\ \text{while } uv\_temp_j \neq \max(uv\_temp) \\ \quad j \leftarrow j + 1 \\ j \end{cases}$$

$$start := start(uv\_temp)$$

$$v\_peaks(uv\_temp) := \begin{cases} \text{for } j \in 1..(start - 1) \\ \quad \begin{cases} Peak1_j \leftarrow 0 \\ Peak2_j \leftarrow 0 \end{cases} \\ \quad \text{for } j \in start..ndata \\ \quad \quad Peak1_j \leftarrow \begin{cases} uv\_temp_j & \text{if } uv\_temp_j < uv\_temp_{j-1} \\ 0 & \text{otherwise} \end{cases} \\ \quad \quad \text{for } j \in (start - 1)..ndata \\ \quad \quad \quad Peak2_j \leftarrow \begin{cases} uv\_temp_j & \text{if } Peak1_j > Peak1_{j-1} \\ 0 & \text{otherwise} \end{cases} \\ \quad \quad Peak2 \end{cases}$$

$$uh\_temp_i := \begin{cases} uh_i & \text{if } uh_i \geq 0 \\ 0 & \text{otherwise} \end{cases}$$

$$start(uh\_temp) := \begin{cases} j \leftarrow 1 \\ \text{while } uh\_temp_j \neq \max(uh\_temp) \\ \quad j \leftarrow j + 1 \\ j \end{cases}$$

$$start := start(uh\_temp)$$

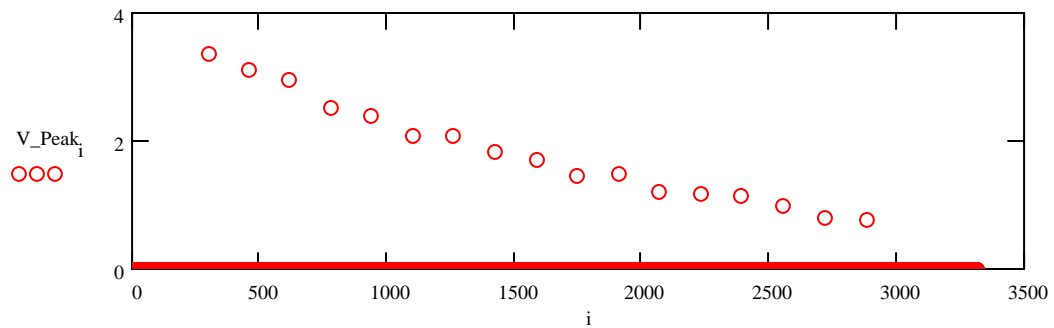


```

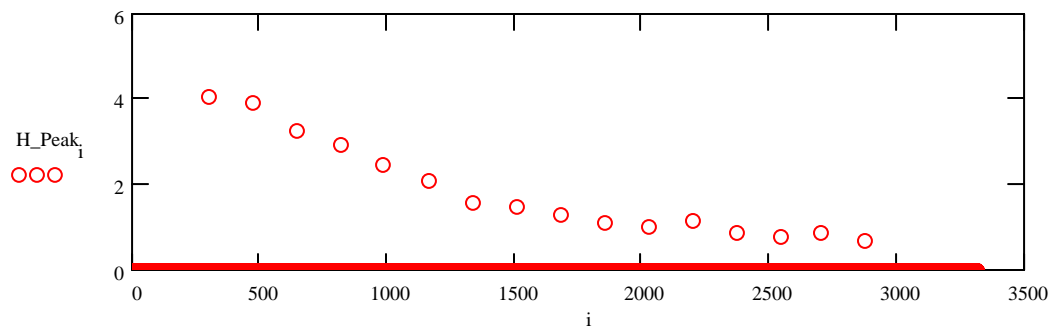
h_peaks (uh_temp) :=
  for j ∈ 1..(start - 1)
    Peak1j ← 0
    Peak2j ← 0
  for j ∈ start .. ndata
    Peak1j ←
      uh_tempj if uh_tempj < uh_tempj-1
      0 otherwise
  for j ∈ (start - 1) .. ndata
    Peak2j ←
      uh_tempj if Peak1j > Peak1j-1
      0 otherwise
  Peak2

```

V\_Peak := v\_peaks (uv\_temp)      k := 3000.. ndata      V\_Peak<sub>k</sub> := 0



H\_Peak := h\_peaks (uh\_temp)      k := 3000.. ndata      H\_Peak<sub>k</sub> := 0



Calculate the vertical and horizontal percent critical damping ...

```

δ(V_Peak) :=
i ← 1
Total ← 0
while V_Peaki ≠ 0
  i ← i + 1
t ← 1
temp1 ← V_Peaki
i ← i + 1
while i ≤ ndata
  while V_Peaki ≠ 0
    i ← i + 1
    break if i = ndata
  break if i = ndata
  t ← t + 1
  temp2 ← V_Peaki
  Cr_Damp ← ln( temp1 / temp2 )
  Total ← Total + Cr_Damp
  temp1 ← temp2
  i ← i + 1
δ ← ( Total / (t - 1) )
δ

```

$$V\delta := \delta(V\_Peak)$$

$$V\_Critical\_Damping := \left[ \frac{V\delta}{\sqrt{(4 \cdot \pi^2) - V\delta^2}} \right] \cdot 100$$

$$V\_Critical\_Damping = 1.464$$

```

δ(H_Peak) :=
i ← 1
Total ← 0
while H_Peaki ≠ 0
  i ← i + 1
t ← 1
temp1 ← H_Peaki
i ← i + 1
while i ≤ ndata
  while H_Peaki ≠ 0
    i ← i + 1
    break if i = ndata
  break if i = ndata
  t ← t + 1
  temp2 ← H_Peaki
  Cr_Damp ← ln( temp1 / temp2 )
  Total ← Total + Cr_Damp
  temp1 ← temp2
  i ← i + 1
δ ← ( Total / (t - 1) )
δ

```

$$H\delta := \delta(H\_Peak)$$

$$H\_Critical\_Damping := \left[ \frac{H\delta}{\sqrt{(4 \cdot \pi^2) - H\delta^2}} \right] \cdot 100$$

$$H\_Critical\_Damping = 1.872$$

Determine the windspeed and direction ...

$$\text{Anna\_temp}_i := \left( \begin{array}{l} \text{Anemometer}_i \text{ if } \text{Anemometer}_i \geq 0 \\ 0 \text{ otherwise} \end{array} \right)$$

start := 3

$$\text{peaks}(\text{Anna\_temp}) := \left( \begin{array}{l} \text{for } j \in 1..(\text{start} - 1) \\ \quad \left| \begin{array}{l} \text{Peak1}_j \leftarrow 0 \\ \text{Peak2}_j \leftarrow 0 \end{array} \right. \\ \text{for } j \in \text{start}.. \text{ndata} \\ \quad \text{Peak1}_j \leftarrow \left( \begin{array}{l} \text{Anna\_temp}_j \text{ if } \text{Anna\_temp}_j < \text{Anna\_temp}_{j-1} \\ 0 \text{ otherwise} \end{array} \right) \\ \text{for } j \in (\text{start} - 1).. \text{ndata} \\ \quad \text{Peak2}_j \leftarrow \left( \begin{array}{l} \text{Anna\_temp}_j \text{ if } \text{Peak1}_j > \text{Peak1}_{j-1} \\ 0 \text{ otherwise} \end{array} \right) \\ \text{Peak2} \end{array} \right)$$

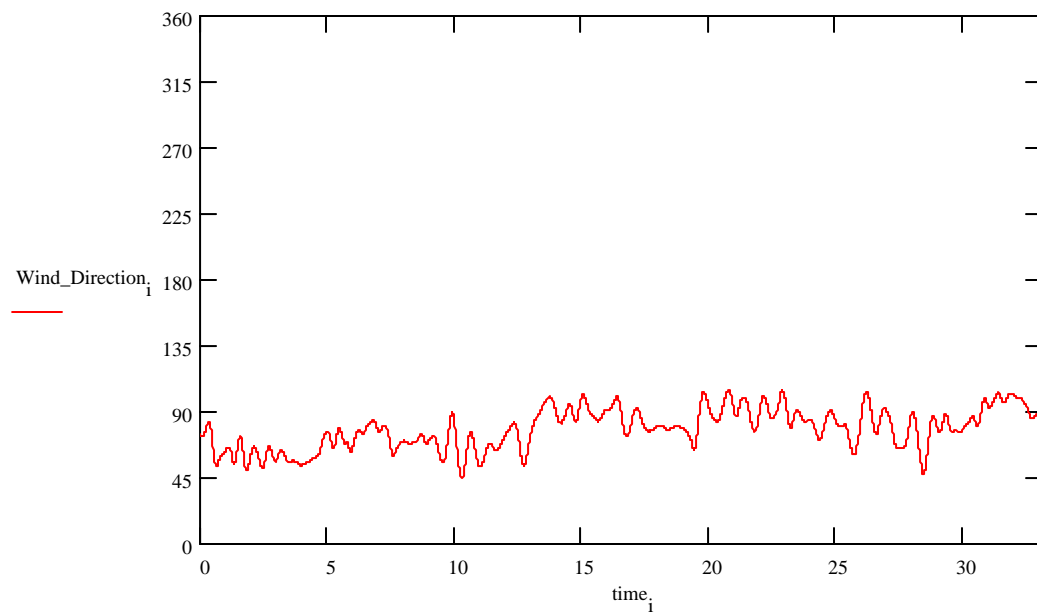
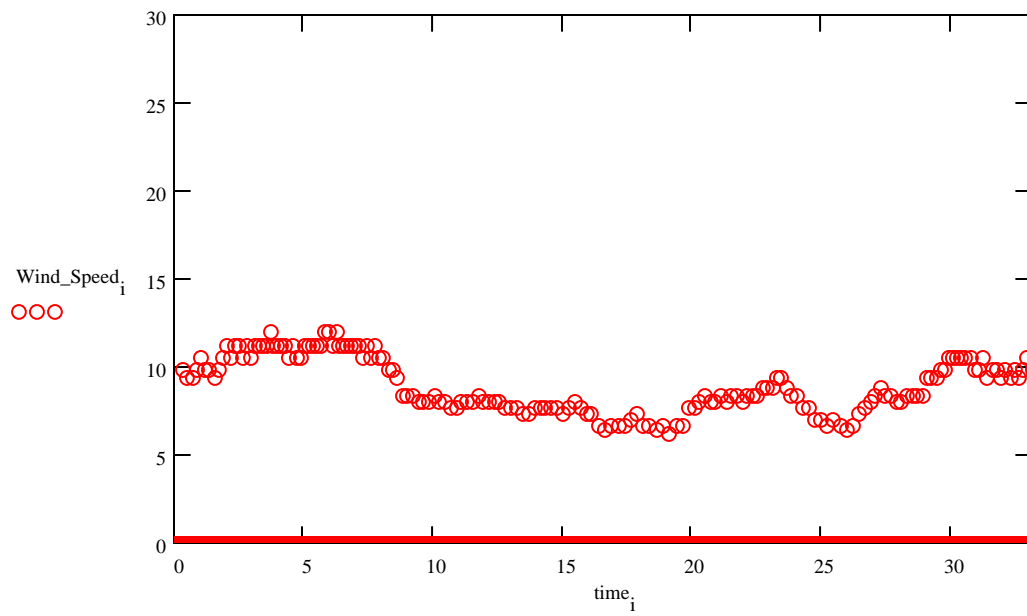
Peak := peaks(Anna\_temp)

$$\text{Wind}(\text{Peak}) := \left( \begin{array}{l} \text{for } i \in 1.. \text{ndata} \\ \quad t_i \leftarrow \left( \begin{array}{l} \text{time}_i \text{ if } \text{Peak}_i \neq 0 \\ 0 \text{ otherwise} \end{array} \right) \\ \text{for } i \in 1.. \text{ndata} \\ \quad \left| \begin{array}{l} \text{start} \leftarrow \left( \begin{array}{l} i \text{ if } \text{Peak}_i \neq 0 \\ 0 \text{ otherwise} \end{array} \right) \\ \text{break if } \text{start} \neq 0 \end{array} \right. \\ \text{temp} \leftarrow t_{\text{start}} \\ \text{for } i \in \text{start} + 1.. \text{ndata} \\ \quad \left| \begin{array}{l} \text{Speed}_i \leftarrow \left( \begin{array}{l} \frac{1.69}{t_i - \text{temp}} \text{ if } \text{Peak}_i \neq 0 \\ 0 \text{ otherwise} \end{array} \right) \\ \text{temp} \leftarrow \left( \begin{array}{l} t_i \text{ if } \text{Peak}_i \neq 0 \\ \text{temp} \text{ otherwise} \end{array} \right) \end{array} \right. \\ \text{Speed} \end{array} \right)$$

Wind\_Speed := Wind(Peak)

Wind\_Direction<sub>i</sub> := Vane<sub>i</sub>

Plot the wind speed and direction ...



APPENDIX B  
SAMPLE SSTAN INPUT FILE OF THE LAB MAST ARM

Lab Mast Arm Analysis

53,1,0 M=4 R=0

Coordinates

1	x=0	y=0	z=0
2	x=0	y=12	z=0
3	x=0	y=24	z=0
4	x=0	y=36	z=0
5	x=0	y=48	z=0
6	x=0	y=60	z=0
7	x=0	y=72	z=0
8	x=0	y=84	z=0
9	x=0	y=96	z=0
10	x=0	y=108	z=0
11	x=0	y=120	z=0
12	x=0	y=132	z=0
13	x=0	y=144	z=0
14	x=0	y=156	z=0
15	x=0	y=168	z=0
16	x=0	y=180	z=0
17	x=12	y=168	z=0
18	x=24	y=168	z=0
19	x=36	y=168	z=0
20	x=48	y=168	z=0
21	x=60	y=168	z=0
22	x=72	y=168	z=0
23	x=84	y=168	z=0
24	x=96	y=168	z=0
25	x=108	y=168	z=0
26	x=120	y=168	z=0
27	x=132	y=168	z=0
28	x=144	y=168	z=0
29	x=156	y=168	z=0
30	x=168	y=168	z=0
31	x=180	y=168	z=0
32	x=192	y=168	z=0
33	x=204	y=168	z=0
34	x=216	y=168	z=0
35	x=228	y=168	z=0

36 x=240 y=168 z=0  
 37 x=252 y=168 z=0  
 38 x=264 y=168 z=0  
 39 x=276 y=168 z=0  
 40 x=288 y=168 z=0  
 41 x=300 y=168 z=0  
 42 x=312 y=168 z=0  
 43 x=324 y=168 z=0  
 44 x=336 y=168 z=0  
 45 x=348 y=168 z=0  
 46 x=360 y=168 z=0  
 47 x=372 y=168 z=0  
 48 x=384 y=168 z=0  
 49 x=396 y=168 z=0  
 50 x=408 y=168 z=0  
 51 x=420 y=168 z=0  
 52 x=432 y=168 z=0  
 53 x=444 y=168 z=0

:

Boundary

1 DOF=F,F,F,F,F,F  
 2,53 DOF=R,R,R,R,R,R

:

Beam

52,52

1 I=93.88060905,93.88060905 J=187.7612181 a=6.38675969 e=29000000  
 m=0.004687009  
 2 I=90.29147225,90.29147225 J=180.5829445 a=6.304292883 e=29000000  
 m=0.00462649  
 3 I=86.79500783,86.79500783 J=173.5900157 a=6.221826076 e=29000000  
 m=0.00456597  
 4 I=83.39000353,83.39000353 J=166.7800071 a=6.139359269 e=29000000  
 m=0.004505451  
 5 I=80.07524711,80.07524711 J=160.1504942 a=6.056892461 e=29000000  
 m=0.004444932  
 6 I=76.84952631,76.84952631 J=153.6990526 a=5.974425654 e=29000000  
 m=0.004384412  
 7 I=73.71162888,73.71162888 J=147.4232578 a=5.891958847 e=29000000  
 m=0.004323893  
 8 I=70.66034256,70.66034256 J=141.3206851 a=5.80949204 e=29000000  
 m=0.004263374  
 9 I=67.6944551,67.6944551 J=135.3889102 a=5.727025233 e=29000000  
 m=0.004202854  
 10 I=64.81275426,64.81275426 J=129.6255085 a=5.644558426 e=29000000  
 m=0.004142335

- 11 I=62.01402777,62.01402777 J=124.0280555 a=5.562091618 e=29000000  
m=0.004081815
- 12 I=59.29706339,59.29706339 J=118.5941268 a=5.479624811 e=29000000  
m=0.004021296
- 13 I=56.66064886,56.66064886 J=113.3212977 a=5.397158004 e=29000000  
m=0.003960777
- 14 I=54.10357193,54.10357193 J=108.2071439 a=5.314691197 e=29000000  
m=0.003900257
- 15 I=51.62462035,51.62462035 J=103.2492407 a=5.23222439 e=29000000  
m=0.003839738
- 16 I=49.22258186,49.22258186 J=98.44516372 a=5.149757583 e=29000000  
m=0.003779219
- 17 I=46.89624421,46.89624421 J=93.79248843 a=5.067290775 e=29000000  
m=0.003718699
- 18 I=44.64439516,44.64439516 J=89.28879032 a=4.984823968 e=29000000  
m=0.00365818
- 19 I=42.46582244,42.46582244 J=84.93164488 a=4.902357161 e=29000000  
m=0.00359766
- 20 I=40.35931381,40.35931381 J=80.71862762 a=4.819890354 e=29000000  
m=0.003537141
- 21 I=38.32365701,38.32365701 J=76.64731401 a=4.737423547 e=29000000  
m=0.003476622
- 22 I=36.35763979,36.35763979 J=72.71527957 a=4.65495674 e=29000000  
m=0.003416102
- 23 I=34.46004989,34.46004989 J=68.92009978 a=4.572489933 e=29000000  
m=0.003355583
- 24 I=32.62967507,32.62967507 J=65.25935014 a=4.490023125 e=29000000  
m=0.003295064
- 25 I=30.86530307,30.86530307 J=61.73060615 a=4.407556318 e=29000000  
m=0.003234544
- 26 I=29.16572165,29.16572165 J=58.33144329 a=4.325089511 e=29000000  
m=0.003174025
- 27 I=27.52971854,27.52971854 J=55.05943707 a=4.242622704 e=29000000  
m=0.003113505
- 28 I=25.95608149,25.95608149 J=51.91216298 a=4.160155897 e=29000000  
m=0.003052986
- 29 I=24.44359825,24.44359825 J=48.88719651 a=4.07768909 e=29000000  
m=0.002992467
- 30 I=22.99105658,22.99105658 J=45.98211316 a=3.995222282 e=29000000  
m=0.002931947
- 31 I=21.59724421,21.59724421 J=43.19448842 a=3.912755475 e=29000000  
m=0.002871428
- 32 I=20.26094889,20.26094889 J=40.52189779 a=3.830288668 e=29000000  
m=0.002810909
- 33 I=18.98095838,18.98095838 J=37.96191676 a=3.747821861 e=29000000  
m=0.002750389

34	I=17.75606042,17.75606042 J=35.51212083 a=3.665355054 e=29000000 m=0.00268987			
35	I=16.58504275,16.58504275 J=33.17008549 a=3.582888247 e=29000000 m=0.002629351			
36	I=15.46669312,15.46669312 J=30.93338625 a=3.500421439 e=29000000 m=0.002568831			
37	I=14.39979929,14.39979929 J=28.79959858 a=3.417954632 e=29000000 m=0.002508312			
38	I=13.383149,13.383149 J=26.76629799 a=3.335487825 e=29000000 m=0.002447792			
39	I=12.41552999,12.41552999 J=24.83105998 a=3.253021018 e=29000000 m=0.002387273			
40	I=11.49573001,11.49573001 J=22.99146003 a=3.170554211 e=29000000 m=0.002326754			
41	I=10.62253682,10.62253682 J=21.24507364 a=3.088087404 e=29000000 m=0.002266234			
42	I=9.794738157,9.794738157 J=19.58947631 a=3.005620597 e=29000000 m=0.002205715			
43	I=9.011121769,9.011121769 J=18.02224354 a=2.923153789 e=29000000 m=0.002145196			
44	I=8.270475404,8.270475404 J=16.54095081 a=2.840686982 e=29000000 m=0.002084676			
45	I=7.571586811,7.571586811 J=15.14317362 a=2.758220175 e=29000000 m=0.002024157			
46	I=6.913243735,6.913243735 J=13.82648747 a=2.675753368 e=29000000 m=0.001963637			
47	I=6.294233926,6.294233926 J=12.58846785 a=2.593286561 e=29000000 m=0.001903118			
48	I=5.713345129,5.713345129 J=11.42669026 a=2.510819754 e=29000000 m=0.001842599			
49	I=5.169365094,5.169365094 J=10.33873019 a=2.428352946 e=29000000 m=0.001782079			
50	I=4.661081567,4.661081567 J=9.322163133 a=2.345886139 e=29000000 m=0.00172156			
51	I=4.187282295,4.187282295 J=8.374564590 a=2.263419332 e=29000000 m=0.001661041			
52	I=3.746755026,3.746755026 J=7.493510052 a=2.180952525 e=29000000 m=0.001600521			
1	1	2	53	m=1
2	2	3	53	m=2
3	3	4	53	m=3
4	4	5	53	m=4
5	5	6	53	m=5
6	6	7	53	m=6
7	7	8	53	m=7
8	8	9	53	m=8



9	9	10	53	m=9
10	10	11	53	m=10
11	11	12	53	m=11
12	12	13	53	m=12
13	13	14	53	m=13
14	14	15	53	m=14
15	15	16	53	m=15
16	15	17	1	m=16
17	17	18	1	m=17
18	18	19	1	m=18
19	19	20	1	m=19
20	20	21	1	m=20
21	21	22	1	m=21
22	22	23	1	m=22
23	23	24	1	m=23
24	24	25	1	m=24
25	25	26	1	m=25
26	26	27	1	m=26
27	27	28	1	m=27
28	28	29	1	m=28
29	29	30	1	m=29
30	30	31	1	m=30
31	31	32	1	m=31
32	32	33	1	m=32
33	33	34	1	m=33
34	34	35	1	m=34
35	35	36	1	m=35
36	36	37	1	m=36
37	37	38	1	m=37
38	38	39	1	m=38
39	39	40	1	m=39
40	40	41	1	m=40
41	41	42	1	m=41
42	42	43	1	m=42
43	43	44	1	m=43
44	44	45	1	m=44
45	45	46	1	m=45
46	46	47	1	m=46
47	47	48	1	m=47
48	48	49	1	m=48
49	49	50	1	m=49
50	50	51	1	m=50
51	51	52	1	m=51
52	52	53	1	m=52
:				
Mass				

25 M=57/386.4,57/386.4,57/386.4,0,0,0 : 3 - light signal head  
37 M=57/386.4,57/386.4,57/386.4,0,0,0 : 3 - light signal head  
51 M=85/386.4,85/386.4,85/386.4,0,0,0 : 5 - light signal head

:

APPENDIX C  
FABRICATION OF TAPERED IMPACT DAMPER

Parts List

Part #	Part	Part Description	Quantity
1	Damper Shell	6" ID, t = 0.125", ASTM A513, Type 1	1
2	Damper Cap	Steel Cap	1
3	Damper Internal Weight	15lb Steel Cylindrical Weight	1
4	Damper Spring	Century Spring Brand (Spring Stock #147) Stiffness = 0.69lb/in, Length = 8.5", OD = 1.062"	1
5	Hex Nut	1/4"-20 Hex Nut (steel)	1
6	Eye Bolt	1/4"x2" Steel Eye Bolt (zinc plated)	1
7	Eye Bolt	1/4"x8" Steel Eye Bolt (zinc plated)	1
8	Cap Screw	#8-32x3/4 SS Machine Screws (Flat Hd Phillips) (Only needed if Part 2 is used)	4
9	Alternate Damper Cap	Cast Aluminum Upright Cap with (3) Stainless Steel Set Screws (Covers 6.25" OD Pipe)	1

Cap Fabrication (Part 2)

- See Cap Fabrication Drawing for Tapered Impact Damper
- Hot Dip Galvanize the Cap after Fabrication

Weight Fabrication (Part 3)

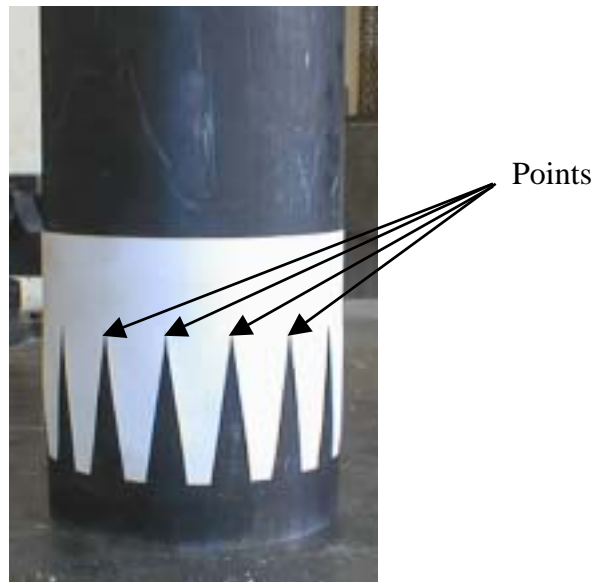
- See Weight Fabrication Drawing for Tapered Impact Damper
- Hot Dip Galvanize the Weight after Fabrication

Alternate Cap (Part 9)

- Can be Purchased Pre-Fabricated
- See Alternate Cap Preparation Drawing for Tapered Impact Damper

### Shell Fabrication (Part 1)

- See Shell Fabrication Drawing for Tapered Impact Damper
- Cut part 1 to 3'- 6".
- Wrap the Shell Stencil around the bottom of part 1. Provide 2' - 9 5/8" between the top of part 1 and the points of the stencil.



- Scribe and cut out the steel below the stencil. The total length of part 1 should still be 3'- 6".



- Heat the area directly between each point and bend each flap inward. Each adjacent flap should be touching. This will create the tapered portion of the shell.



- Weld the flaps together and grind the tapered surface smooth.



- Hot Dip Galvanize the Shell after Fabrication

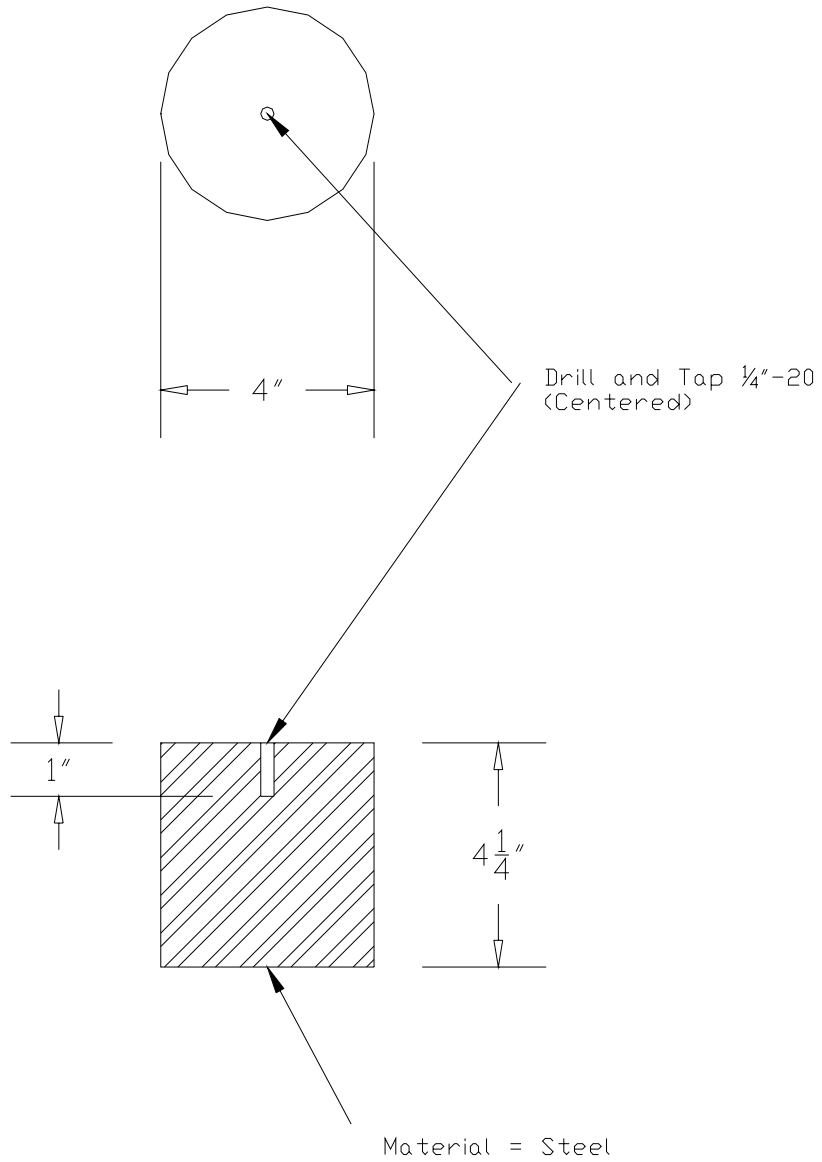
### Sequence of Tapered Impact Damper Assembly using *Part 2*

- Refer to the Overall Fabrication Drawing for Tapered Impact Damper
- Insert part 6 into the threaded hole of part 3 to create the weight assembly.
- Insert part 7 through the threaded hole of part 2 to where part 5 can be attached to part 7. This will create the cap assembly.
- Attach one end of part 4 to part 7 and the other end of part 4 to part 6. This will create the cap/spring/weight assembly.
- Lower the cap/spring/weight assembly into part 1.
- Adjust part 7 on the cap assembly until the bottom of part 3 is 2” from the bottom of part 1. This can be done through the hole at the bottom of part 1. (Note: part 1 must be vertical when making the 2” measurement and the weight and spring combination needs to be at rest)
- Match the holes in part 1 with those from part 2. Fasten them together with part 8 (4 places).
- Tighten part 5 against part 2.
- Cut off portion of part 7 remaining above part 5.

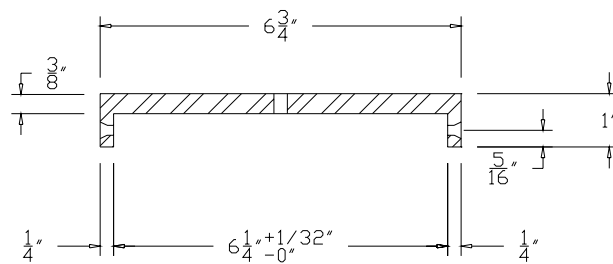
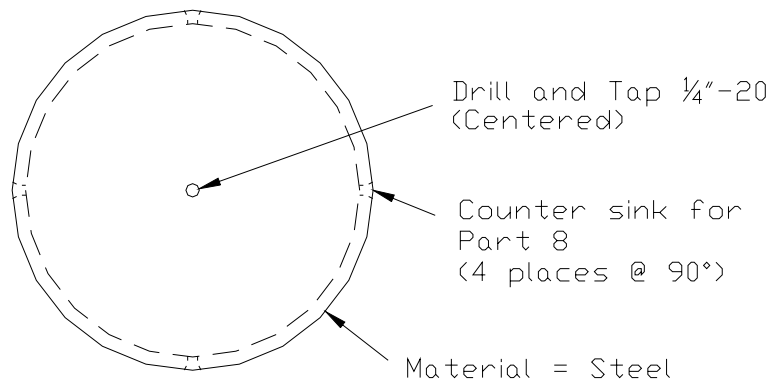
### Sequence of Tapered Impact Damper Assembly using *Part 9*

- Refer to the Overall Fabrication Drawing for Tapered Impact Damper with Alternate Cap
- Insert part 6 into the threaded hole of part 3 to create the weight assembly.
- Insert part 7 through the threaded hole of part 9 to where part 5 can be attached to part 7. This will create the cap assembly.
- Attach one end of part 4 to part 7 and the other end of part 4 to part 6. This will create the cap/spring/weight assembly.
- Lower the cap/spring/weight assembly into part 1.
- Adjust part 7 on the cap assembly until the bottom of part 3 is 2” from the bottom of part 1. This can be done through the hole at the bottom of part 1. (Note: part 1 must be vertical when making the 2” measurement and the weight and spring combination needs to be at rest)
- Tighten the set screws of part 9 against the shell.
- Tighten part 5 against part 9.
- Cut off portion of part 7 remaining above part 5.

Weight Fabrication Drawing for  
Tapered Impact Damper



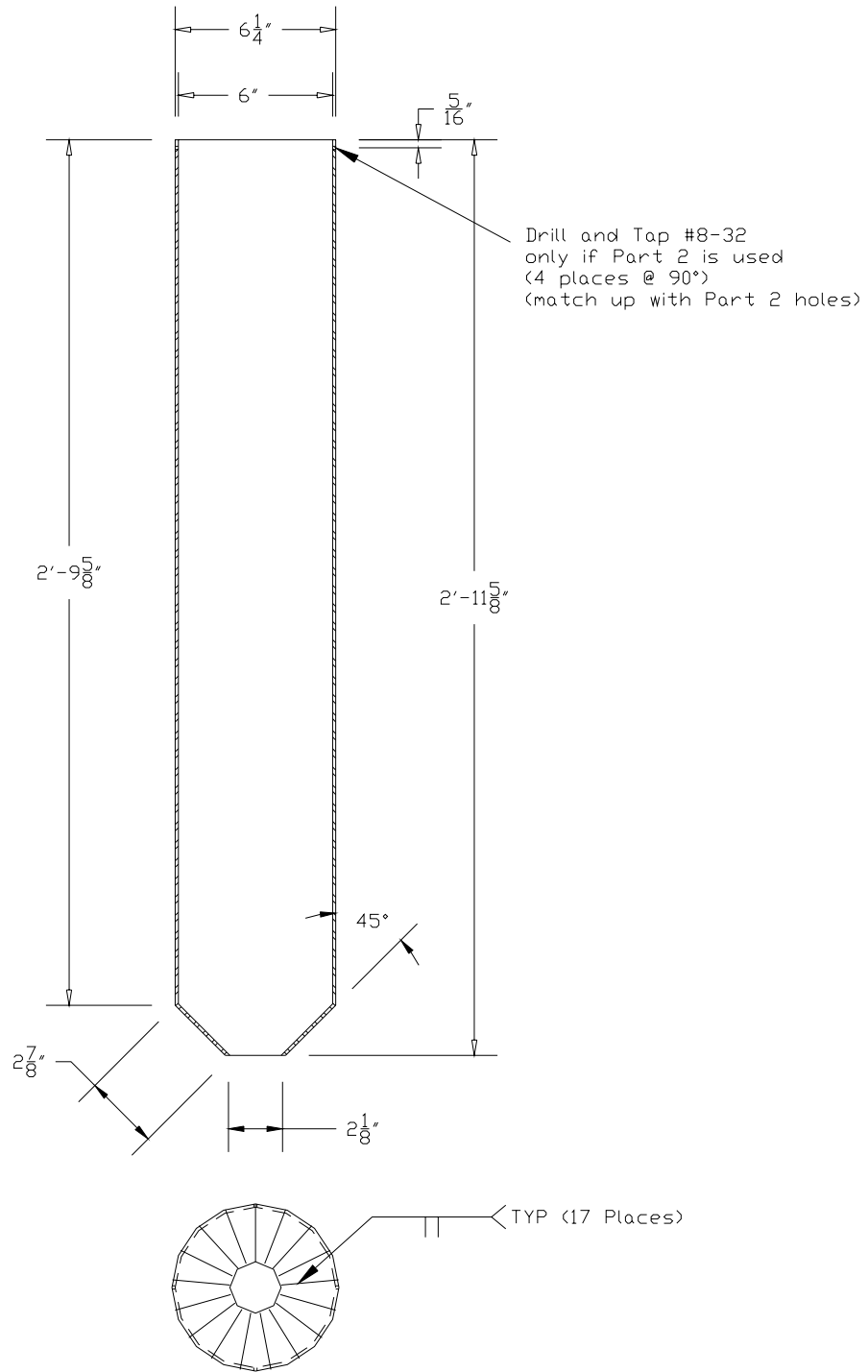
Cap Fabrication Drawing for  
Tapered Impact Damper



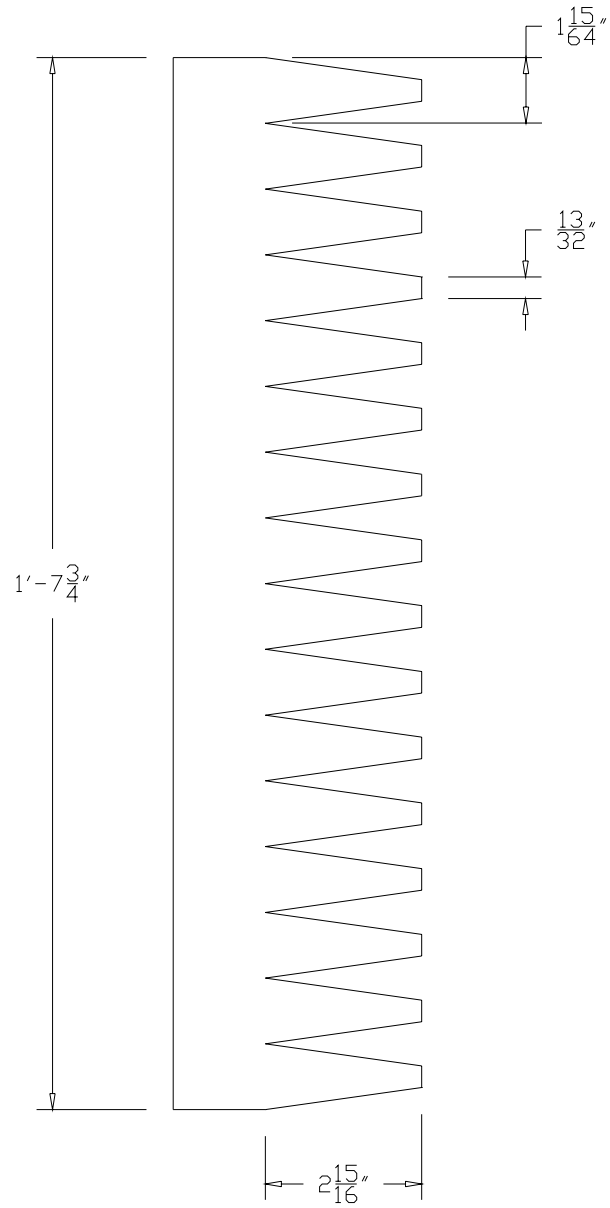
Note: Only build if Part 9 is not used



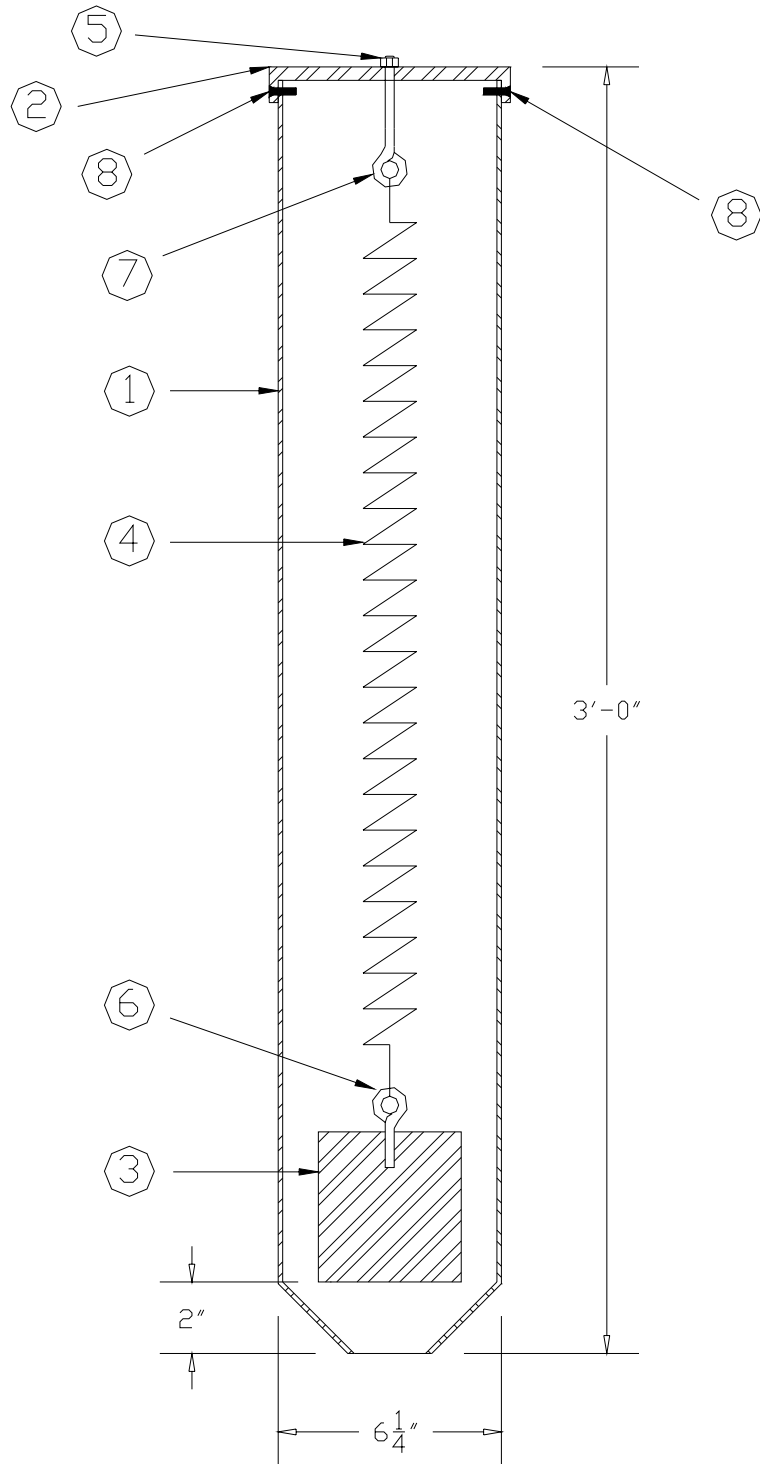
Shell Fabrication Drawing for  
Tapered Impact Damper



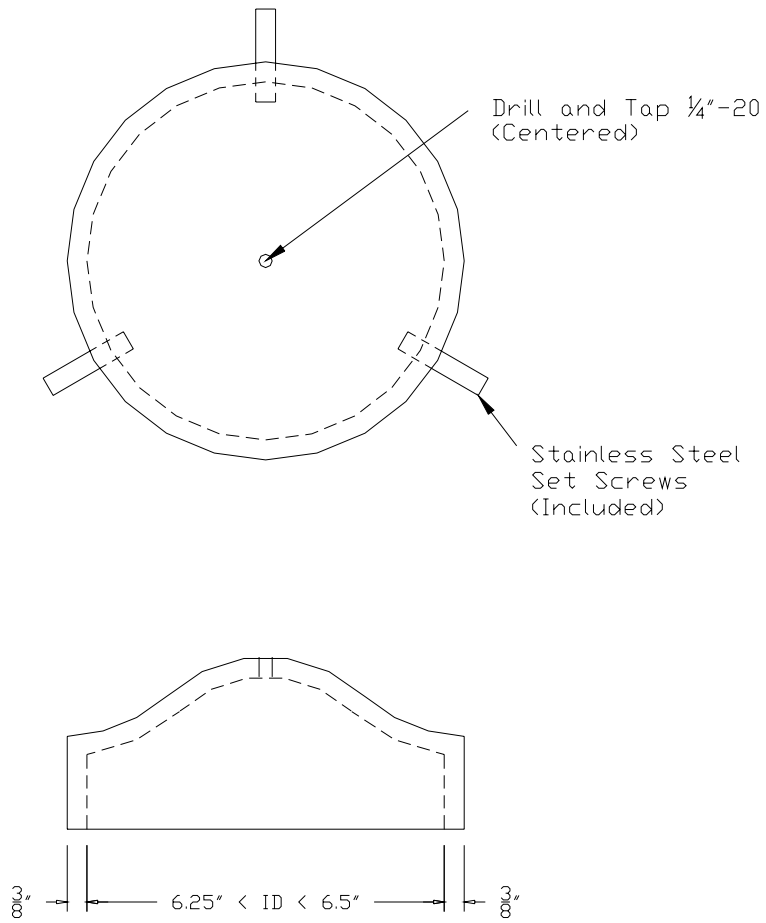
Stencil for Tapered End of Shell  
on the Tapered Impact Damper



Overall Fabrication Drawing for  
Tapered Impact Damper



Alternate Cap Preparation Drawing  
for Tapered Impact Damper



Note: Only use if Part 2 is not used

Overall Fabrication Drawing for  
Tapered Impact Damper  
(with Alternate Cap)

